ADDIS ABABA INSTITUTE OF TECHNOLOGY

SCHOOL OF GRADUATE STUDIES

DEPARTMENT OF CIVIL ENGINEERING

Prediction of swelling behavior of Addis Ababa expansive soil using simple mathematical model

A thesis submitted to the School of Graduate Studies of Addis Ababa Institute of Technology in partial fulfillment of the requirements for the degree of Master of Science in Civil Engineering (GEOTECHNIQUES)

By

ELEYAS ASSEFA

Advisor: **Dr. ing. SAMUEL TADESSE**

Addis Ababa

2012

ADDIS ABABA INSTITUTE OF TECHNOLOGY

SCHOOL OF GRADUATE STUDIES

DEPARTMENT OF CIVIL ENGINEERING

Prediction of swelling behavior of Addis Ababa expansive soil using simple mathematical model

By

ELEYAS ASSEFA

2012

Approved by Board of Examiners

Dr. Samuel Tadesse Advisor	____________________ Signature	________________ Date
Dr. Mesele Haile External Examiner	____________________ Signature	________________ Date
Prof. Alemayehu Teferra Internal Examiner	____________________ Signature	________________ Date
Ato Kibru Fitret Chairman	____________________ Signature	________________ Date

Declaration

This thesis is my original work and has not been presented for a degree in any other university, and that all sources of material used for the thesis have been duly acknowledged.

Candidate's name ______________________________

Signature _____________________________________

Acknowledgement

Though only my name appears on the cover of this thesis, a great many people have contributed to its production. I owe my gratitude to all those people who have made this thesis possible and because of whom my graduate experience has been one that I will cherish forever.

My deepest gratitude is to my advisor, Dr. ing. Samuel Tadesse. I have been amazingly fortunate to have an advisor who gave me the freedom to explore on my own and at the same time the guidance to recover when my steps faltered. He taught me how to question thoughts and express ideas. His patience and support helped me to overcome many crisis situations and finish this thesis.

Abstract

Damage due to soil swelling is very noticeable in wide spectrum of structures such as roads, buildings, canal linings, landfill liners, etc. To evaluate severity of swelling and to design for the best and most economical stabilization strategy, an accurate assessment of the swell potential is required.

The main reason of swelling behavior is water absorption of soil mass in time. And the time required for completion of swelling is relatively long. In view of that several attempts have been made by researchers to obtain time-swell relationships for expansive soils. Some progress has been made toward characterizing swelling characteristics, despite the complexity of the behavior.

In this study a simple hyperbolic mathematical model is used to predict the swelling behavior of an expansive soil from Addis Ababa. The formula was first proposed by Richard and Abbot, 1975.

The model was formed in one equation with many parameters. The main advantage of this model is that only one parameter is needed to run the model. The main parameters that are needed to run the model are the applied pressure and initial dry density. The other parameters of the model including the initial slope of the swell-time curve, the final slope, the reference swell, and the peak swell were investigated experimentally.

Based on the experimental results, empirical relationships were developed for determination of these parameters as functions of the applied pressure and initial dry density. The model prediction were compared with the experimental results and showed good agreements for all levels of applied pressure and initial dry density of the tested soil.

Contents

List of figures

List of tables

List of acronyms

Am	American
ASTM	American society for testing and materials
AU	African Union
Bole H. S	Bole High School
C. Bole A.	Close to Bole air port
Canad. Geotech. J.	Canadian geotechnical journal
CSA	Central statistical agency of Ethiopia
ECA	Economic commission for Africa
Engg. Mech.	Engineering mechanics
Eq.	Equation
Fig.	Figure
Found. Eng.	Foundation engineering
Int. Conf.	International conference
Mag.	Magazine
No.	Number
Proc.	Proceedings of
Reg.	Regional
Res.	Research
Sci.	Scientific
Soil mech.	Soil mechanics
UNDP	United Nations development program
UNICEF	United Nations children's fund

List of nomenclatures

LL	Liquid limit
MDD	Maximum dry density
OMC	Optimum moisture content
PI	Plasticity index
PL	plastic limit
S	Vertical swelling
T	Time
P’s	Corrected swelling pressure
Ps	Uncorrected swelling pressure
E_1	The first slope of stress strain curve
E_2	The second slope of stress strain curve
ϵ_c	Strain of concrete
f_c	Stress of concrete
f_o	The reference stress
n	Curve-shape parameter
k	The initial slope of swell time curve
kp	The final slope of swell time curve
So	Reference swell
n	Curve-shape parameter.

Chapter one
Introduction

1.1 General

Expansive soils are found in many parts of the world, especially in arid or semiarid regions, and temperate climate zones. Severe damage of structures, such as foundation and floor crack, roadway distress, has been reported in many countries (Daniel and Wu, 1993; Alawaji, 1999). Krohn and Slosson, 1980 estimated that, in the United States alone, the costs associated with damage caused by expansive soil amounts about $7 billion per year. Jones and Holtz, 1973 pointed out that the damage due to swelling soils is more than twice as much the combined damages from natural disasters such as floods, hurricanes, earthquakes, and tornadoes. Therefore, the problems related to expansive soils have attracted wide attention throughout the world.

Not all soils create problems due to swelling when brought into contact with water source. Only soils with high swelling potential will cause damage to buildings. An accurate estimation of the swelling potential of a soil is an essential step for the selection of effective treatment alternatives or preparation of adequate designs.

The swelling potential of a soil is a measure of its ability to swell. Many research workers have used different techniques to define the swelling potential of a soil. Holtz and Gibbs, 1956 defined the swelling potential of the soil as the total volume change of a soil from its air dry state to its saturated condition under a surcharge load of 7kPa. Seed et al., 1962 defined swelling potential as the percentage of swell of a laterally confined specimen after soaking in water under a confining pressure of 7kPa, after being compacted to maximum density at optimum water content in the standard AASHTO compaction test. However, in most cases, the two components of the swelling potential; namely the percent swell and the swelling pressure, are used to estimate the swelling potential of a soil.

Several attempts have been made by researchers to obtain time-swell relationships for expansive soils. Some progress has been made toward characterizing swelling characteristics, despite the complexity of the behavior. Seed *et al.*, 1962 reported that the time required for completion of swelling is relatively long.

1.2 Problems due to expansive soils in Addis Ababa

In the capital, Addis Ababa, it has been noticed that expansive soils covers large parts of the city where recent constructions are carried out. During the past decades, rapid expansion of the city and the growth of population due to migration from different parts of the country led to the construction of various structures, particularly low-cost buildings in the suburbs. This situation resulted in an increase in the length of the street network and buried utility lines. The existence of expansive soils in the Addis Ababa area has caused structural damages on light buildings, asphalt pavement, and buried utility lines. City planners and engineers did not appear to pay attention to the problems associated with expansive soil during site selection and construction of low-rise and low-cost buildings.

1.3 Objective of the study

The prime objective of this research program is to predict the swell-time curve of swell tests on expansive soil of Addis Ababa at different levels of applied pressure and different dry density using the model presented by Richard and Abbott, 1975.

1.4 Scope of the thesis

The scope of this study is mainly limited to one-dimensional swelling to investigate and predict the swelling behavior of expansive soil. For this anticipated purpose, disturbed samples were collected from locations of Addis Ababa which were confirmed by different Investigators to be covered by expansive soils.

Also the relationship between different model parameters and the effects of initial dry density, surcharge load and time are studied. The swelling tests are performed using swell overburden test method and the variables considered in the experimental program include initial dry density, time and surcharge pressure. And the influence of these variables on the vertical swell is reported and mathematical model is used to predict the swelling behavior of expansive soil.

1.5 Thesis organization

The thesis is divided into six Chapters. In the first Chapter, “Introduction”, the objective of the thesis is briefly outlined.

The second Chapter, “Literature review”, provides a summary of available information which is used for further experimental development in this research program.

The third Chapter, “Description of the study area”, the study area is briefly outlined.

The fourth Chapter, “Experimental study”, outlines in detail the experimental program for achieving the designated objective. The soil used in the test program, the laboratory equipment used in preparing and testing the specimens, and the test procedures which were run are also outlined. Typical results of the swelling tests are presented.

In the fifth Chapter, “Evaluation of the proposed model”, the results of the data analyses using the proposed model are discussed in detail.

The six Chapter “Summary and conclusion”, summarizes the findings from this research program and provides recommendations regarding the direction for future.

Chapter two
Literature review

2.1 General

Expansive clay soils swell when wetted and shrink when they dry out, hence giving rise to ground movement. A further understanding of the swelling mechanism and properties of this type of soil will lead to an increased confidence level.

Assessing the amount of swelling is an important stage in designing any civil engineering structures on expansive soils. Many researchers have developed different equations that could be used to predict the swelling potential of expansive clays from their index properties (Chen, 1988; Abduljauwad, 1993; Al-Homoud and Al-Suleiman, 1997; Li and Du, 1997; Bonner and Shakoor, 1998; Al-Rawas, 1999); they provided helpful information for practicing engineers. In addition, a small number of studies have been conducted on swelling/shrinking soils mapping and hazard assessment (Ramana, 1993; Basma *et al*., 1995; Oteo *et al*., 1995; USGS, 2000; Meisina, 2002).

Previous researchers have studied swelling behavior, mechanics of swelling, and compressibility of expansive soil mixtures (Komine and Ogata, 1994; Alawaji, 1999). They assessed the effect of factors affecting swelling and compressibility of expansive soils such as initial water content and initial dry density.

Current engineering and geologic practices for characterization of expansive clays involve time-consuming and expensive standard engineering tests for determination of swelling potential.

A major concern in geotechnical engineering is identification of expansive soils and estimation of their swelling magnitudes when subjected to changes in environment (Subba Rao and Satyadas, 1987; Day, 1994; Al-Homoud *et al.*, 1995).

2.2 Factors influencing swelling of soils

The mechanism of swelling in expansive clays is complex and is influenced by a number of factors. Expansion is a change of particle spacing and this is a result of changes in the soil water system that disturb the internal stress equilibrium. The factors influencing the swell potential of a soil can be considered in three different groups; the soil characteristics that influence the basic nature of the internal force field, the environmental factors that influence the changes that may occur in the internal force system, and the state of stress.

2.2.1 Effect of clay mineral type

The mineralogical composition and clay fraction content are the main factors governing the swelling characteristics of expansive clayey soils. However, the determination of mineralogical composition needs relatively sophisticated test equipment and elaborate test procedures which may not be generally available for practical purposes.

Lambe and Whitman, 1969 reported that swelling ability varies with the type of clay mineral and decreases in the order; motmorillonite, illite and kaolinite and also depends considerably on exchangeable ions.

2.2.2 Effect of clay content

El-Sohby and Rabba, 1981 studied the effect of clay content on swelling and swelling pressure with different clay percentage being mixed. In one case with sand and, in the other with silt. According to the experimental results; depending on the soil properties and the applied pressure, the swelling and the value of swelling pressure increases as the percentage of clay increases. The results of tests are shown in Fig. 2.1, Fig. 2.2 and Fig. 2.3

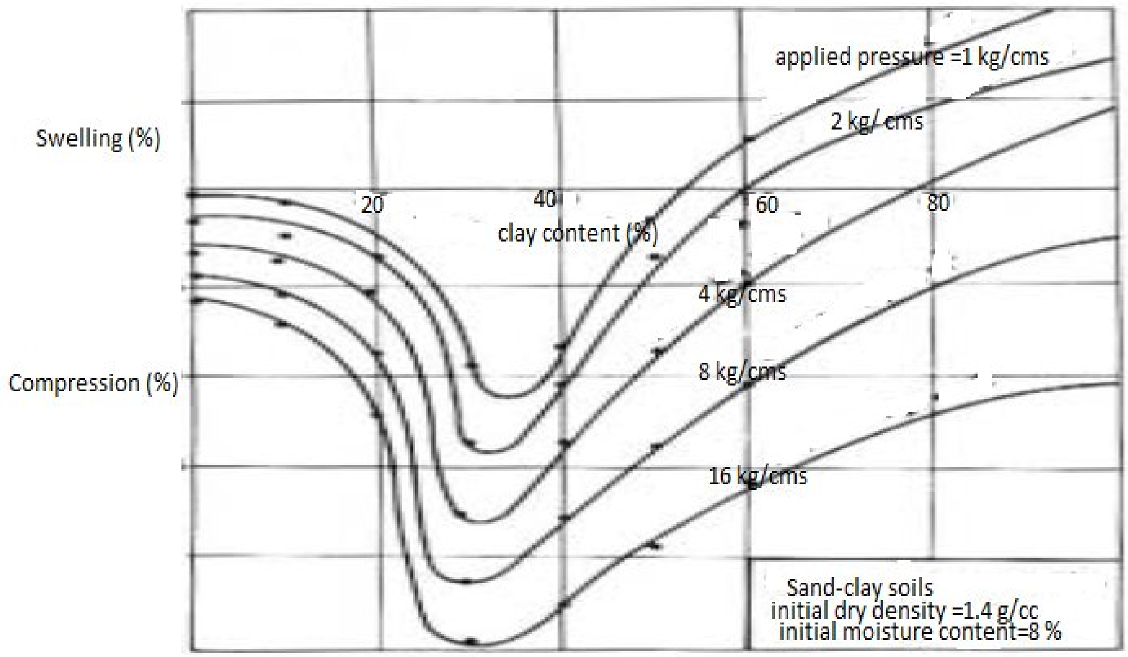

Figure 2.1 Effect of clay content on swelling (After El-Sohby and Rabba, 1981)

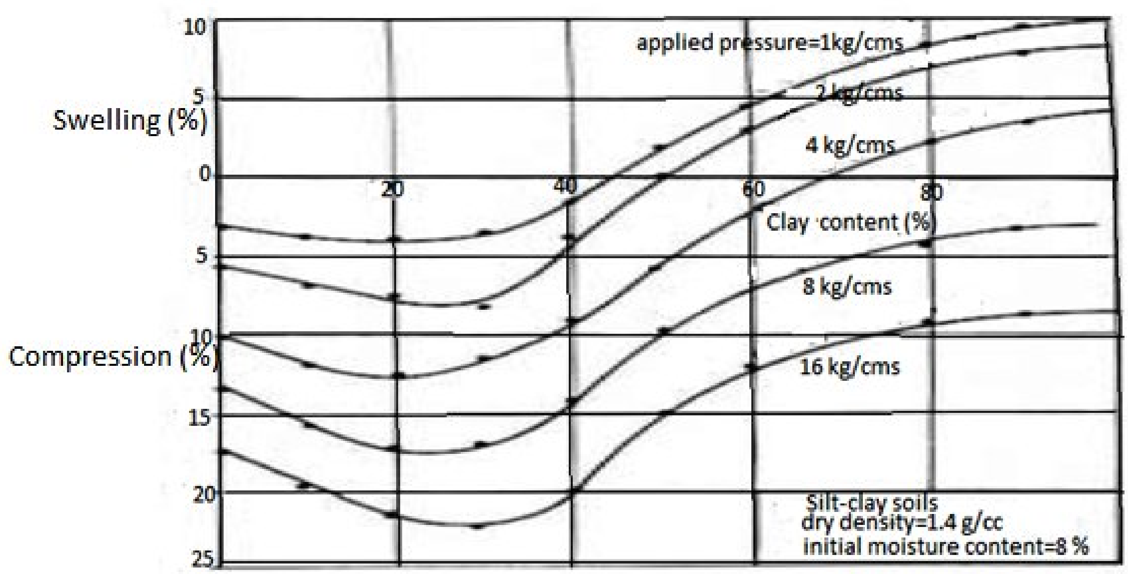

Figure 2.2 Effect of clay content on swelling (After El-Sohby and Rabba, 1981)

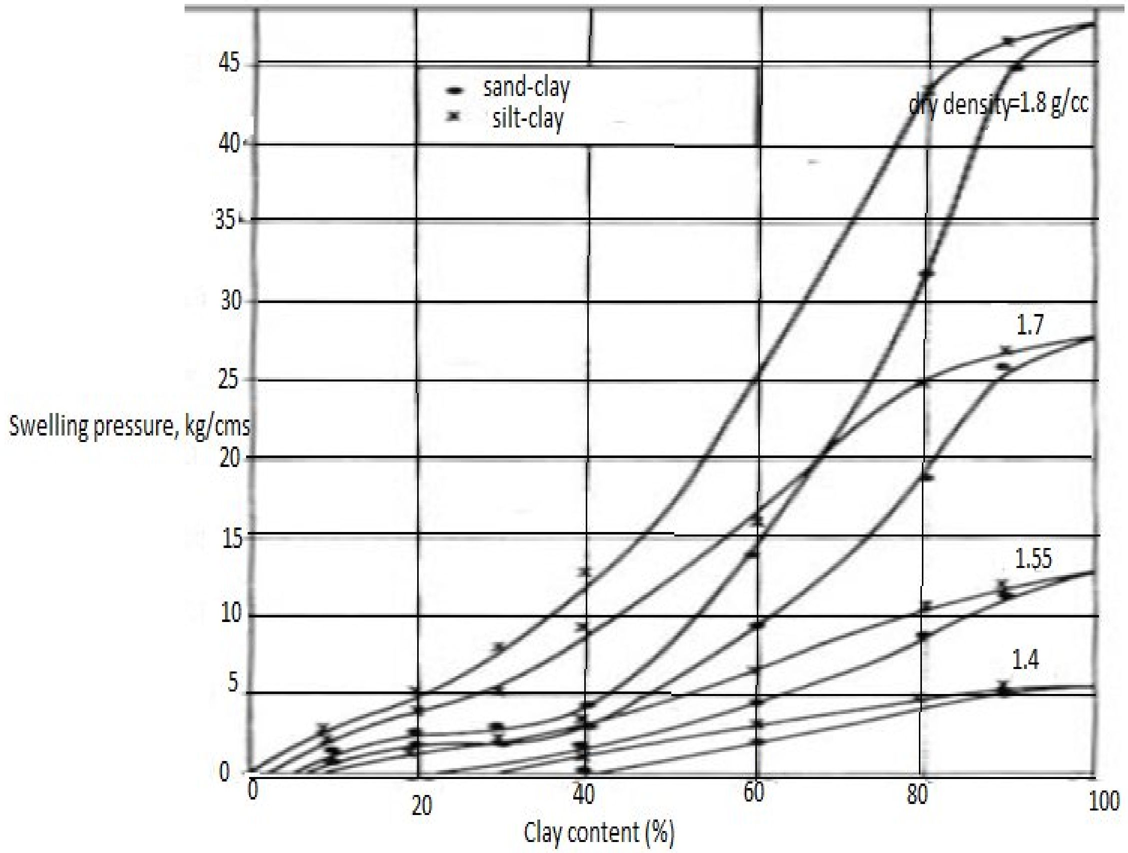

Figure 2.3 Effect of clay content on swelling pressure (After El-Sohby and Rabba, 1981)

2.2.3 Effect of initial water content

In order to study the initial water content on the amount of swelling and swelling pressure El-Sohby and Rabba ,1981 prepared remolded specimens having different initial water contents at the same initial dry density. The effect of initial water content on the amount of swelling under different vertical pressures is shown in Fig. 2.4.

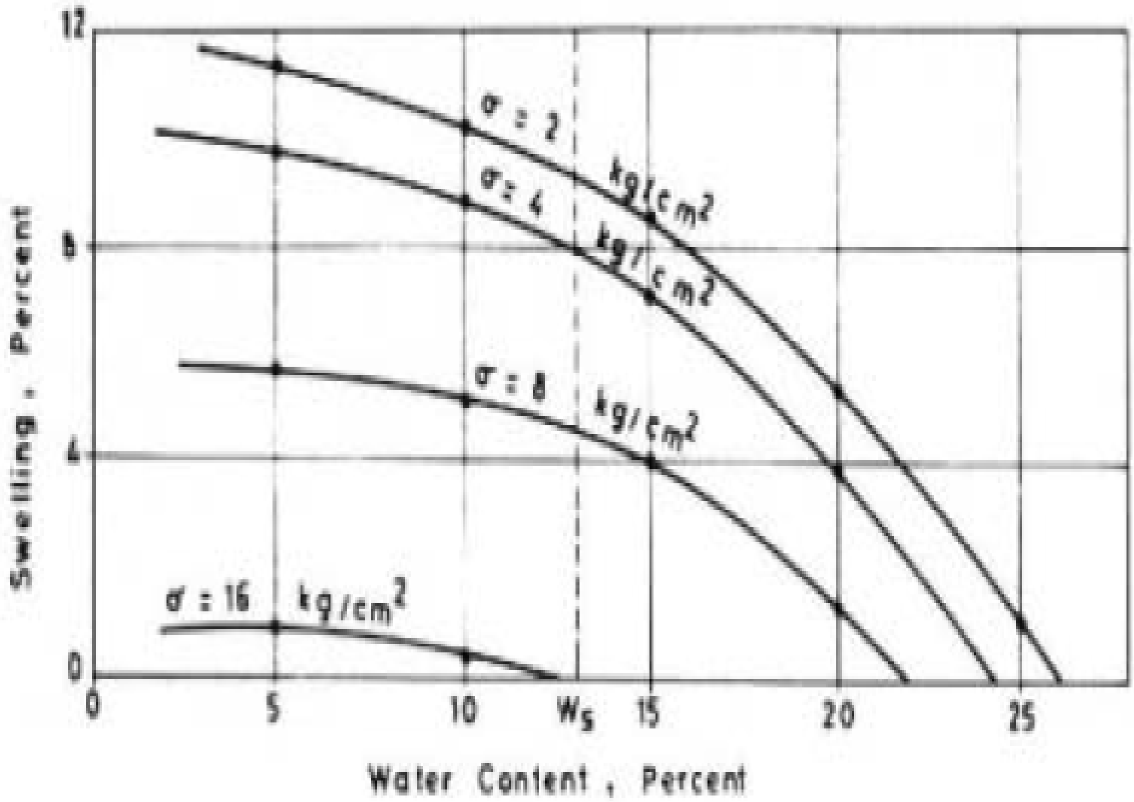

Figure 2.4 Effect of initial water content on swelling (After El-Sohby and Rabba, 1981)

It is evident from Fig. 2.4 that the initial water content has a considerable influence on the percentage swelling of the remolded samples. These results may be expected, since as the initial water content increases, for specimens having the same initial dry unit weight, the initial degree of saturation will also increase and the affinity of soil to absorb water will decrease. It follows that the amount of water absorbed for complete saturation will become smaller, and consequently the amount of swelling will decrease as the initial water content increase. The effect of the initial water content on the swelling pressure is shown in Fig. 2.5

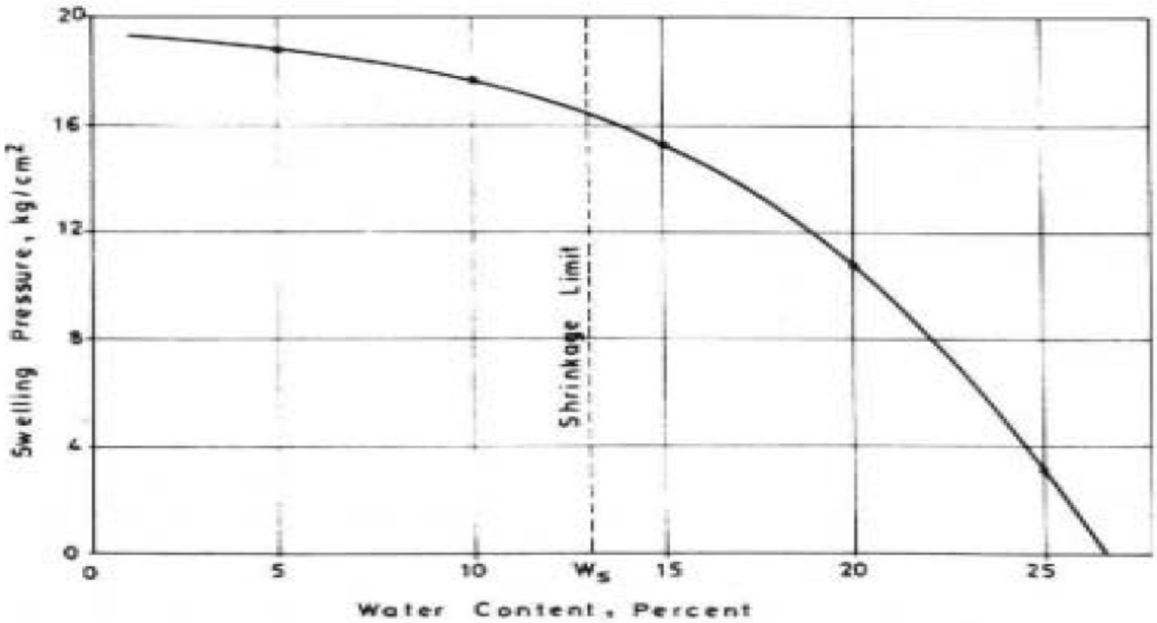

Figure 2.5 Effect of initial water content on swelling pressure (After El-Sohby and Rabba, 1981)

As it can be seen from the figure as the initial water content increases the swelling pressure decreases, but the relationship is non-linear.

2.2.4 Effect of initial dry density

El-Sohby and Rabba, 1981 carried out conventional oedometer test to study the effect of initial dry density on swelling and swelling pressure of soils. For each specimen the swelling under different pressure and, consequently, the swelling pressure is determined. The results of these tests can be seen in Fig. 2.6 and Fig. 2.7.

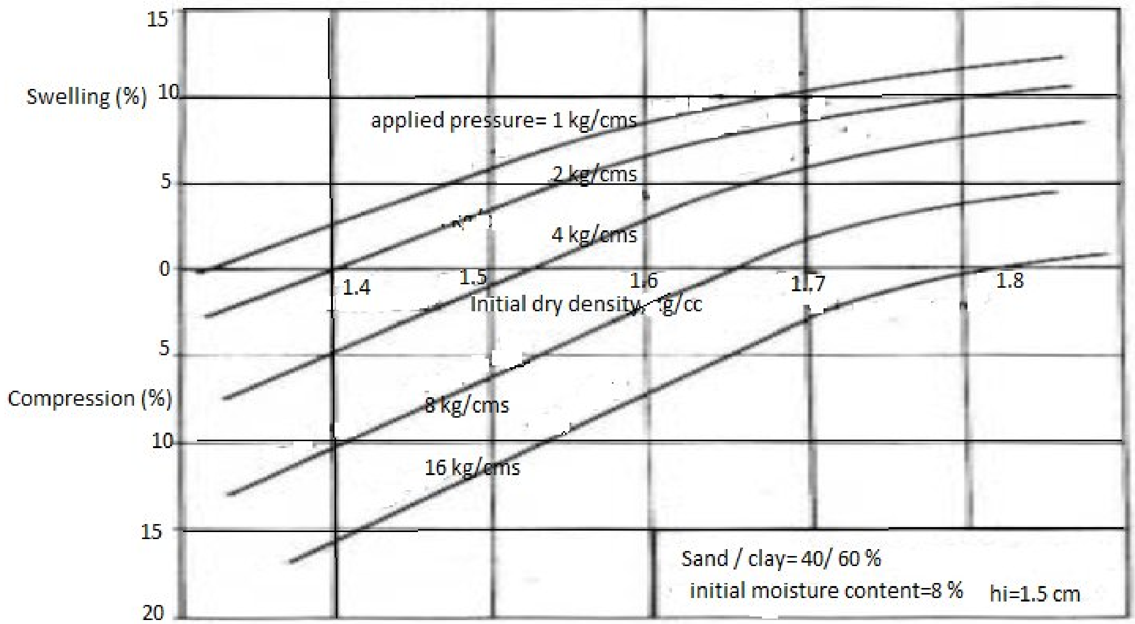

Figure 2.6 Effect of intial dry density on swell (After El-Sohby and Rabba, 1981)

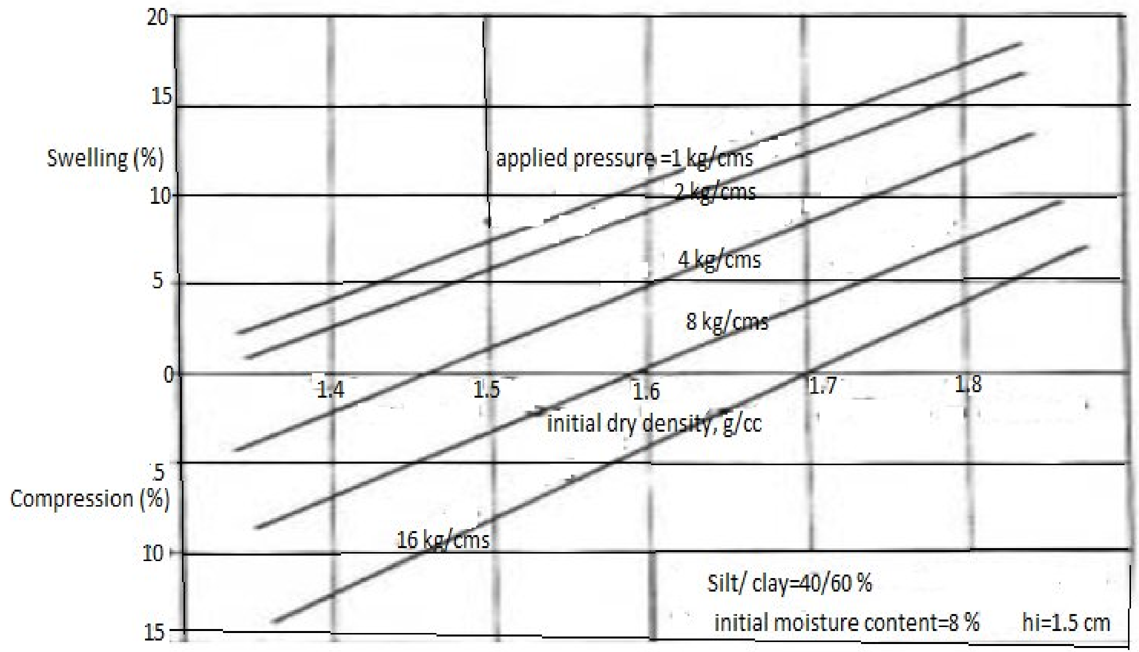

Figure 2.7 Effect of initial dry density on swelling pressure (After El-Sohby and Rabba, 1981)

The results of these tests showed that as the initial dry density increases both of the percent swell and the value of swelling pressure increase. This is because during water absorption into the soil media water particles will apply more forces to the surrounding soil particles to achieve the complete saturation for higher initial dry densities.

2.2.5 Effect of time

The main reason of swelling behavior is water absorption of soil mass in time (Seed, 1961). The time required for the soil to reach its maximum swell potential may vary considerably depending essentially on the initial density, permeability, and the thickness of the sample. According to Chen, 1988; for remolded samples, generally 24 hours is sufficient to obtain 95 percent of the total available swell. At the same time, for undisturbed high density clay shale, it may require several days or even a week before complete saturation can be achieved. For remolded samples, the initial added water must be evenly distributed. This requires a minimum curing time of six hours for reproducible results.

2.2.6 Effect of surcharge load

Swell can be prevented if expansive clays can be loaded with a surcharge large enough to counteract the expected swell pressures. Swell is very sensitive to changes in pressure. Low surcharge pressure may lead to erratic and erroneous test results. Since most footing foundations can exert a pressure of about 47.9 kPa on the soil, it is recommended that this value be used for a surcharge load (Chen, 1988).

2.3 Measurement of swell parameters by oedometer tests

The one-dimensional consolidation apparatus (i.e., oedometer) has become widely used for testing swelling soils. (Holtz and Gibbs, 1956; Jennings and Knight 1957 and Lambe and Whitman, 1969) were among the first to report the use of oedometer tests for predicting heave in swelling soils. The most commonly used testing procedures for determining the swelling parameters are as follows:-

2.3.1 Free swell oedometer test method

In the free swell oedometer test, the soil specimen is allowed to absorb water under a load of 7kPa and is put aside to fully expand and reach equilibrium. Then the soil is gradually consolidated back to its original volume in the conventional manner. The swelling pressure is defined as the stress necessary to consolidate the specimen back to its original volume (Hardy, 1965; Sridharan, Rao and Sivapullaiah, 1986).

A modified form of the free swell method is described in ASTM D4546. This method was first proposed by Jennings, 1973 as the simple oedometer test. In this testing procedure, the specimen is first loaded to the in-situ vertical overburden pressure and then unloaded to the seating load and inundated. When swelling has ceased, the specimen is gradually consolidated back to its original volume in the conventional manner. The stress necessary to consolidate the specimen back to the void ratio corresponding to the situation before inundation is defined as the swelling pressure. This modification provides a correction to the initial reading at the seating load in an effort to more closely duplicate the in-situ void ratio of the swell.

Another modified form of the free swell method is described in ASTM D4546 as Method B. In this testing procedure, the specimen is subjected to a vertical pressure exceeding the seating load and then saturated. The magnitude of vertical pressure is usually equivalent to the in-situ vertical overburden pressure or structural loading, or both. After swell has occurred the specimen is loaded in increments until its initial void ratio or height is obtained. The load required to bring the specimen back to its original void ratio or height is termed the swelling pressure.

Alternative procedure similar to the free swell method is the swell-consolidation test procedure. This procedure is used extensively in the Rocky mountain regions in United States to determine the in-situ swell potential (Chen, 1978; Porter and Nelson, 1980; Kumar, 1984). In this case, the specimens are subjected to a vertical stress generally in the range from 25 kPa to 100 kPa. The applied stresses are dependent upon the anticipated field conditions. After about 24 hours, distilled water is added to the specimen. When the swelling has ceased, the applied load is increased in increments until the specimen has been compressed to its original height. The stress required to compress the specimen to its original height before inundation is termed the swelling pressure.

Shanker, Rao and Swamy, 1982 carried out swelling measurements on disturbed and remolded black cotton clays using a modified form of the free swell method. The specimens were allowed to swell freely under various surcharge loads and then consolidated the specimen to their original volume. The load required to bring the specimen back to its original volume is termed the swelling pressure. It was found that the magnitude of surcharge load does not have any effect on the magnitude of the measured swelling pressure. The similar observations were also reported by Chen, 1975. In this case the swelling pressure is defined as the stress required to compress the specimen back to its original height before inundation. These results contradict the assertions of Justo, 1984 who found that when the surcharge load becomes smaller than 5 kPa the predicted swelling pressure will increase.

There have been a number of controversies regarding the results of free swell oedometer tests. The most serious criticism of this method is that does not represent the normal sequence of loadings experienced by the soil in the field. The soil in the field will not absorb water and swell with the structural loads applied later. But rather vice versa (Brackley, 1975; Justo, 1984; Elsayed and Rabba, 1986).

2.3.2 Loaded swell oedometer test method

In the loaded swell oedometer test, a number of “identical” specimens are subjected to different initial applied loads and allowed to swell freely. The resulting final volume changes are then plotted against the corresponding applied load or stresses. The stress corresponding to zero volume change is termed the swelling pressure (Skempton, 1961; Gizienski and Lee, 1965; Nobel, 1966; Matyas, 1969).

Pidgeon, 1987 suggested that the linear relationship between the amount of swell and the logarithm of the applied stress could be accepted as a universal soil property. A number of research workers in various parts of the world have found above relationship to apply to test carried out on undisturbed or remolded specimens of both transported and residual soils. These soils contained both calcium and sodium montmorillonite clay minerals.

2.3.3 Constant volume oedometer test

In the constant volume test procedure, a specimen is allowed to absorb water without any increase in volume by increasing the applied pressure as the test proceeds until the sample reaches equilibrium. The applied load at this point is referred to as the "uncorrected" swelling pressure, Ps. The soil specimen is then further loaded and unloaded following the conventional oedometer test procedure.

Maintaining a constant volume may be achieved in different way such as by using a proving ring or a null-type measuring system. Several attempts have been made to measure swelling pressure using proving rings (Palit, 1953; Alpan, 1957; Finn and Storm, 1958; Seed, 1962; Sing 1967). The apparatus used by Palit, 1953 consisted of a cell 76.2 mm diameter and 101.6 mm height containing the soil specimen. Swelling of the soil was prevented using a piston and proving ring connected to the frame while the pressure was measured continuously. Seed, 1962 used a similar apparatus, except that a proving bar replaced the proving ring. Proving rings or bars have the advantage that required vertical load can be automatically applied to the specimen to maintain the specimen at a constant volume. However, the measurement of swelling pressure using a proving ring necessitates some deformation of the ring resulting in an equal amount of swelling in the soil which will cause the measured swelling pressure decrease. (Seed, Mitchell and Chan, 1962) have illustrated this effect by measuring the swelling pressure of identical specimens using proving rings of different stiffness. The swelling pressure measured using the stiffest measuring system yielded the highest swelling pressure. In order to more accurately measure swelling pressure by the constant volume procedure, attempts have been made to increase the stiffness of the measuring device (Seed, 1962; Kassif, 1965). However, even with the use of extremely stiff proving rings or load cell, some swelling of the soil specimen would still occur due to the compression of the apparatus. In addition, the accuracy of the measurement of small loads may be lost if extremely stiff load measuring device are used. This leads to the null-type measuring system wherein a very small (measurable) volume change is allowed and is then balanced by adjusting the applied load on the specimen. Therefore, a constant volume is maintained until there is no further tendency for swelling (Holtz and Gibbs, 1956; Salas and Serratosa, 1957; Iyer, 1972; Agarwal and Sharma, 1973; Shanker, Rao and Swamy, 1982; Sridharan , Rao and Sivapullaiah, 1986). The null-type measuring system has the advantage that the effects of the compressibility of the oedometer apparatus can be compensated during the test.

The constant volume method has been recommended by many research workers (Frydman and Calabresi, 1987 and ASTM D4546) due to the advantage that it doesn’t involve volume change and does not incorporate hysteresis into the estimation of the in-situ stress state (i.e., swelling pressure). However, the constant volume method suffers from a serious limitation that the sampling disturbance has not been taken into account. The vertical pressure corresponding to the end of wetting at constant volume is used by many engineers as the swelling pressure (Justo, Delgado and Ruiz, 1984; Sridharan, Rao and Sivapullaiah, 1986; Chen, 1988). In order to eliminate this limitation, swelling pressure could be determined using a similar construction procedure as that proposed by Casagrande for the determination of pre-consolidation pressure to compensate for the effect of sampling disturbance was proposed by Fredlund et al. ,1980. It has been adopted by the ASTM standards. The void ratio, e, versus log pressure curve obtained is used to find a corrected swelling pressure by using the modified Casagrade type of geometrical construction as shown in Fig. 2.8.

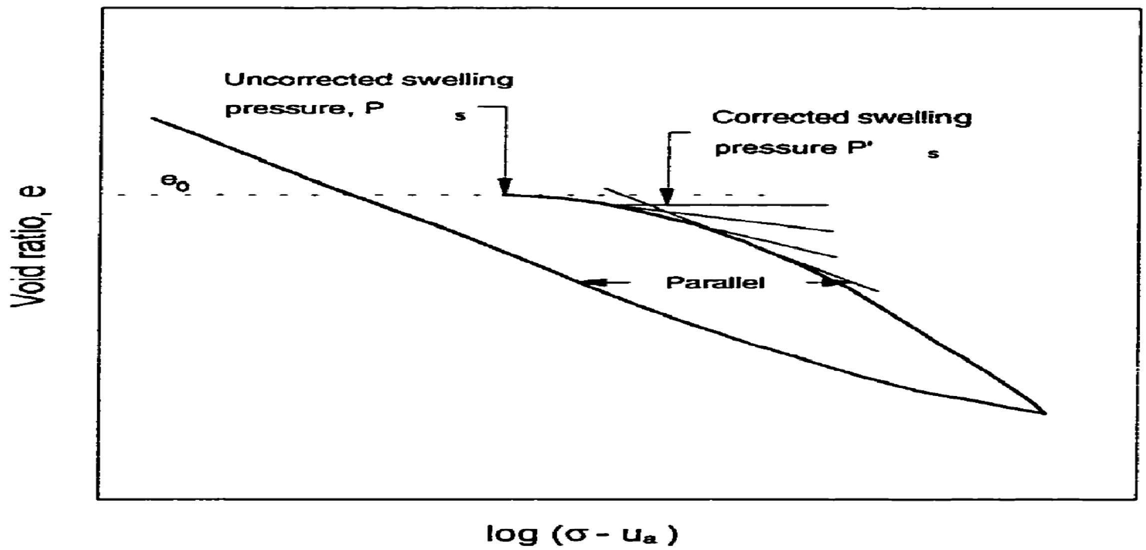

Figure 2.8 Construction procedures to correct for the effect of sampling disturbance (Fredulund, 1980)

2.3.4 Double oedometer test method

The double oedometer test procedure was first described by Jennings and Knight, 1957, primarily for use in the study of collapsing soils. It has now become widely accepted for testing swelling soil and has been modified over the years.

This method is based on subjecting two identical samples to consolidation test. The first sample is consolidated at its natural moisture content while the second sample is first allowed to absorb water and swell under light load followed by consolidation. The data from both tests can be plotted on a conventional, two-dimensional void ratio versus log applied pressure plot. Many double oedometer tests show a cross-over of the two curves at high pressures. The applied pressure at this cross-over point is referred to as the swelling pressure. This method usually results in higher swelling pressure measurements than from the free swell method. The higher swelling pressure occurs because the swelling pressure is not that magnitude required to bring the specimen to its initial volume. Rather, the swelling pressure corresponds to the volume of the specimen after it has been compressed at the natural water content by a pressure equal to the swelling pressure. Justo, 1984 found that when the initial degree of saturation of the specimen is high, the two curves of the double oedometer test become asymptotic or overlap at high pressures. On the other hand, when the specimen is dry, the two curves cross-over at the swelling pressure. For this reason, Justo, 1984 suggested that the adjustment of the test results indicated by Jennings, 1973 might be correct for wet clays, but not for dry soils.

The double oedometer method has the same limitations as the free swell method. Wetson, 1980 indicate that the double oedometer method gives a swell prediction about one and one half to two times the swell which occurs under field stress conditions. Jennings, 1973 suggested that the method could over-estimate in-situ heave for very dry soil and sandy clay and suggested that it is better to use the simple oedometer test under those conditions.

2.3.5 Direct model method

The direct model method was first described in the Texas highway department manual of testing procedures and primarily used for estimating heave in undisturbed soils. The direct model method is essentially a series of loaded swell oedometer tests. The specimens are subjected to their field overburden pressure (or the load that will exist at the end of construction) and then saturated. The resulting final volume changes are plotted versus the applied loads and the applied load corresponding to zero volume change is called the swelling pressure.

The swelling pressure and heave predicted is generally significantly below the actual swelling pressure and heave experienced in the field. Jennings, 1969 used the method to back-analyze a known and recorded heave on an existing building and that the resulting prediction was only about 50% of the observed heave.

2.3.6 Comparisons of test methods

In order to compare the swelling pressure value obtained from different methods, a testing program was conducted by Ali and Elturabi, 1984. In this program, both undisturbed and compacted specimens were used. Identical specimens were subjected to the two testing procedures; namely the free swell oedometer tests and the constant volume oedometer tests. The results obtained indicated that the free swell method usually gave higher swelling pressure values than those obtained from the constant volume method.

The fact that difference values of the swelling pressure are obtained when using different testing methods was also observed by Sayed and Rabbaaa, 1986. Test results are presented in Table 2.1

Table 2.1 Comparative values of swelling pressures using various testing methods but "identical" specimens (Sayed and Rabbaa, 1975)

Method	Swelling Pressure (kPa)
Free swell	2,200
Constant volume	1,900
Loaded swell	1,800
Double oedometer	3400

The discrepancies in the swelling potential (vertical swell and swelling pressure) are due to differences in loading and wetting conditions in the oedometer tests. The free swell test does not represent the normal sequence of load wetting in the field. The soil in the field will not absorb water and swell first with the structural load applied later, but rather vice versa.

The constant volume method also does not simulate the *in situ* condition, where the applied load after the structure is in service does not change with time. In addition, it does not present the expected amount of heave under the application of a certain load (structure load).

The swell overburden method has the important advantage of being more representative of actual field loading and wetting conditions (El Sayed and Rabbaa, 1986). The data obtained by this method can provide useful information for design, such as swelling pressure corresponding to zero volume change, the expected vertical heave under the loads imposed by the structure, and the loads that could be applied to develop a certain swelling within tolerable limits.

Sorochan, 1991 suggested that the swelling pressure should be determined using the loaded swell method since this method most closely reflects the process undergone by the soil in the field.

2.4 Prediction of swelling using a hyperbolic equation

In tropical countries, where there is a large seasonal variation in moisture and rainfall, light residential or commercial buildings founded on expansive soils are generally subjected to undesirable cracking and differential movements. Therefore it becomes necessary for soil engineers in their day-to-day practice to predict the total probable heave under given loading conditions of buildings founded on these soils.

Despite the complexity of the behavior of expansive soil, several attempts have been made in the past to characterize swelling, swelling pressure-time relationships of expansive clays. Several methods are presently available to predict the swelling of expansive soil. These methods have had only a limited success since the influence of various factors on swelling behavior is extremely complex and the swelling problem can only be solved by an approach based on the observed properties of swelling soils.

2.4.1 Review of swelling-time relationships

Seed et al, 1961 reported that considerable time is required for complete swelling to take place. Blight, 1965; Tsytovich and Zaratsky, 1967; and Myslivec, 1969 have presented various swelling-time relationships. Thurairajah, 1970 has obtained a linear relationship for the variation of swelling with square root of time. Komorink & Zeitlen, 1970 have noted that the vertical movement follows a time function similar to that of consolidation. Srinivasan, 1970 has reported that the time required for the water to enter into a swelling clay system is a function of the permeability of soil, hydraulic gradient, soil structure, etc.

An attempt was made by V.Dakshanamurthy, 1978 to represent the swelling-time relationship by a hyperbolic equation.

Konder, 1963 showed that the non-linear stress-strain curves of soils may be approximated by hyperbola to a high degree of accuracy. The hyperbolic equation proposed by Konder is

$$(\sigma_1 - \sigma_3) = \frac{\varepsilon}{a + b\varepsilon} \text{ -- } (2.1)$$

In which σ_1 and σ_3 are the major and minor principal stresses respectively, ε is the axial strain, and a and b are constants whose values can be determined experimentally. From the property of the rectangular hyperbola, a transformed plot of $\frac{\varepsilon}{\sigma_1 - \sigma_3}$ versus ε is a straight line .The equation of the transformed plot is given by:

$$\frac{\varepsilon}{\sigma_1 - \sigma_3} = a + b\varepsilon \text{ -- } (2.2)$$

In most of the swelling tests, it appears that plots of swelling versus time can be represented by hyperbola having equations of the form given below:

$$S = \frac{T}{\alpha + \beta T} \text{ -- } (2.3)$$

Where, S=axial swelling

T=time

α and β are appropriate constants.

The validity of these relationships can be demonstrated if a transformed plots of $\frac{T}{S}$ versus T results in a straight line. The maximum value of swelling can be predicted by taking the limit of Eq. 2.3:

$$\text{Limit of S as } T \rightarrow \infty \left(\frac{1}{\frac{\alpha}{T} + \beta} \right) = \frac{1}{\beta} \text{ ……………………..………………… } (2.4)$$

Thus the inverse of the slope of the transformed plot gives the maximum swelling.

V.Dakshanamurthy, 1978 has carried out a comprehensive experimental program on two soils viz.; (1) pure sodium montmorillonite obtained commercially and (2), a local expansive soil. Based on the analysis of the tested data V.Dakshanamurthy, 1978 arrived at the following conclusions

(1) The swelling-time relationship for expansive clay can be represented by a hyperbolic equation.
(2) The maximum swelling which will take place at infinite time is equal to the inverse of the slope β.

2.5 proposed Model

2.5.1 General

A versatile model presented by Richard and Abbott, 1975 has been used to represent the stress-strain spectrum of different types of concrete as well as triaxially confined soils. This model was used by Almusallam and Alsayed, 1995 to capture the complete stress-strain curves (hardening and softening parts) for normal, high strength and light weight concrete tested under various loading conditions. Few basic and practical soil constitutive models were discussed and summarized by Lade P.V., 2005. According to Lade P.V., 2005 some empirical models need to have two different formulas to generate the complete stress-strain curve and other models could not take into account the influences of different factors influencing the stress-strain curves. Also, it was found that some models require complicated computations to evaluate their parameters.

However, the model presented by Almusallam and Alsayed, 1995 was found to have the ability to consider the influence of different parameters affecting the stress strain curve characteristics with only single parameter, which is the ultimate compressive strength of the concrete, needed to run the model. The other parameters of the model are determined using the best fitting curve technique as a function of the compressive strength of the concrete. The model was presented by Almusallam and Alsayed, 1995 and found to provide good predictions of the experimental results for hardening and softening parts.

Alshenawy, 2002 extended the application of the above model to predict the complete differential cavity pressure-cavity volume change curve of an expansion of a thick-walled hollow cylinder test for both coarse and fine Ottawa sands. Based on the experimental result, the confining pressure was chosen to be the input parameter to run the model. The other parameters were expressed as a function of the confining pressure and determined using the best-fitting curve technique. The computational results of the model were then compared with the experimental results and showed good agreements for both coarse and fine sands at all levels of confining pressures. The model was found to be able to predict the complete differential cavity pressure-cavity volume change curve at any value of confining pressure other than used in the tests.

Al-Karni, 2006 extended the application of the model to predict the stress-strain curve of consolidated drained triaxial test on granular soil. The main parameters involved are the confining pressure, the angle of friction, and the relative density. The other parameters were evaluated as a function of these parameters using best-fitting curve technique. The results of the model was compared with the experimental results and found to be in a good agreement.

Recently Abdullah I. Al-Mhaidib, 2008 used this mathematical model to predict the swelling behavior of an expansive soil from Saudi Arabia.

2.5.2 Mathematical form of the model

The formula was first proposed by Richard and Abbot, 1975; a general stress-strain equation applicable to normal weight concrete as well as triaxially confined soils The same formula was later successfully utilized by Almusallam and Alsayed, 1995 to model the stress-strain response of normal and light weight concrete, as well as high-strength concrete (Michel S. Samann, 1997).

The four parameter formula is given as follows

$$fc = \frac{(E1 - E2) \in c}{\left[1 + \left(\frac{(E1 - E2) \in c}{fo}\right)^n\right]^{\frac{1}{n}}} + E2 \in c \qquad \text{.. (2.5)}$$

Where E_1 and E_2 are the first and second slopes of the stress-strain response, respectively, ϵ_c and f_c are the concrete strain and stress, respectively, f_o is the reference stress at the intercept of the second slope with the stress axis, and n is a curve-shape parameter which controls the curvature in the transition zone.

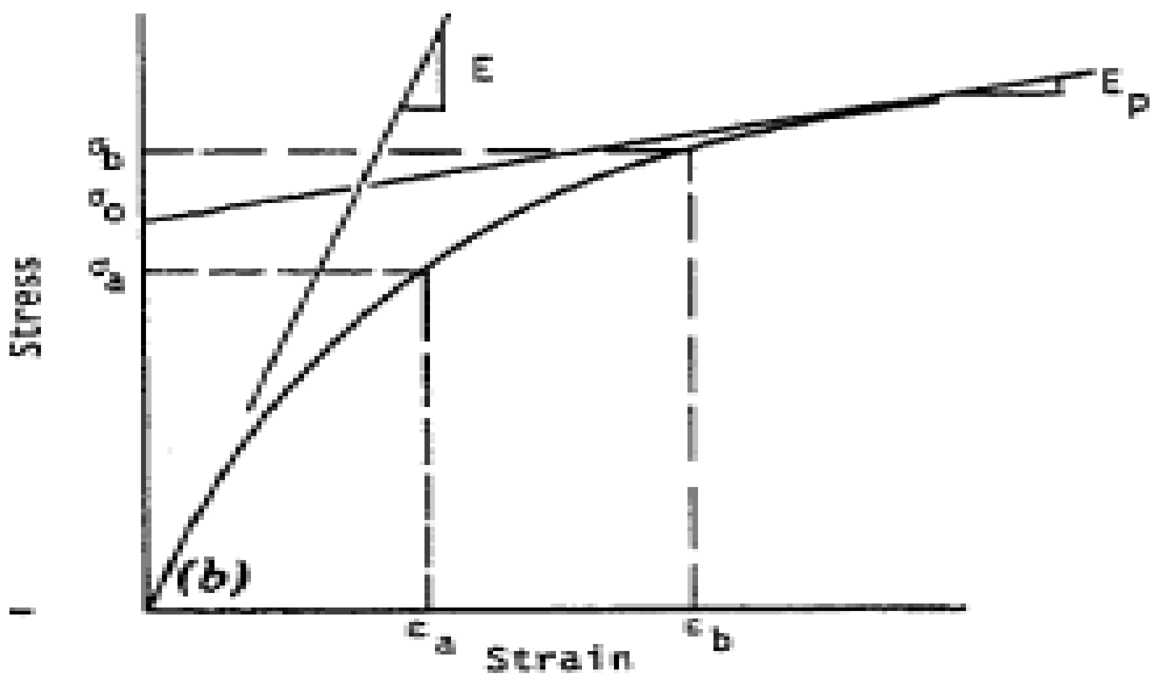

Figure 2.9 by equation 2.5

Ralph M. Richard and Barry J. Abbott,1975 concluded that the proposed equation provides a simple and useful means of describing material stress-strain behavior accurately beyond the proportional limit there by the completing the Ramberg-Osgood expression.

Moreover, it is noted that the proposed equation with n=1 corresponds to the equation presented by Duncan, J.M. and Chang, C.-Y., 1970, which is widely used to describe non linear soil behavior.

2.5.3 Proposed model to predict swelling behavior

The mathematical form of the model presented by Richard and Abbott, 1975 shown in Eqn. 2.5 may be rewritten to relate the percentage of swell (*S*) of expansive soil to time (*T*) as follows:

$$S = \frac{(k-kp)T}{\left[1+\left(\frac{(k-kp)T}{So}\right)^{n}\right]^{\frac{1}{n}}} + kpT \text{ ---------- } (2.6)$$

Where *S* is the percentage of swell that corresponds to time *T*, *k* is the initial slope of the curve; *kp* is the final slope of curve, *So* is a reference swell and *n* is a curve-shape parameter.

The value of *n* can be expressed as follows:

$$n = \frac{\ln m}{\ln\left[\frac{S1}{S0} - \frac{kp}{k-kp}\right]} \text{ ---------- } (2.7)$$

Where *m* is a constant and *S1* can be calculated from:

$$S1 = Sp\left[2\frac{T1}{Tp} - \left[\frac{T1}{Tp}\right]^{2}\right] \text{ ---------- } (2.8)$$

Where *Sp* is the peak swell, *Tp* is the corresponding time and *T*1 can be obtained from:

$$T1 = \frac{So}{k-kp} \text{ ---------- } (2.9)$$

Chapter three
Description of the study area

3.1 Location, topography and population size

Addis Ababa, the capital of Ethiopia, is located in the central highlands of Ethiopia. With an elevation ranging from 2000-2800masl, being the highest capital in Africa. Its topography is constituted by hills, rivers and streams.

City Government of Addis Ababa bounded by 9° 00'N and 10° 00'N Latitudes, 37° 30'E and 39° 00'E Longitudes. It is the seat of International Organization (UNDP, UNICEF, ECA, AU, etc.), high level of governmental and Non-governmental organizations.

The city is expanding from time to time horizontally in the expansion areas in the east, south, west, and in limited extent in the north. The population of the city have been grown from 443,728 in 1961 to 1,167,315 in 1978 and 2,112,737 in 1994 (CSA, 1999). The Authority publishes regular abstracts, the latest one in January 2003 containing estimates of population of the city are more than 2.3 million.

3.2 Climate

The Climate of Addis Ababa is Woina Dega type (Daniel Gemechu, 1974).The Rainfall has unimodal pattern, one distinct rainy and dry season. The dry season is October through May and the wet one is from June to September being the highest rainfall peak in August. The long-term mean annual rainfall observed at Addis Ababa Observatory is 1254mm (Berhanu, 2002).

The maximum temperature of Addis Ababa ranges between 20^0c (in wet season) to 25^0c (in dry season), while the minimum falls between 7 - 12^0c in the year. This indicates that daily variation of temperature is highly pronounced.

Wind speed is generally moderate, ranging between 0.5 to 0.9 m/s. The average daily sunshine hours are 9.5 hours in November & December, and far low, 3 hours, in July and August. Pan-evaporation records at Addis Ababa Observatory showed that the average monthly pan-evaporation during dry season (November) is about 180mm and in wet season (July) falls to 75mm.

3.3 Geology and geo-structures

Addis Ababa generally lies in the western margin of the Ethiopian rift and consists of different volcanic rocks that range from basic to acidic composition, belonging to the trap series (Tamiru et.al. 2003).

The north and north eastern area (the Entoto Mountain, the northern and north eastern Addis Ababa) is covered with trachytes, rhyolites, basalts and several episodes of pyroclastic materials of older volcanism occur on the upper part and foothill sides of Entoto ridge. Overlying these, younger basaltic rocks (Addis Ababa Basalt) are found covering the central and southern part of the city.

Outcrops of ignimbrites north of Bole area (Eastern Addis) and Lideta area (Central Addis) have been observed underlying the Addis Ababa basalt. Younger volcanic of trachy-basalt, trachytes, ignimbrites and tuff belonging to the Wochecha, Furi and Yerer volcanoes are recognized overlying un-conformably on the Addis Ababa basalt in the western, south-western and eastern part. Akaki, Dukem and Debrezeit area are covered with olivine basalt, scoria, scoriaceous basalts and vesicular basalts (Tamiru et.al. 2003).

In the upper part, in some places, intercalation of tuffs, sand and gravels are also recognized. In north-east, east and in smaller extent in the western part of Debre Zeit, outcrops of trachytes, rhyolitic ignimbrites and tuffs are recognized covering the area.

The lacustrine covers Bole, Lideta, Mekanisa, Akaki-Aba Samuel area and Dukem-Debre Zeit area. Some alluvial deposit also occur along Big & small Akaki rivers in the southern and south-western part of Addis and minor deposit also occur along Kebena river in the area north-west of Bole.

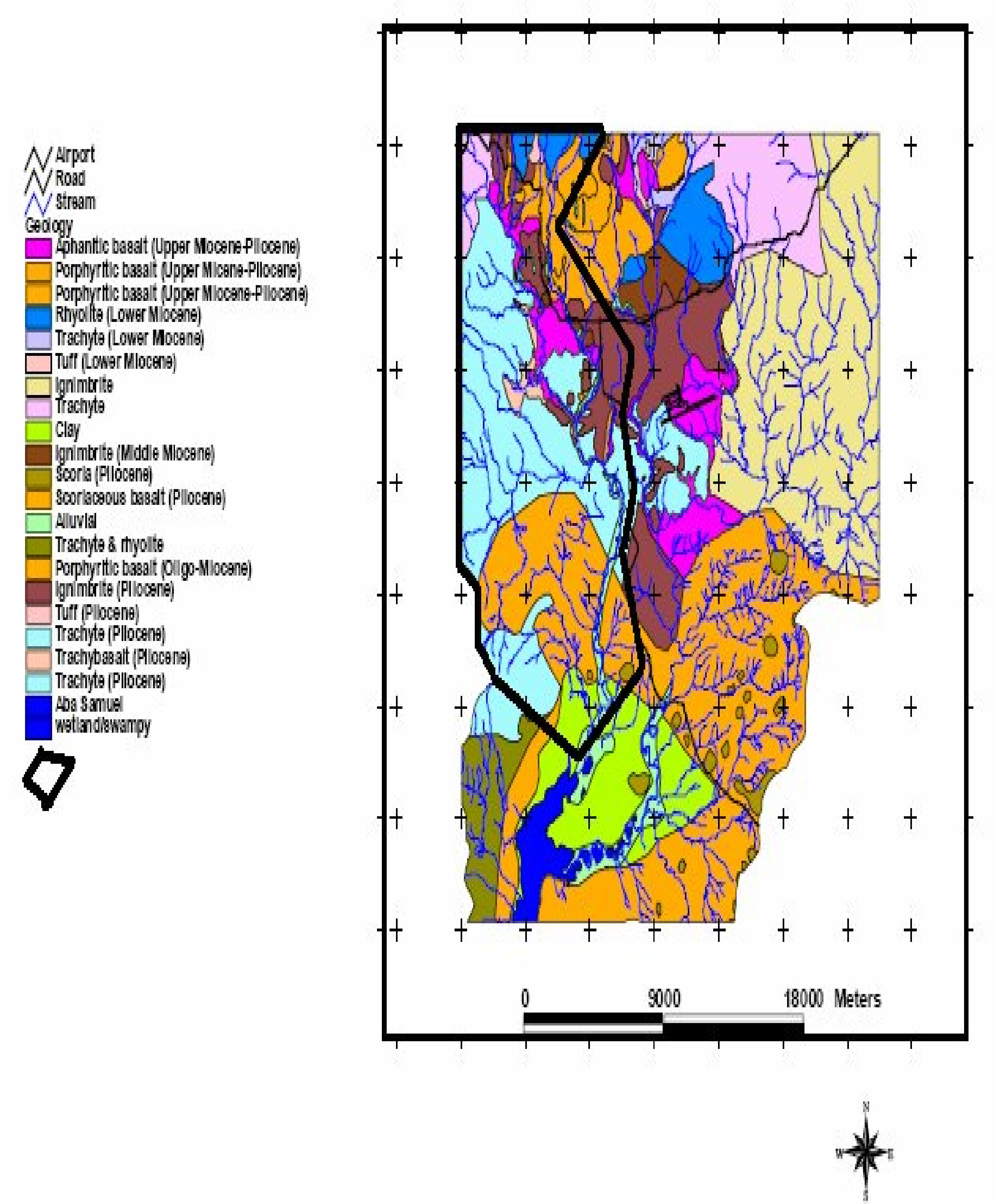

Figure 3.1The geologic map of Addis Ababa (modified after Tamiru et.al. 2003)

Chapter four
Experimental study

4.1 Material

The data collection stage involved gathering of relevant information from literature followed by field work soil sampling. Sampling sites were selected within the city of Addis Ababa based on information from previous studies and they revealed that expansive soil samples collected from different parts of Addis Ababa fall in under one group which is inorganic clays of high plasticity (Teferra and Yohannes, 1986 and Yeheyis 2001). Within the selected areas random sampling strategy was employed. Three representative soil samples one from Akaki-Kality sub city and the others two from Bole sub city are used in this study.

The average geotechnical properties of investigated soils are shown in Table 4.1. Liquid limit, plastic limit, specific gravity, and particle size all were determined in accordance with ASTM test procedures. According to the unified classification system, theses soils are classified as inorganic clay of high plasticity (CH).

Table 4.1 Average geotechnical properties of the tested soils

Parameter	Kality	Bole H. S.	C. Bole A.
Depth, m	2.3	2	1.9
Sand content (grain size 2 to 75μm), %	6.10	3.8	2.8
Silt content (grain size 75μm to 2μm), %	17.41	17.56	15.4
Clay content (grain size <2μm)	76.49	78.64	81.8
Liquid limit, LL, %	103	107	112.4
Plastic limit, PL, %	36	38	40
Plasticity index, PI, %	67	69	72.4
Specific gravity of solids,	2.73	2.76	2.8

4.2 Sample preparation

To ensure uniformity of testing, block samples were dried, pulverized into a powder in batches and screened through sieve No. 40. The batches were thoroughly mixed to obtain a uniform bulk sample. Individual samples were oven-dried for about 24 hours and then thoroughly mixed to the chosen molding moisture content. They were then stored in air-tight plastic bags and sealed in plastic wraps to avoid loss in moisture content, and were allowed to cure at room temperature for 24 hours to achieve uniform distribution of moisture content.

A prescribed weight of the wet soil, producing a required dry unit weight, was pressed into a mold and then dynamically compacted using small hand held tamper. Immediately after preparation, the 50 mm-diameter and 20 mm-thick oedometer samples were transferred to the oedometer and the swell tests were performed.

4.3 Swell Test

The direct measurement of volume change that occurs when a soil undergoes heave is usually obtained by the use of the conventional one dimensional oedometer. The oedometer testing technique is the oldest and the most commonly used method for testing expansive soils (Justo, 1979). The amount of swell measured in an oedometer test is dependent on test procedure (i.e. stress path and soaking conditions).

The American society for testing and materials (ASTM) standardized the swell oedometer test procedures under the designation No. D4546. This standard describes three alternate oedometer testing procedures. Free swell, constant volume swell, and swell overburden tests to evaluate the amount of volume change. The swell overburden method has the important advantage of being more representative of actual field loading and wetting conditions. It was therefore chosen and the tests were conducted according to ASTMD4546. The sample was put into the oedometer and subjected to seating pressure 7 kPa for a period of 5 minutes. Then, deformation dial gauge was adjusted for the initial zero reading, and after 5 minutes the specified vertical pressure was applied. Water was introduced to the specimen after 5 minutes of applying the vertical pressure. Thereafter, the expansion of the specimen was allowed until the rate of expansion reaches a negligible value, at which the test was terminated.

4.4 Testing program

Using swell overburden method a total of 24 tests were carried out by varying the initial dry density and the applied vertical pressure. Table 4.2 shows set numbers of each set performed in this study with respect to their initial water content, initial dry density and applied load.

Table 4.2 Set numbers

No.	Soil from Kality	No.	Soil from Bole H. School	No.	Soil from near to Bole Airport	No.	Soil from near to Bole Airport.
	Combinations		Combinations		Combinations		Combinations
1	MDD=1.3 g/cm^3, OMC=29 % and P=25 kPa	7	MDD=1.28 g/cm^3, OMC=39 % and P=25 kPa	13	MDD=1.3 g/cm^3, OMC=29 % and P=25 kPa	19	MDD=1.28 g/cm^3, OMC=39 % and P=25 kPa
2	MDD=1.3 g/cm^3, OMC=29 % and P=50 kPa	8	MDD=1.28 g/cm^3, OMC=39 % and P=50 kPa	14	MDD=1.3 g/cm^3, OMC=29 % and P=50 kPa	20	MDD=1.28 g/cm^3, OMC=39 % and P=50 kPa
3	MDD=1.3 g/cm^3, OMC=29 % and P=100 kPa	9	MDD=1.28 g/cm^3, OMC=39 % and P=100 kPa	15	MDD=1.3 g/cm^3, OMC=29 % and P=100 kPa	21	MDD=1.28 g/cm^3, OMC=39 % and P=100 kPa
4	MDD=1.3 g/cm^3, OMC=29 % and P=7 kPa	10	MDD=1.28 g/cm^3, OMC=39 % and P=7 kPa	16	MDD=1.3 g/cm^3, OMC=29 % and P=7 kPa	22	MDD=1.28 g/cm^3, OMC=39 % and P=7 kPa
5	DD=1.25 g/cm^3, OMC=29 % and P=7 kPa	11	DD=1.25 g/cm^3, OMC=39 % and P=7 kPa	17	DD=1.25 g/cm^3, OMC=29 % and P=7 kPa	23	DD=1.25 g/cm^3, OMC=39 % and P=7 kPa
6	DD=1.2 g/cm^3, OMC=29 % and P=7 kPa	12	DD=1.2g/cm^3, OMC=39 % and P=7 kPa	18	DD=1.2 g/cm^3, OMC=29 % and P=7 kPa	24	DD=1.2 g/cm^3, OMC=39 % and P=7 kPa

4.5 Test results

The test results presented in the main body of the paper are only the typical ones which can show the swell time relationships. The results of all other samples are in Appendix A. The typical plots of percentage vertical swelling ($S = \frac{\Delta H}{H} * 100$) versus time (T in minutes) are presented in Fig. 4.1 and Fig. 4.2. An observation of these figures suggests that the shape of the curves has the form of hyperbolae, wherein the swelling reaches an asymptotic value at a time about 1400 minutes.

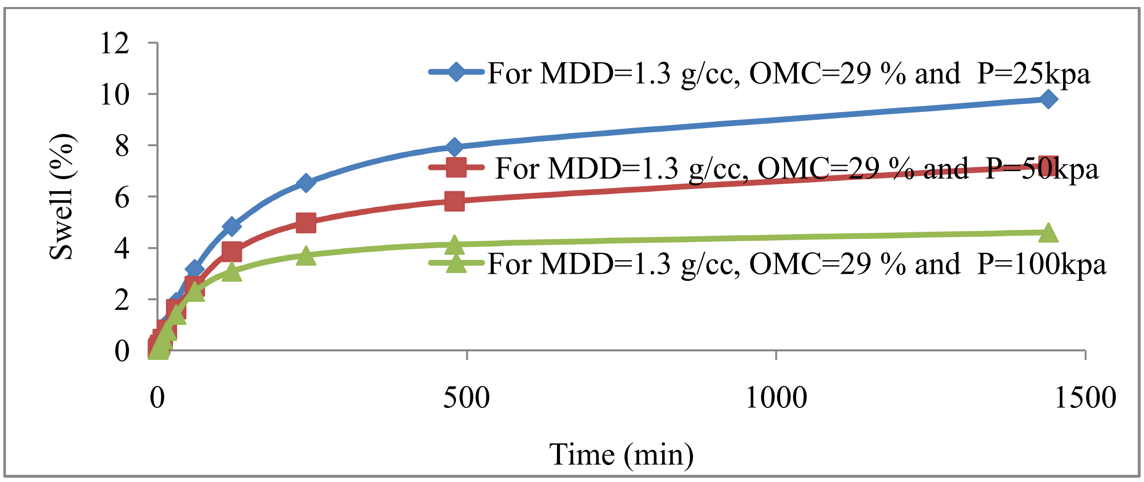

Figure 4.1 Vertical swell vs. time relationship for Kality soil (different applied pressure)

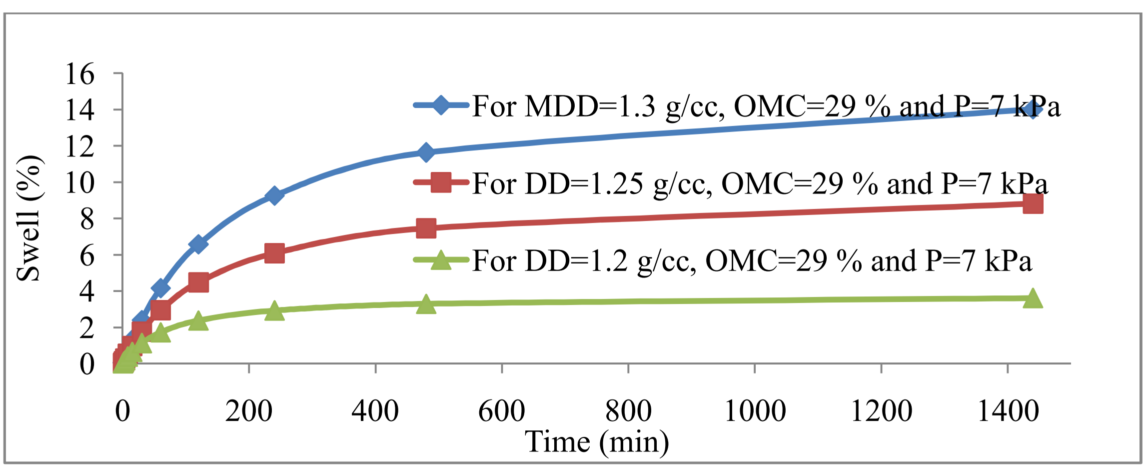

Figure 4.2 Vertical swell vs. time relationship for Kality soil (different dry density)

Plots of percentage vertical swelling, S versus time (T in minutes), have been transformed into plots of T/S versus T. Typical transformed plot is presented in Fig 4.3. It can be seen that these are essentially straight lines; which is the characteristic feature of the hyperbola and confirms the assumption made earlier in Chapter two.

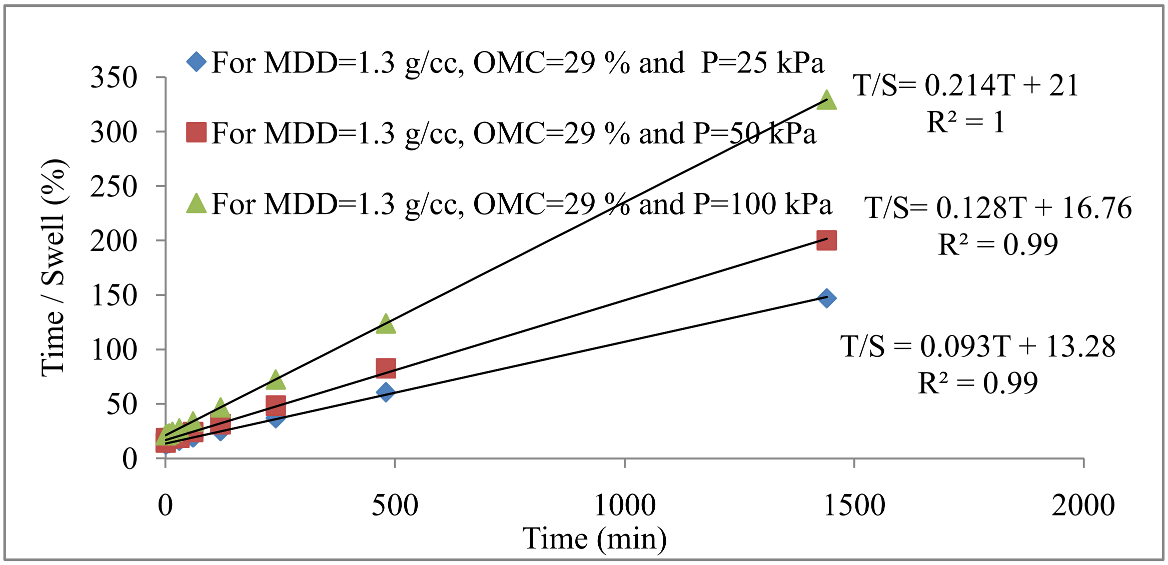

Figure 4.3 Determination of the coefficients rate of swelling for Kality soil.

The constants, *a* and *b*, can be obtained by means of linearzing the nonlinear curve. Typical plots of percentage vertical swelling, S versus time, *T* (Fig. 4.1), have been transformed into plots of *T/S* versus *T* (Fig. 4.3). The rate of swelling can be known by the value of the slope, *b*, which shows the flow of swelling path. Therefore, *b* is then defined as coefficient of the rate of swelling. The coefficients of the rate of swelling for each tested specimens, are presented in Table 4.3.

Table 4.3 Swelling properties of expansive soil

Test No.	Coefficient rate of swell, b	Maximum swell (%), 1/b	Measured swell (%)	Divergence (%)
1	0.093	10.75	9.8	9.69
2	0.128	7.81	7.2	8.47
3	0.214	4.67	4.61	1.30
4	0.064	15.63	14.02	11.48
5	0.104	9.61	8.82	8.96
6	0.264	3.79	3.61	4.99
7	0.578	1.73	1.69	2.37
8	0.749	1.34	1.29	3.88
9	1.219	0.82	0.802	2.24
10	0.371	2.69	2.61	3.07
11	0.417	2.39	2.31	3.46
12	0.512	1.95	1.89	3.17
13	0.11	9.09	8.03	13.21
14	0.181	5.52	5.06	9.19
15	0.274	3.65	3.60	1.39
16	0.068	14.71	12.41	18.50
17	0.113	8.85	7.9	12.02
18	0.434	2.30	2.235	3.09
19	0.758	1.32	1.3	1.48
20	1.178	0.85	0.84	1.06
21	1.433	0.70	0.60	16.7
22	0.432	2.31	2.245	3.11
23	0.553	1.81	1.765	2.45
24	0.655	1.53	1.49	2.46

Notes:-

$$\text{Divergence} = \left|\frac{\text{Maximum swell - Measured swell}}{\text{Measured swell}}\right| 100\%.$$

4.6 Discussion of test results

4.6. 1 Swell percentage

Typical results for vertical swell with elapsed time are shown in Fig.4.1 and Fig. 4.2. The percentage of vertical swell is defined as the ratio of the increase in height of the sample to its initial height before it was given free access to water.

From Fig. 4.2 it can be observed that vertical swell percentage also increases with increase in dry density for given initial moisture content and applied pressure. This is because the dense soil contains more clay particles in a unit volume and consequently grater movement will occur in a dense soil than in a loose soil upon wetting (Aboulied, 1982). During water absorption into the soil media water particles will apply more forces to the surrounding soil particles to achieve the complete saturation for higher initial dry density.

As expected, the increase in overburden pressure caused a reduction in the swell percentage (Fig. 4.1). Magnitude of surcharge load determines the amount of volume change that will occur for a given moisture content and density.

For full expansion time is necessary. As explained before the main reason of swelling behavior is water absorption of soil mass in time. And the soil suction governs the time needed for water to be absorbed to reach to the complete saturation. Seed, 1962 explained this behavior as; when compacted soil specimen is exposed to water, time is required for the movement of water into the specimen under the hydraulic gradient set up by the negative water pressure within the soil relative to free water i.e., the soil suction. The amount of swell that occurs within a given period of time depends on the quantity of water that enters the soil; thus, the rate of swell is proportional to the hydraulic gradient and the conductivity. These quantities, in turn, are influenced by the soil structure or by the treatment during compaction. As it can be seen from Fig 4.1 and Fig. 4.2 the time of inundation, there is a sharp increase in vertical swelling for the first 200 minutes.

Once water mobility was initiated, the high water adsorptive forces on clay particle surfaces were readily wetted thereby resulting in a high rate of primary swelling. The gradual reduction in the swelling rate during the primary and secondary stages and the eventual cessation of the vertical swelling pressure in the latter stage is attributed to increasing sample saturation due to water migration. The minor initial swell is attributed to swelling of the macrostructure, while the major primary swell and minor secondary swell is attributed to micro structural swelling (Rao *et al.*, 2006).

Dakshanamurthy, 1978 noted two stages of swelling. In the first stage, hydration of dry clay particles, water is adsorbed in successive monolayers on the surface of montmorillonite clay. This is referred to as interlayer or intercrystalline swelling. The second phase of swelling is due to double-layer repulsion. Large volume changes accompany this stage of swelling. Primary swelling developed when the void could no longer accommodate further clay particle swelling. It occurred at a faster rate. After primary swelling was completed, slow continuous swelling occurred.

The vertical swell-time curves of the tested samples could be represented by a hyperbola (Eq. 2.3) which is in agreement with the findings of Dakshanamurthy, 1978. The time/vertical swell versus time relationship could be represented by a straight line as shown in Fig. 4.3. The reciprocal of the slope of the straight line for each pressure and dry density gives the maximum swell.

The coefficients of the rate of swelling for each tested specimens is presented in Table 4.3 shows a good agreement between the maximum swelling predicted and the maximum swelling observed under different testing conditions. It is observed that the predicted values are in general higher than the observed values by about 6.16 % on the average. This is expected because the asymptotic values are always more than the experimental peak values.

4.6.2 Swell pressure

The relationships between the maximum swell percentage and the applied overburden pressure for samples under different testing conditions are shown in Fig. 4.4.

A straight line was obtained using the semi-log graph. The swell pressures were determined by extrapolating the linear relationship (i.e. at 0 % vertical swell). The values of swell pressure for all samples are shown in Table 4.4.

Table 4.4 Swell percentage under different overburden pressure

Test No.	Vertical swell (%) 25 (kPa)	Vertical swell (%) 50 (kPa)	Vertical swell (%) 100 (kPa)	Empirical equation from fig. 5.4	Swelling pressure (kPa)
1,2 and 3	9.8	7.2	4.61	S=-3.74ln (P)+21.84	343.6
7, 8 and 9	1.69	1.29	0.802	S=-0.64ln (P)+3.766	359.4
13, 14 and 15	8.03	5.06	3.6	S=-3.19ln (P)+18.06	287.6
19, 20 and 21	1.3	0.84	0.6	S=-0.5ln (P) +2. 88	322.5

Typical example for test No. 1, 2 and 3 has been carried out as follows.

S=-3.74ln (P) +21.84, setting S=0, (i.e. at 0 % vertical swell) and solving for P yields, P (Swelling pressure) =Exp (21.84/3.74)=343.6

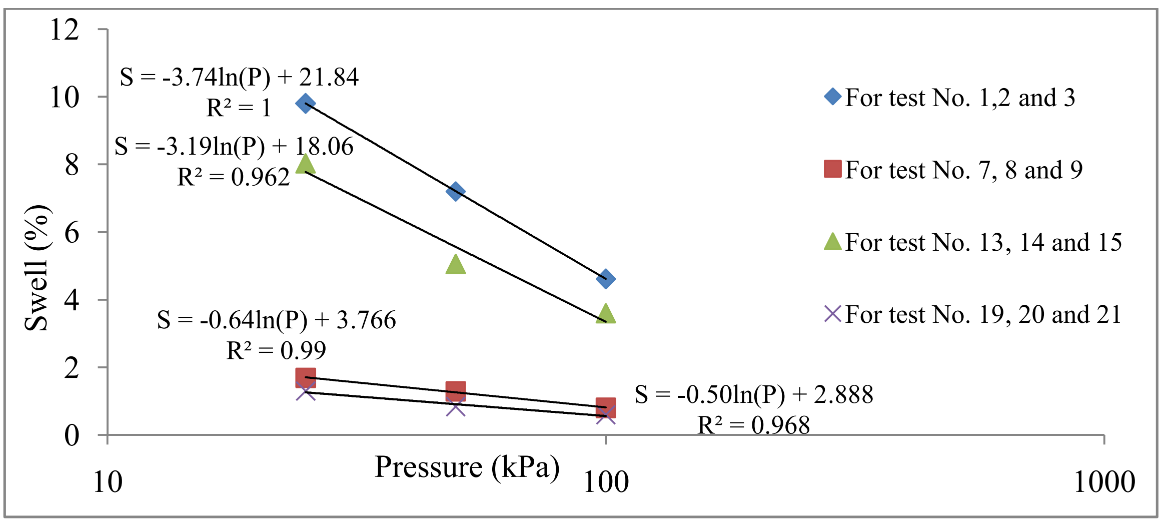

Figure 4.4 Relationship between swell percentage and overburden pressure

Chapter five
Evaluation of the proposed model

5.1 Evaluation of the model parameters

The parameters that needed to be determined in order to execute the model in Eqn. (2.6) are: the initial slope of the curve, K; the final slope of curve, Kp; the reference swell, So; and the peak swell, Sp. Using vertical swell vs. time plot one can determine the parameters of the model in this manner.

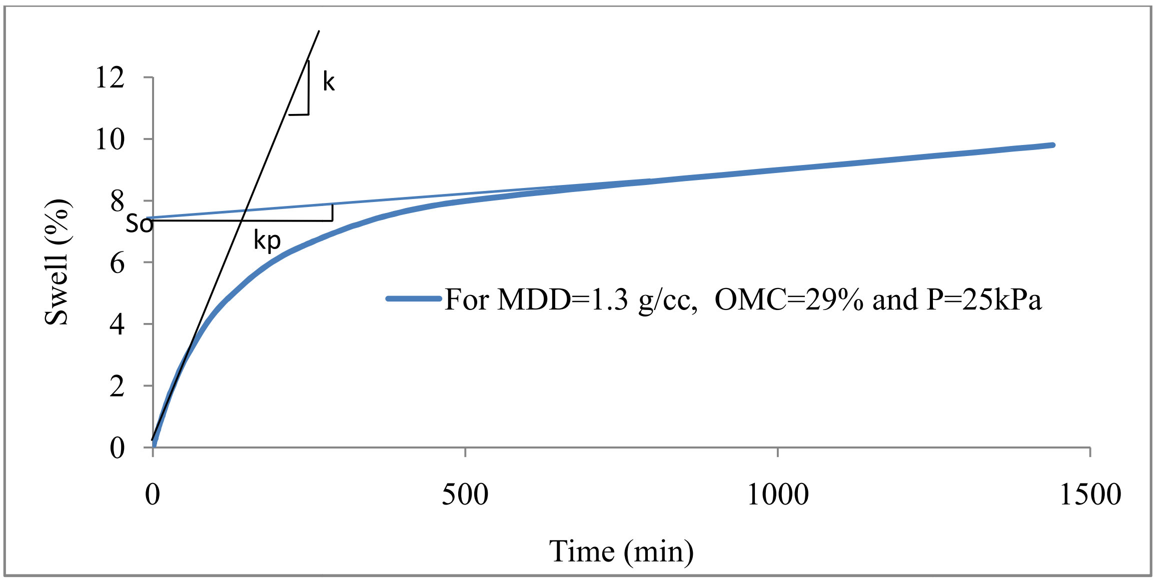

Figure 5.1 Illustration of Parameter determination for Kality soil

By way of the above geometrical construction the following parameters have been determined approximately. As it can be seen from Fig. 5.1:-

- Initial slope of the curve, k = (1.88-0.038)/(30-0.5)=0.0624
- Final slope of the curve, Kp= (9.8-8.0)/(1440-520)=0.00195
- The reference swell, So=7.38
- The peak swell, Sp= 9.8

Similar fashion were employed for all cases and attached to Appendix B.

Results of model parameters are presented in Table 5.1

Table 5.1 Variation of model parameters with applied pressure

Test pit No.	Test No.	P (kPa)	Kp	So	K	Sp
1(Kality)	1	25	0.00195	7.38	0.0624	9.8
	2	50	0.00144	5.5	0.0536	7.2
	3	100	0.00049	4.19	0.0460	4.61
2 (Bole H.S.)	7	25	6.25E-05	1.62	0.0403	1.69
	8	50	5.26E-05	1.18	0.0187	1.29
	9	100	3.96E-05	0.78	0.0107	0.8

The initial slope of the curve, K; the final slope of curve, Kp; the reference swell, So; and the peak swell, Sp could be expressed as functions of the applied pressure (P) by a linear equation. Fig. 5.2 illustrates the variation of *K* against the applied pressure. Other empirical relationships are attached in Appendix B.

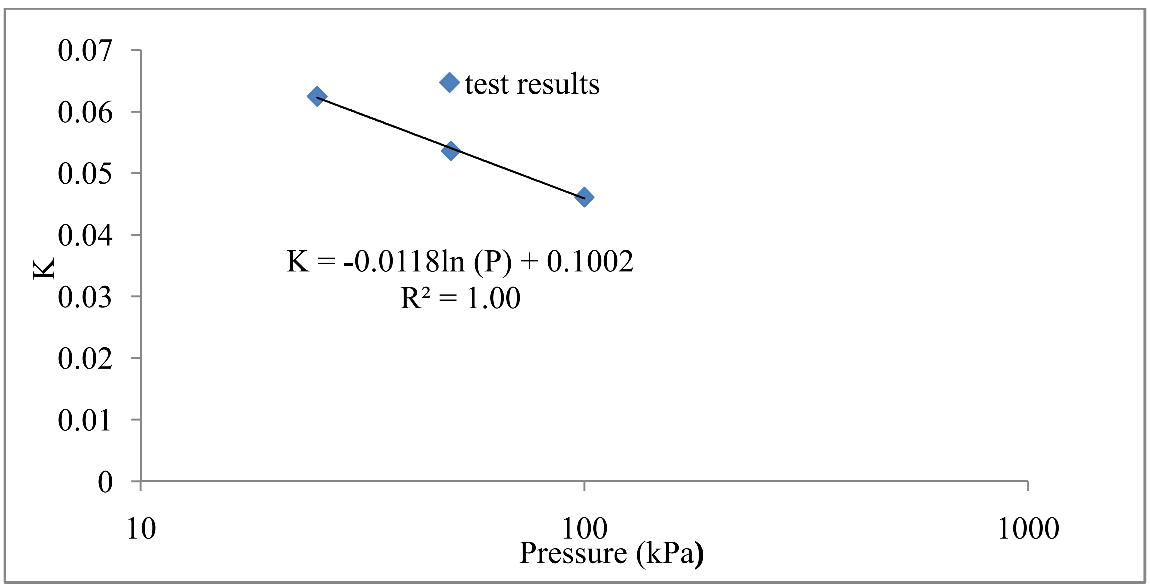

Figure 5.2 Variation of K with applied pressure for test pit No. 1

Model parameters were determined in similar approach as shown in section 5.1 and attached to Appendix B. Results of model parameters against initial dry density are presented in Table 5.2.

Table 5.2 Variation of model parameters with dry density

Test pit No.	Test No.	DD (g/cc)	Kp	So	K	Sp
1 (kality)	4	1.2	0.00032	3.27	0.037	3.61
	5	1.25	0.001406	7.02	0.058	8.81
	6	1.3	0.002468	10.63	0.079	14.01
2 (Bole H.S.)	10	1.2	1.15E-04	1.73	0.0265	1.89
	11	1.25	1.74E-04	2.1	0.0268	2.3
	12	1.28	2.27E-04	2.27	0.0269	2.6

The initial slope of the curve, K; the final slope of curve, Kp; the reference swell, So; and the peak swell, Sp could be expressed as functions of the initial dry density (DD) by a linear equation. Fig. 5.3 illustrates the variation of *K* against the initial dry density. Other empirical relationships are attached to appendix B.

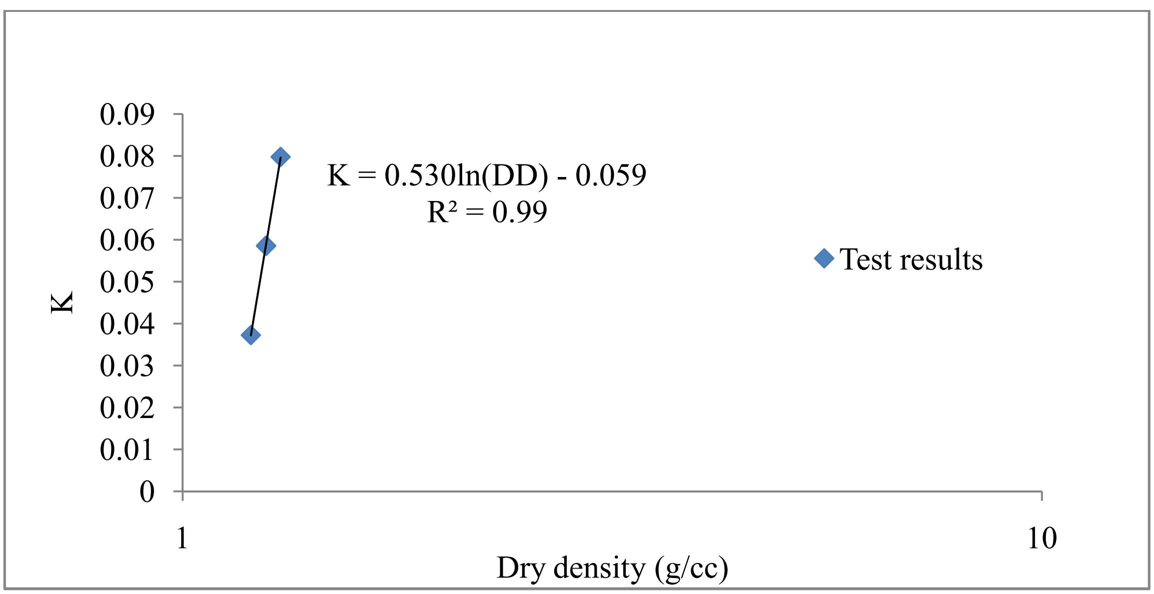

Figure 5.3 Variation of K with dry density for test pit No. 1

The parameter *m* will be evaluated after the calibration of the model and the parameter *n* can be calculated from Eq. 2.7.

5.2 Calibration of the proposed model

The model depends on the determination of the parameter m since the other parameters are evaluated directly from the tests results. This was carried out by testing the model for different values of *m* using the tests results. In this study m is determined by minimizing the error between the predicted results and experimental results. For soils brought from Kality and Bole H. S. area the best values that are applicable to all the applied pressure and dry density levels with marginal deviation were found to be when m=0.0689 and m=0.0162 respectively.

5.2.1. General procedures for the determination of soil constant parameter (m)

1) Employ spreadsheet application, assume any arbitrary value of m and use the value of m as an absolute reference
2) Compute the predicted percent swell using Eqn. 2.6
3) Find out the error, i.e. the difference between the predicted percent swell and the experimental percent swell
4) Square the error to get a positive error and find the total sum of square error
5) Go to tool menu and select solver to pop up solver parameters window
6) For set target cell , give the cell reference of the sum of square of errors
7) The minimization of the errors can be achieved by changing the assumed value of m.
8) Click solve button and repeat this until the same value of sum of square error is obtained.

5.3 Comparison with Test Results

Fig. 5.4 to Fig. 5.7 shows the experimental results of swell-time relationships as well as the curves generated by the proposed model. It can be seen from these figures that the curves generated by the proposed model are in good agreement with the experimental results. The computed data for the proposed model are attached to Appendix C.

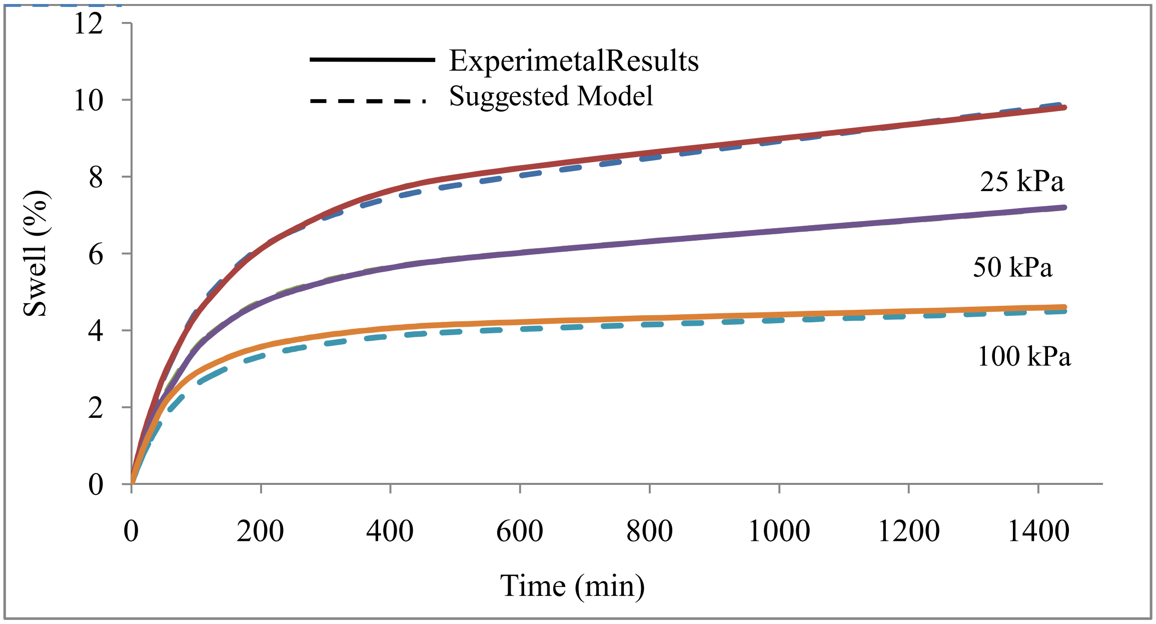

Figure 5.4 Swell vs. time relationship (MDD=1.3 g/cc and OMC=29 %), soil from Kality.

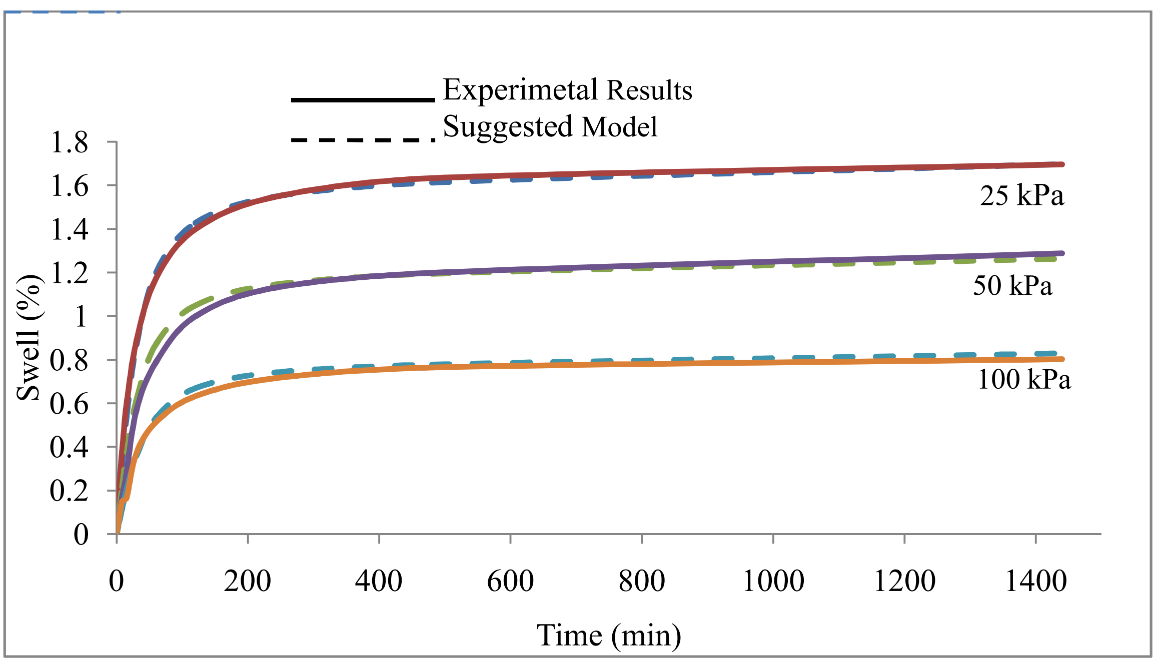

Figure 5.5 Swell vs. time relationship (MDD=1.28 g/cc and OMC=39 %), soil from Bole high school.

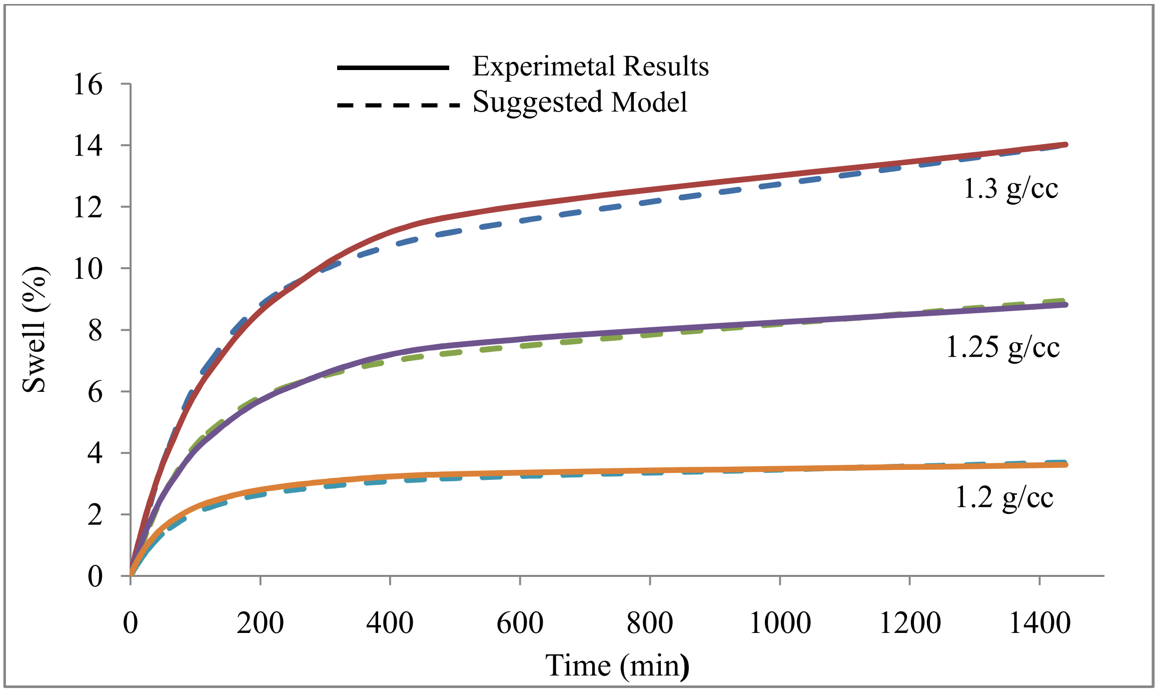

Figure 5.6 Swell vs. time relationship (P=7 kPa and OMC=29 %), soil from Kality.

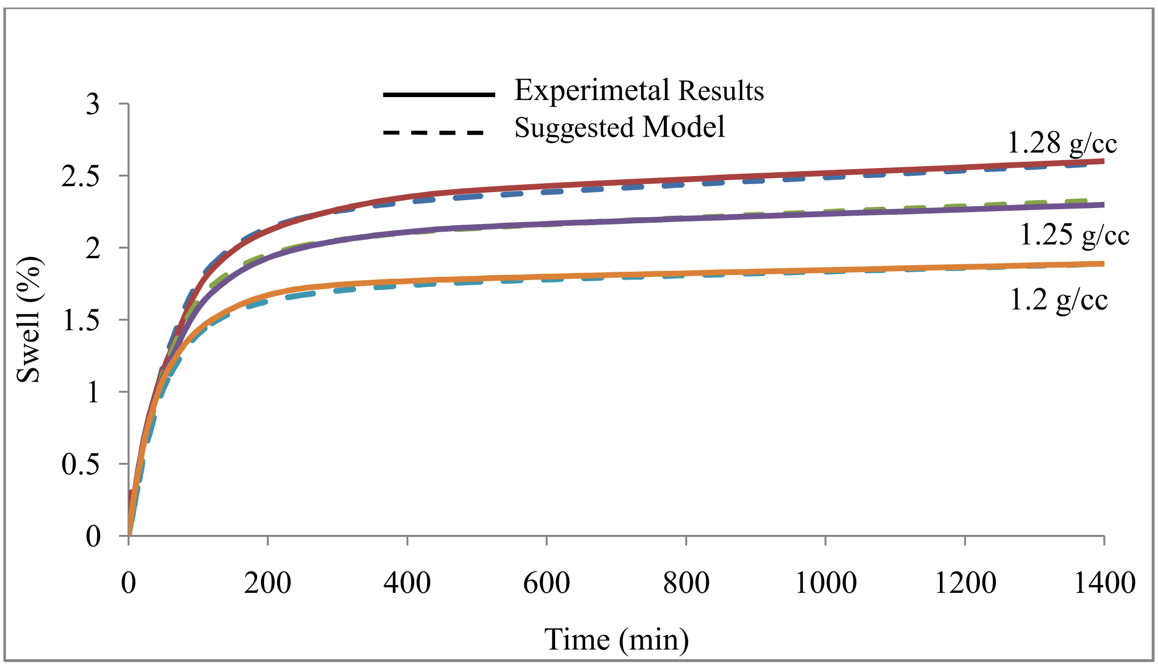

Figure 5.7 Swell vs. time relationship (P=7 kPa and OMC=39 %), soil from Bole high school.

Graphical assessments of calibration were prepared with experimental percent swell on the x-axis and the percent swell by Eqn. 2.6 on the y-axis. Fig 5.8 shows Measured vertical swell and predicted vertical swell were on the 45-degree line (i.e. Perfect prediction). All other figures are attached to appendix c.

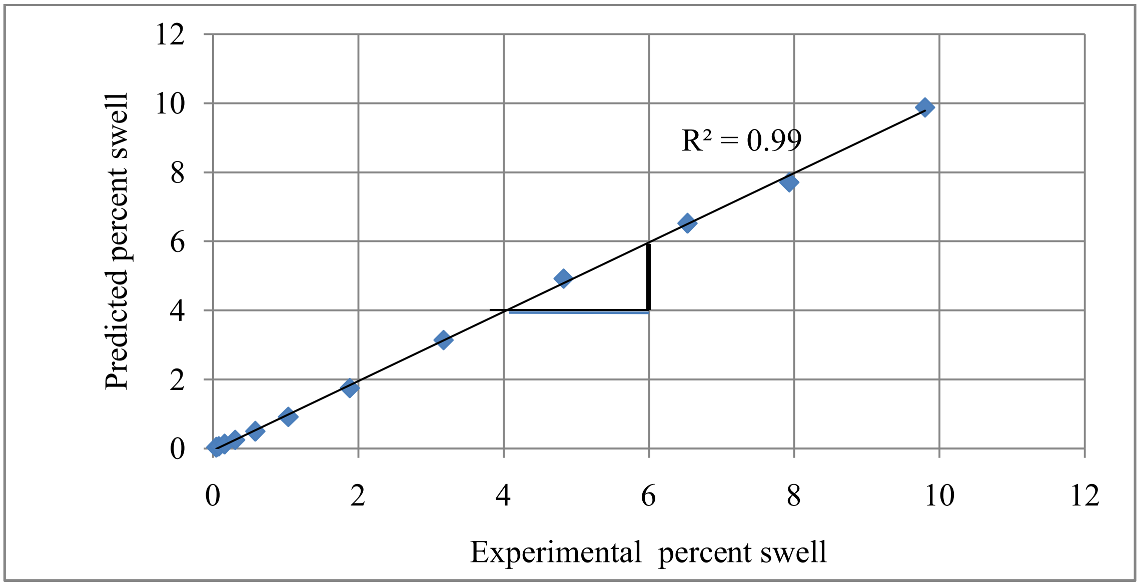

Figure 5.8 Relationship between experimental percent swell and predicted percent swell (MDD=1.3 g/cc, OMC=29 % and P=25 kPa), for Kality soil

5.4 Verification of the model

To verify the proposed model, the predicted vertical swell developed for Kality and Bole H.S. soil were compared to the experimental result obtained for soil close to Bole Airport under similar testing conditions (Fig. 5.9 and Fig. 5.10).

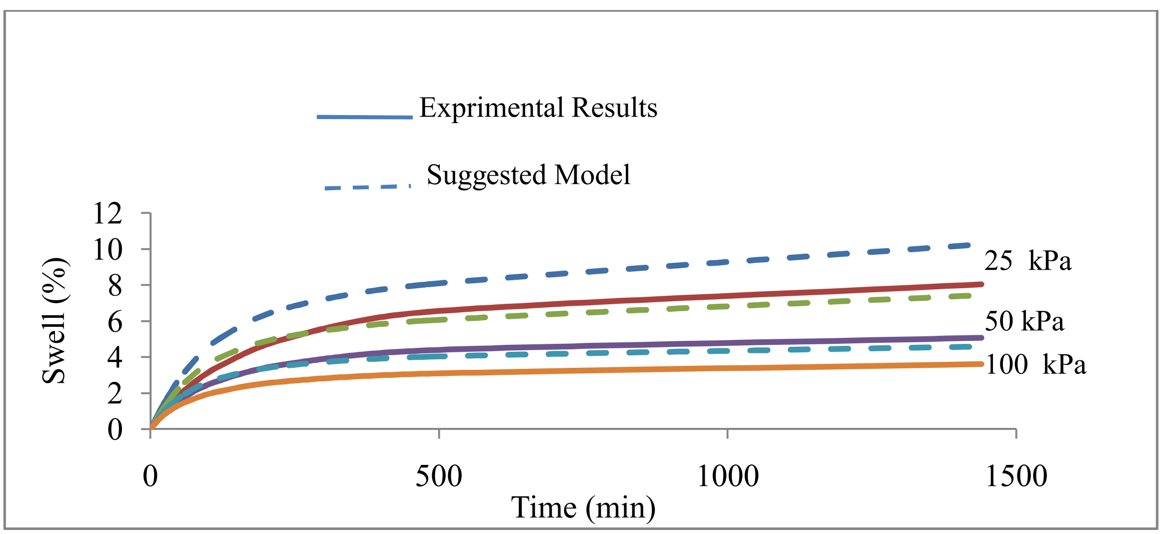

Figure 5.9 Swell vs. time relationship (MDD=1.3 g/cc and OMC=29 %), soil close to Bole air port.

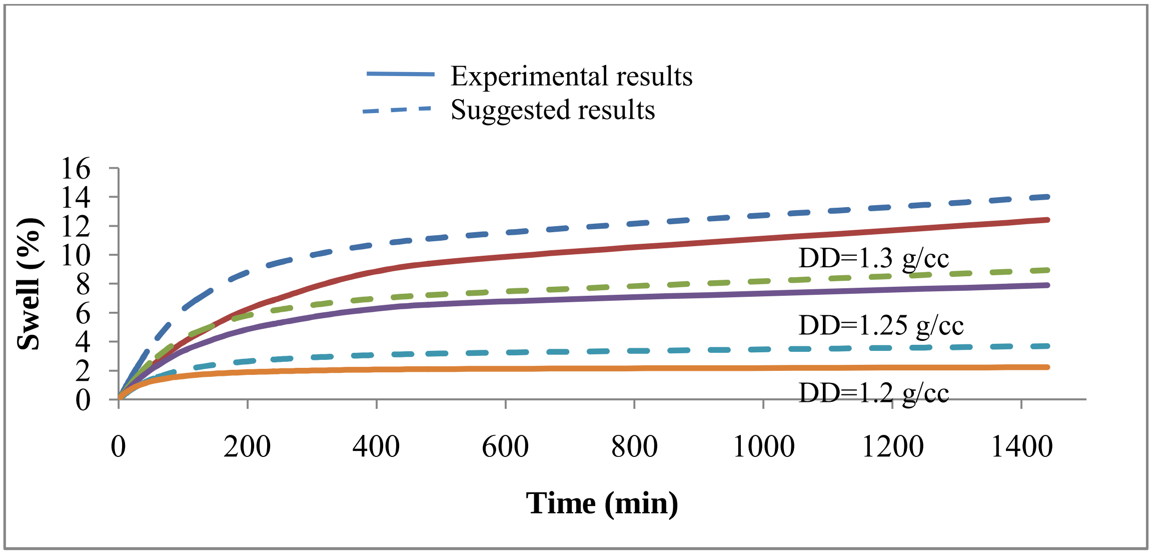

Figure 5.10 Swell vs. time relationship (OMC=29 % and P=7 kPa), soil close to Bole air port.

5.5 comparisons between equation 2.3 and equation 2.6

The measured values of vertical swell were compared with predictive values obtained by using Eqn. 2.3 and Eqn. 2.6. From Fig. 5.11 and Fig. 5.12 it can be observed that Eqn. 2.6 clearly gives more accurate predictions than Eqn. 2.3 and has the advantage of considering the influence of different factors affecting the swell-time curve characteristics including the applied pressure and the initial dry density. In other words Eqn. 2.6 is more general.

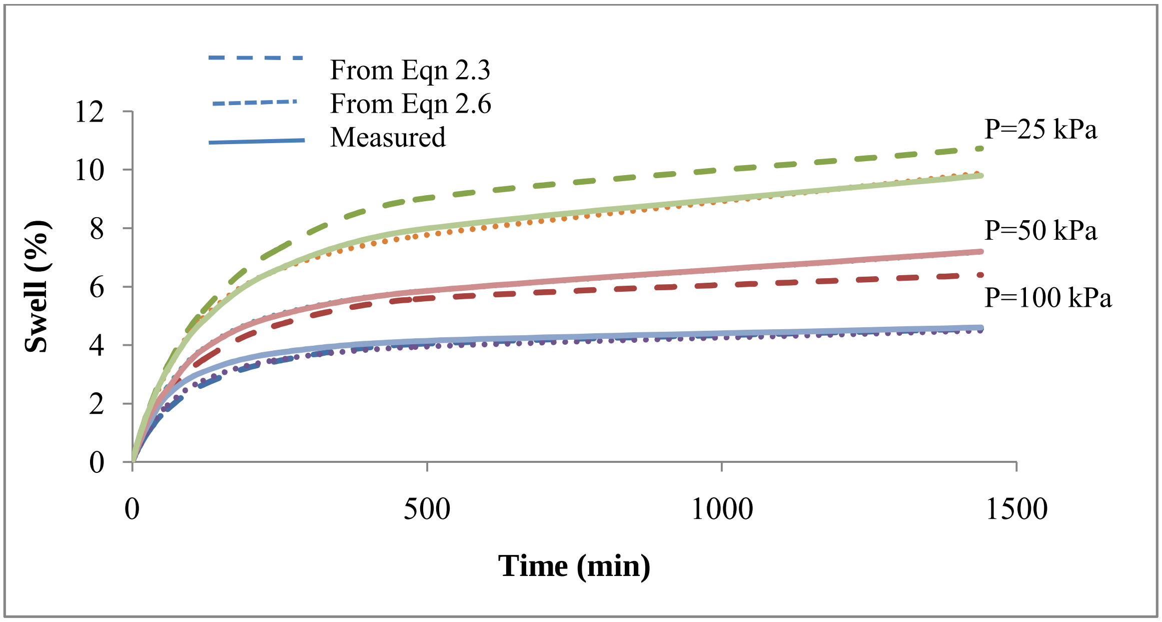

Figure 5.11 Comparisons between Eqn. 2.3 and Eqn. 2.6 (OMC=29 % and MDD=1.3 g/cc) for Kality soil.

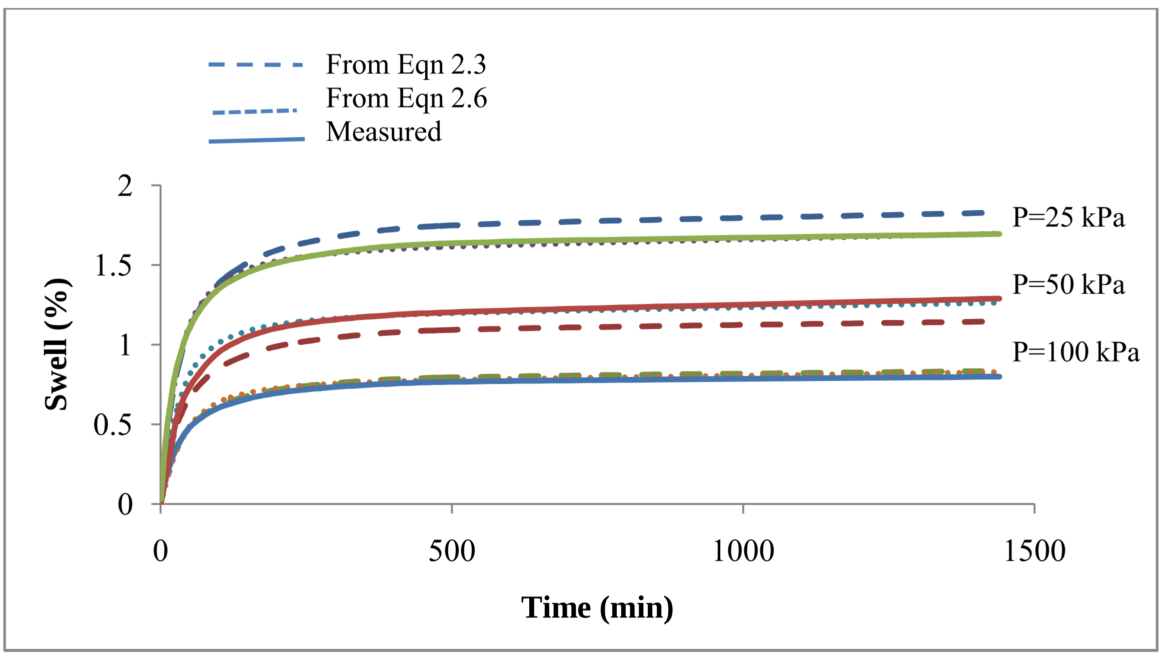

Figure 5.12 comparisons between Eqn. 2.3 and Eqn. 2.6 (OMC=39 % and MDD=1.28 g/cc) for Bole high school soil.

Chapter six
Conclusion and recommendation

6.1 conclusion

The following conclusions were drawn from the theoretical developments and experimental program in this study.

1) For the swell tests, the relationship between the percentage of ultimate vertical swell and the logarithm of applied pressure was approximately linear. Accordingly, the swell pressures were determined by extrapolating the linear relationship (i.e. at 0% vertical swell).
2) The experimental data from the loaded swell oedometer test results show that an increase in surcharge load significantly reduces the vertical swell and as the initial dry density increases the vertical swell increases.
3) A simple hyperbolic mathematical model (Eqn. 2.6) is used to generate the vertical swell–time curve of an expansive soil found in Addis Ababa. The model prediction were compared with the experimental results and showed very good agreements for all levels of applied pressure and initial dry density of the tested soils.

6.2 Recommendations

Further experimental work that covers wide variations in the initial dry unit weight, initial water content and soil type is needed to check the validity of the proposed model (Eqn. 2.6). The results of this study is hoped to simulate further research in this direction.

References

1. A. Alshenawy, 2002. Mathematical modeling of cavity expansion test on dry sand. Emirate. J. *Association of Engineering Geologists*, 30(4), 481–498.

2. A. O. Erol, A. Dhowian, and A. Youssef, 1987. Assessment of Oeodometer methods for heave prediction, proc. 6th int. conf. expansive soils (New Delhi. India), pp.99-103.

3. A. Sridharan, S.A. Rao, and P.V. Sivapullaiah, 1986. Swelling pressure of clays, Geotech. Test. J, vol.9, no. 1, pp 24-33

4. A. Tamiru, 2001, Geological map of Addis Ababa, Addis Ababa university department of Geology and Geophysics.

5. A. Yevnin, and Zaslavsky, 1970 some factors affecting compacted clay swelling, Canadian Getec. J. vol. 7, no. 1, pp78-89

6. A.A. Al-Karni, 2006. Modeling of stress-strain curves of drained triaxial test on sand. Am. J. Applied Sci., 3(11):2108-2113, 2006.

7. A.A. Al-Rawas, 1999. The factors controlling the expansive nature of the soils and rocks of northern Oman. *Engineering Geology*, 53, 327–350.

8. A.A. Basma, A.S. Al-Hamoud, and A. Husein, 1995. Laboratory assessment of swelling pressure of expansive soils. *Applied Clay Science*, 9, 355–368.

9. A.I. Al-mahidib and M.A. Al- Sharmani, swelling characteristics of lime-treated expansive soils. Civil engineering department, king Saud University.

10. A.S. Al-Homoud, and T.I. Al-Suleiman, 1997. Loss in serviceability of pavements due to expansive clay sub-grades. *Environmental and Engineering Geo-science*, III (1), 277–294.

11. Abdullah I. Al-Mhaidib, 2008, Mathematical Model to Predict Swelling of Expansive Soil, *Bulletin of the International Association for Computer Methods and Advances in Geo-mechanics (IACMAG)*

12. C. Bonner, and A. Shakoor, 1998. Predicting the swelling potential of a bentonitic clay from initial water content and dry density values. Proceedings of the 8th International IAEG Congress,

13. C. Meisina, 2002. Swelling/shrinkage hazard assessment applications in Italy, Proceedings of the 9th Congress of International Association for Engineering Geology and Environment, Durban, South Africa, 625–635.

14. C.A. Noble, 1966. Swelling measurement and prediction of heave for lacustrine clay, Cand. Geotech. J, vol. 3, no. 1, pp 32-41.

15. C.S. Oteo, J.L Salinas, F.J. Ayala, and M. Ferrer, 1995. Risk map for swelling of soils in Spain: results. Proceedings of the 1st International Conference on Unsaturated Soils, Paris, Vol. 34, 915–920.

16. D. Teklu, 2003, examining the swelling pressure of Addis Ababa presented to school of graduate studies, Addis Ababa University.

17. D.G Fredulund, 1995 the prediction of heave in expansive soils, presented at Canada-Kenya symposium on unsaturated soils.

18. D.G. Fredulund, 1969. Consolidometer test procedural factors affecting swell properties. Proc. And inte. Conf. expansive clay soils.

19. David Muir Wood, 2004. Geotechnical modeling. Version 2.2

20. E. A. Srochan, 1991. Construction of buildings on expansive soils, Brook field A.A. Balkema publishers, 298 pp.

21. Expansive Soils: Advances in Characterization and Treatment, 2006.Edited by Amer A. Al-Rawas and Mattheus F.A.Goosen, Taylor & Francis, London (UK).

22. F.H. Chen, 1988. Foundation on expansive soils, Amsterdam. Elsevier.

23. Fangsheg Shuai, 1996, Simulation of swelling pressure measurements on expansive soils. Dissertation, university of Saskatchewan, Saskatoon, Canada.

24. Fekrte Arega, 2006. Spectroscopy to drive engineering parameters of expansive soils. M.Sc. Thesis, International institute for Geo-information Science and Earth observation. Nederland.

25. Fekrte Arega, 2012. Remote sensing and Geotechnical investigations of expansive soils. Dissertation, university of Twente. Nederland.

26. H. Komine, and N. Ogata, (1994). Experimental study of swelling characteristics of compacted bentonite. *Canadian Geotechnical Journal*, 31, 478–490.

27. H. Yeheyis, 2001. “The effect of initial moisture content and initial dry density on the characteristics of expansive soils in Addis Ababa,” A thesis presented to school of graduate studies, Addis Ababa University.

28. H.A. Alawaji, 1999, “Swell and compressibility characteristics of sand–bentonite mixtures inundated with liquids,” *Applied Clay Science*, Vol. 15, No. 3–4, pp. 411–430.

29. J.E Jennings, 1961 .A comparison between laboratory prediction and field observation of heave of building on desiccated sub soils, proc. 5th int. conf.

30. J.E. Jennings, R.A. Firth, T. K. Ralph, and N. Negate 1973. An improved method for predicting heave using the oedometer test, proc. 3rd. int. conf. expansive soils (Haifa, Israel),vol. 2 , pp. 149-154.

31. J.L. Justo, (1979) “Design parameters for special soil conditions “. Design parameters in Geotechnical engineering. Proceedings of the seventh int. conf. on soil mech & found. Eng.vol. 5, pp 127-158.

32. J.M. Duncan, and C.Y. Chang, 1970. Nonlinear analysis of stress and strain in soils. J. Soil Mechanics and Foundation Division, ASCE, 96 (SM5): 1629-1653.

33. J.P. Kron, and J.E. Slosson, 1980. Assessment of expansive soils in the United States, proc. 4th Int. conf. expansive soils (Denver, Colorado), vol.1, pp. 596-608.

34. J.T. Pidgeon, 1987. The prediction of differential heave for design of foundation in expansive soil areas, proc. 9th. African reg. conf. soil mech. Found. Eng. (Lagos), pp 117-128.

35. K.S. Subba Rao, and G.C. Satyadas, (1987). Swelling potentials with cycles of swelling and partial shrinkage. *Proceedings 6th International Conference on Expansive Soils*, vol. 1, New Delhi, 137–142.

36. K.V. Ramana, 1993. Humid tropical expansive soils of Trinidad: Their geotechnical properties and areal distribution. *Engineering Geology*, 34, 27–44.

37. S. Li, and Y.Du, 1997. On the swelling–shrinkage properties and mechanisms of compacted expansive soil. Proceedings of the 30th International Geological Congress, China, Vol. 23, 253- 259.

38. M .A Osman, and A.M El Sharief, 1987. Field and laboratory observation of expansive soil heave, proc. 6th. Int. conf. expansive soils (New Delhi, India), pp. 105-110

39. M.Feng, J.K Gan, and D.G. Fredulund, 1998. A laboratory study of swelling pressure using various test methods. International conference on unsaturated soils. Volume 1, pp. 350-355.
40. N. S. Rao, and K. Kodandaramaswamy, 1982. Method to Predict Ultimate Compression in Clays, *Journal of Geotechnical Engineering Division*, ASCE, 108(GT2), 308-314.
41. N. S. Rao, K. Kodandaramaswamy, and J.R. Somayajulu, 1981. Proposed Hyperbolic Relationship Between Settlement and Time, *Journal of Geotechnical Engineering*, 12, 53-62.
42. P.V. Lade, 2005. Overview of constitutive models for soils. Geotechnical Special Publication No.128: Soil Constitutive Model Evaluation, Selection and Calibration. ASCE, pp: 1-34.
43. R.L. Kondner, 1963. Hyperbolic stress-strain response: Cohesive soils. J. Soil Mechanics and Foundation Division, ASCE, 89(SM1): 115-143.
44. R.M. Kouner, 1970. Effect of particle characteristics on soil strength. J. Soil Mechanics and Foundation Division, ASCE, 96 (SM4): 1221-1234
45. R.M. Richard, and B.J. Abbott, 1975. Versatile elastic-plastic stress-strain formula. J. Engg. Mech., ASCE, 10: 511-515.
46. R.W. Day, (1994). Swell-shrink behavior of compacted clay. *Journal of Geotechnical Engineering, ASCE* 120, 618–623.
47. S. F Gizienski, and L.J. Lee, 1965 comparisons of laboratory swell tests to small scale field tests, proc. 1st int. conf. expansive clay soils, Texas A &M press, pp. 108-119
48. S. Frydman, and G. Calbresi, 1987 suggested standard for one dimensional testing, proc. 6th int. conf. expansive soils (New Delhi, India pp. 91-98, 1987).
49. S.N Abduljauwad, 1993. Study on the performance of calcareous expansive clay.
50. S.T. Elsayed, and S.A. Rabba, 1986. Factors affecting behavior of expansive soils in the laboratory and field. A review, Geotechnical Engineering, Vol. 17, no.1, pp.89-107. Engg. Res. United Arab Emirates University, 7: 7-24.
51. T. W Lambe, and R.V. Whitman, 1979 soil mechanics. New York, NY: Jhon Wiley & sons, pp 553

52. T.H. Almusallam, and S.H. Alsayed, 1995. Stress strain relationship of normal, high-strength and lightweight concrete. Mag. Concrete Res., 47: 39-44.

53. Teferra and Yohannes, 1986. Investigation on the expansive soils of Addis Ababa. Journal of EAEA, vol. 7

54. USGS, 2000. Swelling clays map of the conterminous U.S. US Geological Survey.

55. V. Dakshanamurthy, 1978. A New Method to Predict Swelling Using a Hyperbolic Equation, *Journal of Geotechnical Engineering*, 9, 29-38.

56. W.G Holtz and H.J. Gibbs, 1956. Engineering properties of expansive clays, Transactions ASCE, vol.121, pp.641-663.

Appendix A
Swelling test results

Table A1 Swell test result for Kality soil (MDD=1.3 g/cc, OMC=29 % and P=25 kPa)

Initial reading: 8.200

Time (min)	Dial, mm	ΔH, mm	S (%)	T/S
0.5	8.192	0.008	0.040	12.50
1	8.1844	0.016	0.078	12.82
2	8.169	0.031	0.155	12.90
4	8.140	0.060	0.300	13.33
8	8.084	0.116	0.580	13.79
15	7.993	0.207	1.035	14.49
30	7.824	0.376	1.880	15.96
60	7.566	0.634	3.170	18.93
120	7.235	0.965	4.825	24.87
240	6.894	1.306	6.530	36.75
480	6.614	1.586	7.932	60.52
1440	6.240	1.960	9.800	146.94

Table A2 Swell test result for Kality soil (MDD=1.3 g/cc, OMC=29 % and P=50 kPa)

Initial reading: 8.6

Time (min)	Dial, mm	ΔH, mm	S (%)	T/S
0.5	8.593	0.007	0.0350	14.286
1	8.589	0.011	0.060	16.667
2	8.577	0.023	0.115	17.391
4	8.555	0.045	0.225	17.778
8	8.512	0.088	0.440	18.182
15	8.438	0.162	0.810	18.519
30	8.278	0.322	1.610	18.634
60	8.100	0.500	2.500	24.000
120	7.830	0.770	3.850	31.169
240	7.605	0.995	4.975	48.241
480	7.437	1.163	5.815	82.545
1440	7.160	1.440	7.200	200.000

Table A3 Swell test result for Kality soil (MDD=1.3 g/cc, OMC=29 % and P=100 kPa)

Initial reading: 6.25

Time (min)	Dial, mm	ΔH, mm	S (%)	T/S
0.5	6.244	0.006	0.030	16.667
1	6.2382	0.012	0.059	16.949
2	6.227	0.023	0.115	17.391
4	6.205	0.045	0.225	17.778
8	6.162	0.088	0.440	18.182
15	6.095	0.155	0.775	19.355
30	5.972	0.278	1.390	21.583
60	5.792	0.458	2.290	26.201
120	5.635	0.615	3.075	39.024
240	5.508	0.742	3.710	64.690
480	5.423	0.827	4.135	116.082
1440	5.329	0.921	4.605	312.704

Table A4 Swell test result for Kality soil (MDD=1.3 g/cc, OMC=29 % and P=7 kPa)

Initial reading: 8.4

Time (min)	Dial, mm	ΔH, mm	S (%)	T/S
0.5	8.3904	0.0096	0.048	10.42
1	8.381	0.019	0.095	10.53
2	8.3631	0.0369	0.185	10.84
4	8.327	0.073	0.365	10.96
8	8.255	0.145	0.725	11.03
15	8.139	0.261	1.305	11.49
30	7.919	0.481	2.405	12.47
60	7.567	0.833	4.165	14.41
120	7.084	1.316	6.580	18.24
240	6.548	1.852	9.260	25.92
480	6.074	2.326	11.630	41.27
1440	5.596	2.804	14.020	102.71

Table A5 Swell test result for Kality soil (DD=1.25 g/cc, OMC=29 % and P=7 kPa)

Initial reading: 4.676

Time (min)	Dial, mm	ΔH, mm	S (%)	T/S
0.5	4.6686	0.007	0.037	13.514
1	4.6613	0.015	0.074	13.605
2	4.647	0.029	0.145	13.793
4	4.619	0.057	0.285	14.035
8	4.565	0.111	0.555	14.414
15	4.480	0.196	0.980	15.306
30	4.323	0.353	1.765	16.997
60	4.086	0.590	2.950	20.339
120	3.780	0.896	4.480	26.786
240	3.458	1.218	6.090	39.409
480	3.183	1.493	7.465	64.300
1440	2.913	1.763	8.815	163.358

Table A6 Swell test result for Kality soil (DD=1.2 g/cc, OMC=29 % and P=7 kPa)

Initial reading: 9.3

Time (min)	Dial, mm	ΔH, mm	S (%)	T/S
0.5	9.2947	0.005	0.0265	18.87
1	9.2895	0.011	0.053	19.05
2	9.2791	0.021	0.105	19.14
4	9.260	0.040	0.200	20.00
8	9.223	0.077	0.385	20.78
15	9.168	0.132	0.660	22.73
30	9.075	0.225	1.125	26.67
60	8.953	0.347	1.735	34.58
120	8.824	0.476	2.380	50.42
240	8.715	0.585	2.925	82.05
480	8.640	0.660	3.300	145.45
1440	8.578	0.722	3.610	398.89

Table A7 Swell test result for Bole H. S. soil (MDD=1.28 g/cc, OMC=39 % and P=25 kPa)

Initial reading: 2.086

Time (min)	Dial, mm	ΔH, mm	S (%)	T/S
0.5	2.080	0.006	0.030	16.67
1	2.0742	0.012	0.059	16.95
2	2.063	0.023	0.115	17.39
4	2.043	0.043	0.215	18.60
8	2.010	0.076	0.380	21.05
15	1.967	0.119	0.595	25.21
30	1.908	0.178	0.890	33.71
60	1.851	0.235	1.175	51.06
120	1.806	0.280	1.400	85.71
240	1.777	0.309	1.545	155.34
480	1.759	0.327	1.635	293.58
1440	1.747	0.339	1.695	849.56

Table A8 Swell test result for Bole H. S. soil (MDD=1.28 g/cc, OMC=39 % and P=50 kPa)

Initial reading: 8.19

Time (min)	Dial, mm	ΔH, mm	S (%)	T/S
0.5	8.1876	0.00240	0.012	41.67
1	8.1854	0.00470	0.023	42.55
2	8.181	0.00900	0.045	44.44
4	8.1721	0.01790	0.089	44.69
8	8.156	0.03400	0.170	47.06
15	8.133	0.05700	0.285	52.63
30	8.0761	0.11390	0.569	52.68
60	8.032	0.15800	0.790	75.95
120	7.990	0.20000	1.000	120.00
240	7.964	0.22600	1.130	212.39
480	7.950	0.24000	1.200	400.00
1440	7.932	0.25800	1.290	1116.28

Table A9 Swell test result for Bole H. S. soil (MDD=1.28 g/cc, OMC=39 % and P=100 kPa)

Initial reading: 10.64

Time (min)	Dial, mm	ΔH, mm	S (%)	T/S
0.5	10.6378	0.0023	0.0115	43.48
1	10.6355	0.0045	0.0225	44.44
2	10.6313	0.0087	0.0435	45.98
4	10.624	0.0160	0.0800	50.00
8	10.610	0.0300	0.1500	53.33
15	10.592	0.0480	0.2400	62.50
30	10.565	0.0750	0.3750	80.00
60	10.537	0.1030	0.5150	116.50
120	10.514	0.1260	0.6300	190.48
240	10.497	0.1430	0.7150	335.66
480	10.487	0.1530	0.7650	627.45
1440	10.480	0.1600	0.8000	1800.00

Table A10 Swell test result for Bole H. S. soil (MDD=1.28 g/cc, OMC=39 % and P=7 kPa)

Initial reading: 1.488

Time (min)	Dial, mm	ΔH, mm	S (%)	T/S
0.5	1.479	0.0088	0.044	11.3690
1	1.471	0.0172	0.086	11.6380
2	1.455	0.0329	0.164	12.1760
4	1.428	0.0604	0.302	13.2520
8	1.431	0.0573	0.286	27.9280
15	1.389	0.0984	0.492	30.4900
30	1.320	0.1680	0.840	35.7143
60	1.232	0.2555	1.278	46.9600
120	1.118	0.3700	1.850	64.8649
240	1.051	0.4374	2.187	109.7441
480	1.010	0.4784	2.392	200.6800
1440	0.966	0.5217	2.609	552.0400

Table A11 Swell test result for Bole H. S. soil (DD=1.25 g/cc, OMC=39 % and P=7 kPa)

Initial reading: 9.62

Time (min)	Dial, mm	ΔH, mm	S (%)	T/S
0.5	9.6159	0.0041	0.020	24.4
1	9.6119	0.0081	0.040	24.7
2	9.604	0.0160	0.080	25.0
4	9.589	0.0310	0.155	25.8
8	9.562	0.0580	0.290	27.6
15	9.522	0.0980	0.490	30.6
30	9.457	0.1630	0.815	36.8
60	9.377	0.2430	1.215	49.4
120	9.282	0.3380	1.690	71.0
240	9.222	0.3980	1.990	120.6
480	9.192	0.4280	2.140	224.3
1440	9.159	0.4610	2.305	624.7

Table A12 Swell test result for Bole H. S. soil (DD=1.2 g/cc, OMC=39 % and P=7 kPa)

Initial reading: 10.042

Time (min)	Dial, mm	ΔH, mm	S (%)	T/S
0.5	10.038	0.0040	0.020	25.000
1	10.0341	0.0079	0.039	25.316
2	10.0263	0.0156	0.078	25.478
4	10.012	0.0300	0.150	26.667
8	9.985	0.0570	0.285	28.070
15	9.948	0.0940	0.470	31.915
30	9.882	0.1600	0.800	37.500
60	9.805	0.2370	1.185	50.633
120	9.742	0.3000	1.500	80.000
240	9.700	0.3420	1.710	140.351
480	9.686	0.3560	1.780	269.663
1440	9.664	0.3780	1.890	761.905

Table A13 Swell test result for soil close to Bole airport (DD=1.3 g/cc, MC=29 % and P=25 kPa)

Initial reading: 1.628

Time , min	Dial, mm	ΔH, mm	S (%)	T/S
0.5	1.623	0.005	0.025	20.00
1	1.6183	0.0097	0.049	20.62
2	1.609	0.019	0.095	21.05
4	1.591	0.037	0.185	21.62
8	1.555	0.073	0.365	21.92
15	1.495	0.133	0.665	22.56
30	1.381	0.247	1.235	24.29
60	1.193	0.435	2.175	27.59
120	0.926	0.702	3.510	34.19
240	0.615	1.013	5.065	47.38
480	0.327	1.301	6.505	73.79
1440	0.022	1.606	8.030	179.33

Table A14 Swell test result for soil close to Bole airport (DD=1.3 g/cc, MC=29 % and P=50 kPa)

Initial reading: 8.850

Time , min	Dial, mm	ΔH, mm	S (%)	T/S
0.5	8.8456	0.004	0.022	22.73
1	8.8413	0.009	0.043	22.99
2	8.833	0.017	0.085	23.53
4	8.816	0.034	0.169	23.60
8	8.783	0.067	0.335	23.88
15	8.731	0.119	0.595	25.21
30	8.635	0.215	1.075	27.91
60	8.491	0.359	1.795	33.43
120	8.309	0.541	2.705	44.36
240	8.125	0.725	3.625	66.21
480	7.976	0.874	4.370	109.84
1440	7.838	1.012	5.060	284.58

Table A15 Swell test result for soil close to Bole airport (DD=1.3 g/cc, MC=29 % and P=100 kPa)

Initial reading: 1.844

Time , min	Dial, mm	ΔH, mm	S (%)	T/S
0.5	1.840	0.004	0.020	25.0000
1	1.8361	0.008	0.039	25.3165
2	1.8284	0.016	0.078	25.6410
4	1.813	0.031	0.155	25.8065
8	1.783	0.061	0.305	26.2295
15	1.737	0.107	0.535	28.0374
30	1.657	0.187	0.935	32.0856
60	1.548	0.296	1.480	40.5405
120	1.423	0.421	2.105	57.0071
240	1.311	0.533	2.665	90.0563
480	1.229	0.615	3.075	156.0976
1440	1.158	0.686	3.60	400.000

Table A16 Swell test result for soil close to Bole airport (DD=1.3 g/cc, MC=29 % and P=7 kPa)

Initial reading: 10.806

Time , min	Dial, mm	ΔH, mm	S (%)	T/S
0.5	10.800	0.006	0.030	16.67
1	10.795	0.011	0.055	18.18
2	10.7842	0.022	0.109	18.35
4	10.763	0.043	0.215	18.60
8	10.723	0.083	0.415	19.28
15	10.653	0.153	0.765	19.61
30	10.517	0.289	1.445	20.76
60	10.279	0.527	2.635	22.77
120	9.911	0.895	4.475	26.82
240	9.432	1.374	6.870	34.93
480	8.929	1.877	9.385	51.15
1440	8.324	2.482	12.410	116.04

Table A17 Swell test result for soil close to Bole airport (DD=1.25 g/cc, MC=29 % and P=7 kPa)

Initial reading: 10.674

Time , min	Dial, mm	ΔH, mm	S (%)	T/S
0.5	10.6685	0.0055	0.027	18.18
1	10.6631	0.0109	0.054	18.35
2	10.653	0.0210	0.105	19.05
4	10.633	0.0410	0.205	19.51
8	10.594	0.0800	0.400	20.00
15	10.527	0.1470	0.735	20.41
30	10.403	0.2710	1.355	22.14
60	10.204	0.4700	2.350	25.53
120	9.932	0.7420	3.710	32.35
240	9.630	1.0440	5.220	45.98
480	9.363	1.3110	6.555	73.23
1440	9.094	1.5800	7.900	182.28

Table A18 Swell test result for soil close to Bole airport (DD=1.2 g/cc, MC=29 % and P=7 kPa)

Initial reading: 6.692

Time , min	Dial, mm	ΔH, mm	S (%)	T/S
0.5	6.687	0.005	0.025	20.00
1	6.6821	0.010	0.049	20.20
2	6.673	0.019	0.095	21.05
4	6.655	0.037	0.185	21.62
8	6.619	0.073	0.365	21.92
15	6.573	0.119	0.595	25.21
30	6.503	0.189	0.945	31.75
60	6.424	0.268	1.340	44.78
120	6.353	0.339	1.695	70.80
240	6.302	0.390	1.950	123.08
480	6.270	0.422	2.110	227.49
1440	6.245	0.447	2.235	644.30

Table A19 Swell test result for soil close to Bole airport (DD=1.28 g/cc, MC=39 % and P=25 kPa)

Initial reading: 8.814

Time , min	Dial, mm	ΔH, mm	S (%)	T/S
0.5	8.807	0.007	0.035	14.29
1	8.802	0.012	0.060	16.67
2	8.791	0.023	0.115	17.39
4	8.773	0.041	0.205	19.51
8	8.742	0.072	0.360	22.22
15	8.705	0.109	0.545	27.52
30	8.660	0.154	0.770	38.96
60	8.619	0.195	0.975	61.54
120	8.590	0.224	1.120	107.14
240	8.571	0.243	1.215	197.53
480	8.561	0.253	1.265	379.45
1440	8.554	0.26	1.300	1107.69

Table A20 Swell test result for soil close to Bole airport (DD=1.28 g/cc, MC=39 % and P=50 kPa)

Initial reading: 7.2

Time , min	Dial, mm	ΔH, mm	S (%)	T/S
0.5	7.1949	0.0051	0.026	19.61
1	7.190	0.0100	0.050	20.00
2	7.181	0.0190	0.095	21.05
4	7.164	0.0360	0.180	22.22
8	7.138	0.0620	0.310	25.81
15	7.112	0.0880	0.440	34.09
30	7.084	0.1160	0.580	51.72
60	7.062	0.1380	0.690	86.96
120	7.048	0.1520	0.760	157.89
240	7.039	0.1610	0.805	298.14
480	7.035	0.1650	0.825	581.82
1440	7.032	0.1680	0.840	1714.29

Table A21 Swell test result for soil close to Bole airport (DD=1.28 g/cc, MC=39 % and P=100 kPa)

Initial reading: 6.6

Time , min	Dial, mm	ΔH, mm	S (%)	T/S
0.5	6.596	0.004	0.020	25.72
1	6.593	0.007	0.035	26.44
2	6.579	0.014	0.072	27.87
4	6.567	0.026	0.130	30.74
8	6.549	0.044	0.219	36.49
15	6.521	0.079	0.395	46.54
30	6.499	0.101	0.505	68.08
60	6.483	0.117	0.585	111.16
120	6.473	0.127	0.635	197.32
240	6.467	0.133	0.665	369.64
480	6.464	0.136	0.680	714.28
1440	6.326	0.138	0.69	2086

Table A22 Swell test result for soil close to Bole airport (DD=1.28 g/cc, MC=39 % and P=7 kPa)

Initial reading: 8.958

Time , min	Dial, mm	ΔH, mm	S (%)	T/S
0.5	8.9523	0.006	0.029	17.54
1	8.947	0.011	0.055	18.18
2	8.937	0.021	0.105	19.05
4	8.919	0.039	0.195	20.51
8	8.886	0.072	0.360	22.22
15	8.839	0.119	0.595	25.21
30	8.769	0.189	0.945	31.75
60	8.689	0.269	1.345	44.61
120	8.618	0.340	1.700	70.59
240	8.566	0.392	1.960	122.45
480	8.534	0.424	2.120	226.42
1440	8.509	0.449	2.245	641.43

Table A23 Swell test result for soil close to Bole airport (DD=1.25 g/cc, MC=39 % and P=7 kPa)

Initial reading: 7.246

Time , min	Dial, mm	ΔH, mm	S (%)	T/S
0.5	7.241	0.005	0.025	20.00
1	7.2361	0.010	0.050	20.20
2	7.227	0.019	0.095	21.05
4	7.209	0.037	0.185	21.62
8	7.177	0.069	0.345	23.19
15	7.135	0.111	0.555	27.03
30	7.076	0.170	0.850	35.29
60	7.015	0.231	1.155	51.95
120	6.964	0.282	1.410	85.11
240	6.929	0.317	1.585	151.42
480	6.909	0.337	1.685	284.87
1440	6.893	0.353	1.765	815.86

Table A24 Swell test result for soil close to Bole airport (DD=1.2 g/cc, MC=39 % and P=7 kPa)

Initial reading: 1.490

Time , min	Dial, mm	ΔH, mm	S (%)	T/S
0.5	1.4859	0.0041	0.0205	24.39
1	1.482	0.0080	0.0400	25.00
2	1.4741	0.0159	0.0795	25.16
4	1.459	0.0310	0.1550	25.81
8	1.430	0.0600	0.3000	26.67
15	1.385	0.1050	0.5250	28.57
30	1.334	0.1560	0.7800	38.46
60	1.284	0.2060	1.0300	58.25
120	1.244	0.2460	1.2300	97.56
240	1.218	0.2720	1.3600	176.47
480	1.203	0.2870	1.4350	334.49
1440	1.192	0.2980	1.4900	966.44

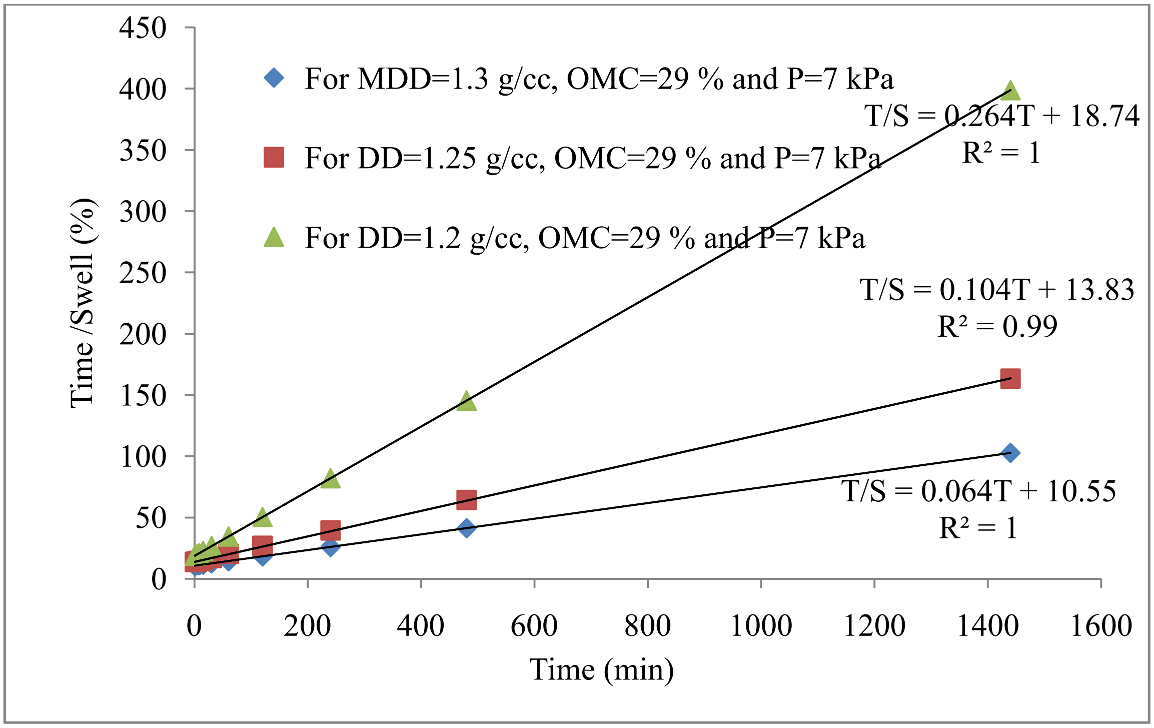

Figure A1 Determination of the coefficients rate of swelling for Kality soil.

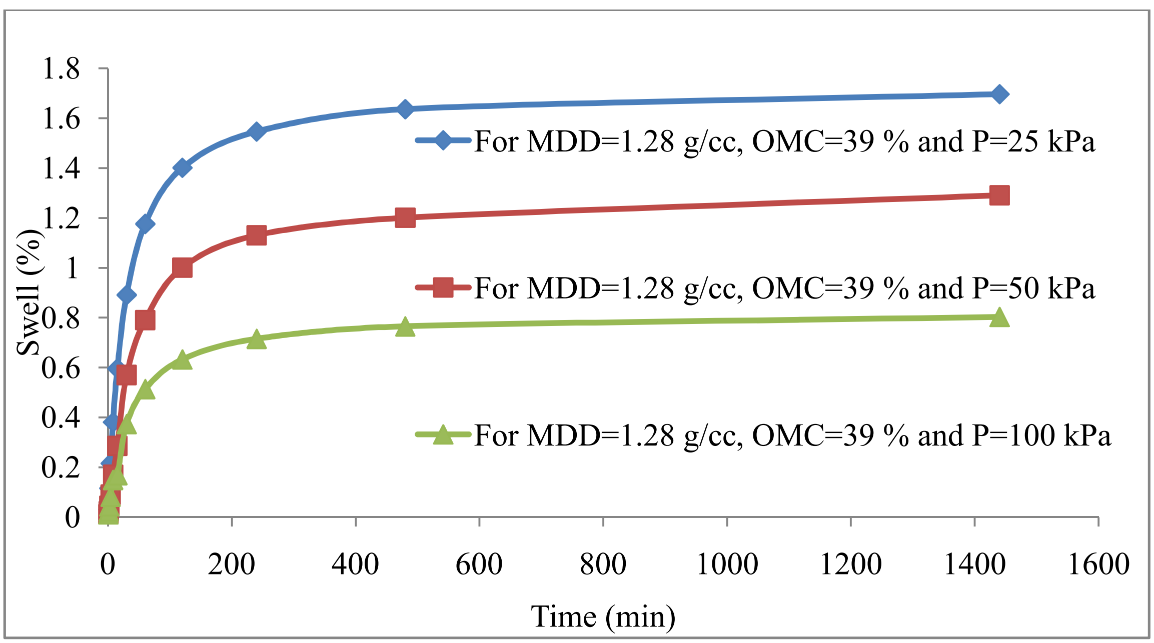

Figure A2 Vertical swell vs. time relationship for Bole high school.

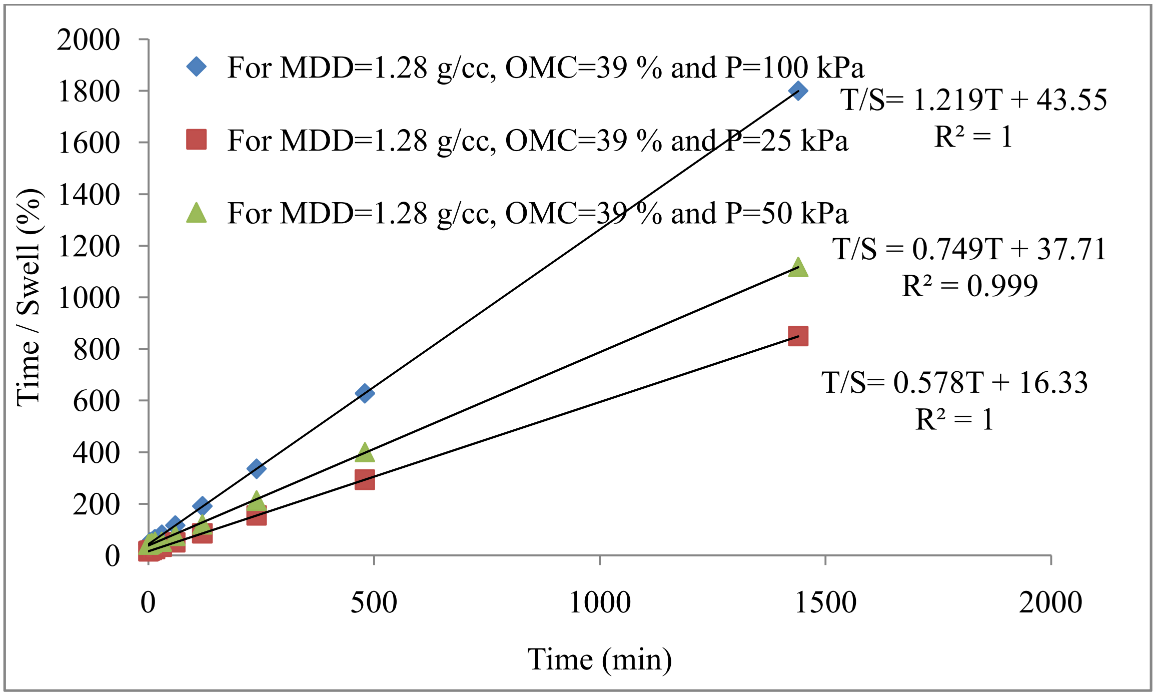

Figure A3 Determination of the coefficients rate of swelling for Bole high school.

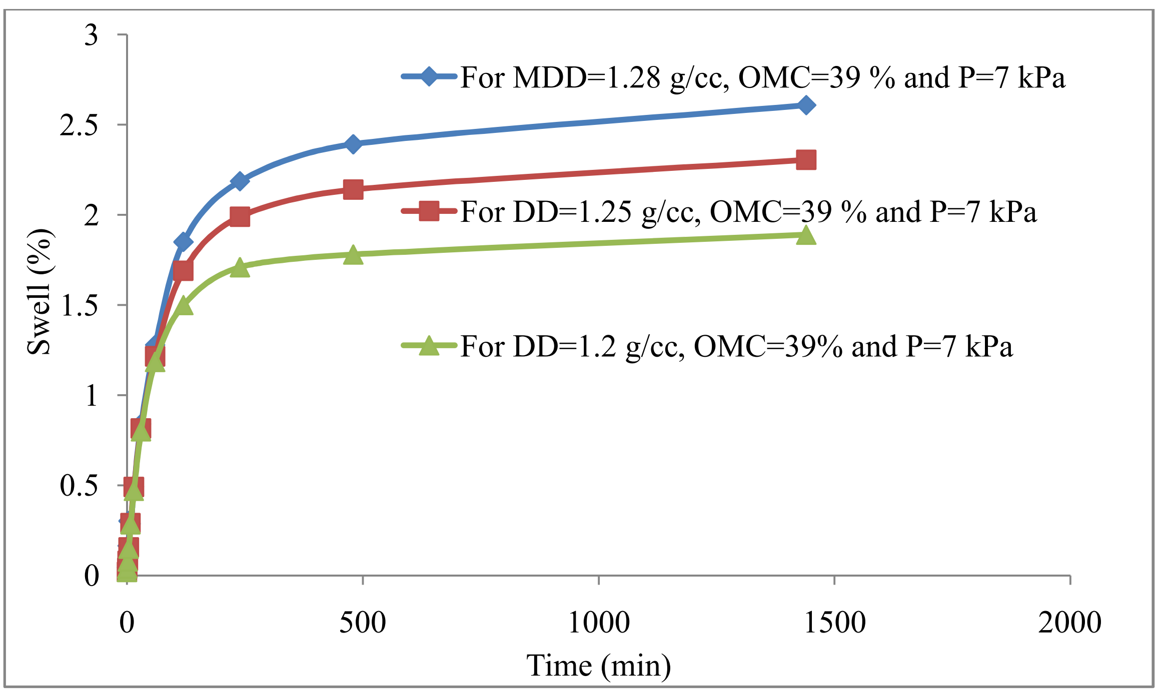

Figure A4 Swell vs. time relationship for Bole high school.

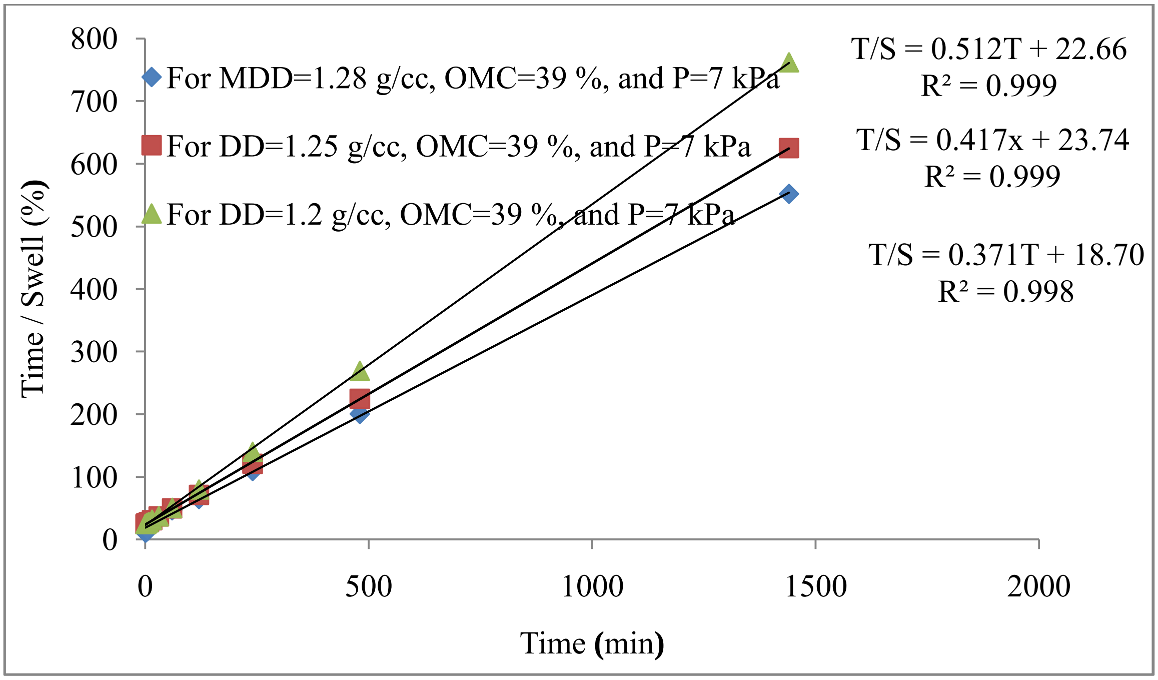

Figure A5 Determination of the coefficients rate of swelling for Bole high school

Appendix B
Model parameters and empirical relationships

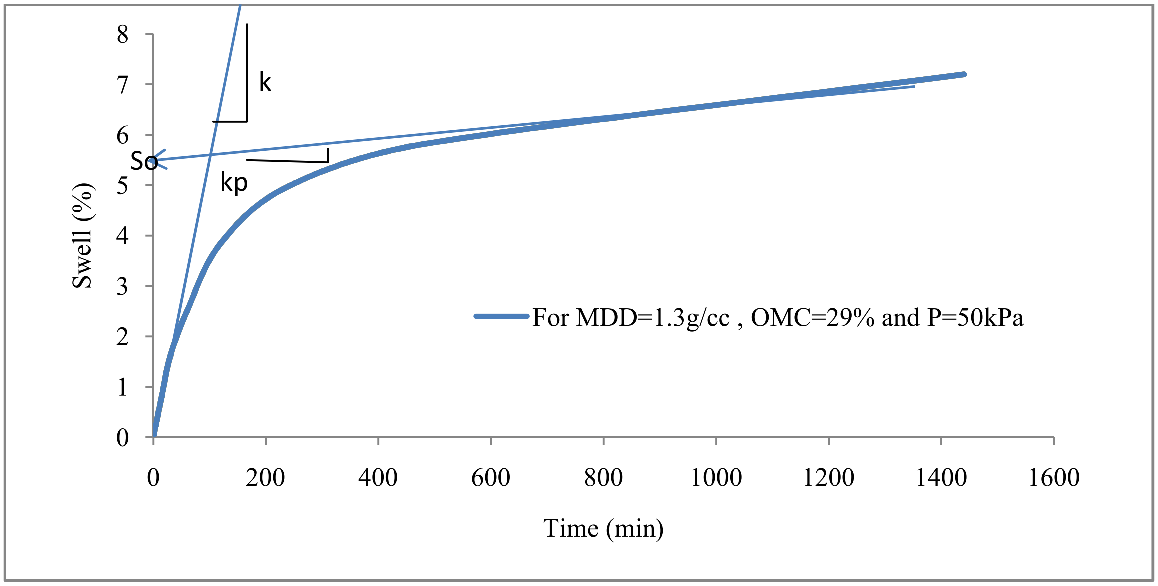

Figure B1 Parameter determination for Kality soil

Initial slope of the curve, *k = 0.0536,* final slope of the curve, *Kp= 0.00144*

The reference swell, *So*=5.5 and the peak swell, *Sp*= 7.2

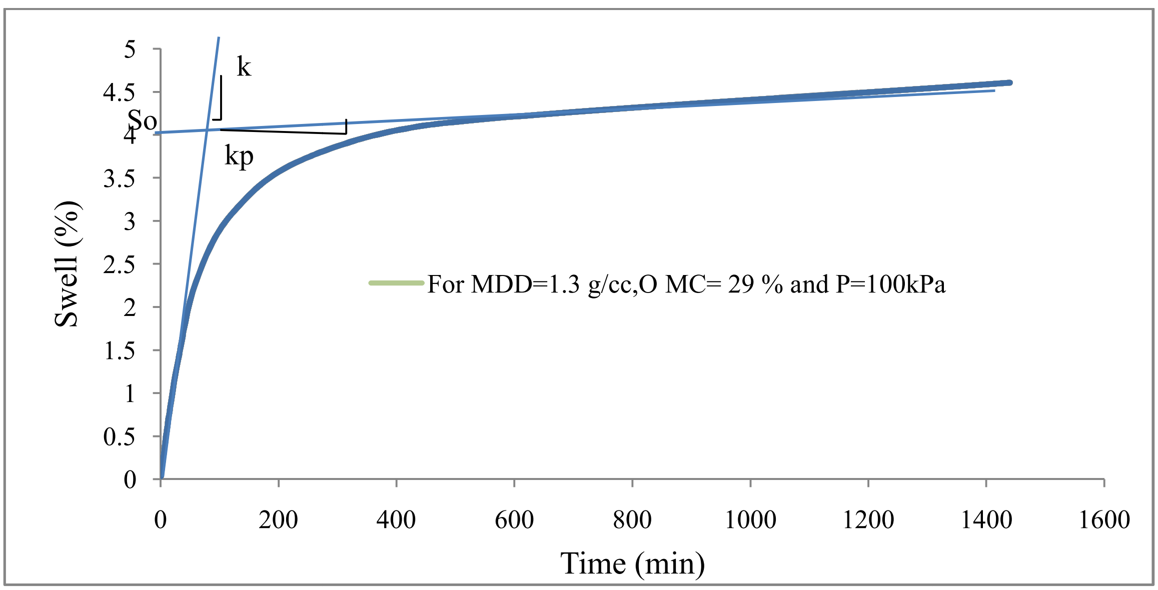

Figure B2 Parameter determination for Kality soil

Initial slope of the curve, *k = 0.0460,* final slope of the curve, *Kp= 0.00049*

The reference swell, *So*=4.19 and the peak swell, *Sp*= 4.61

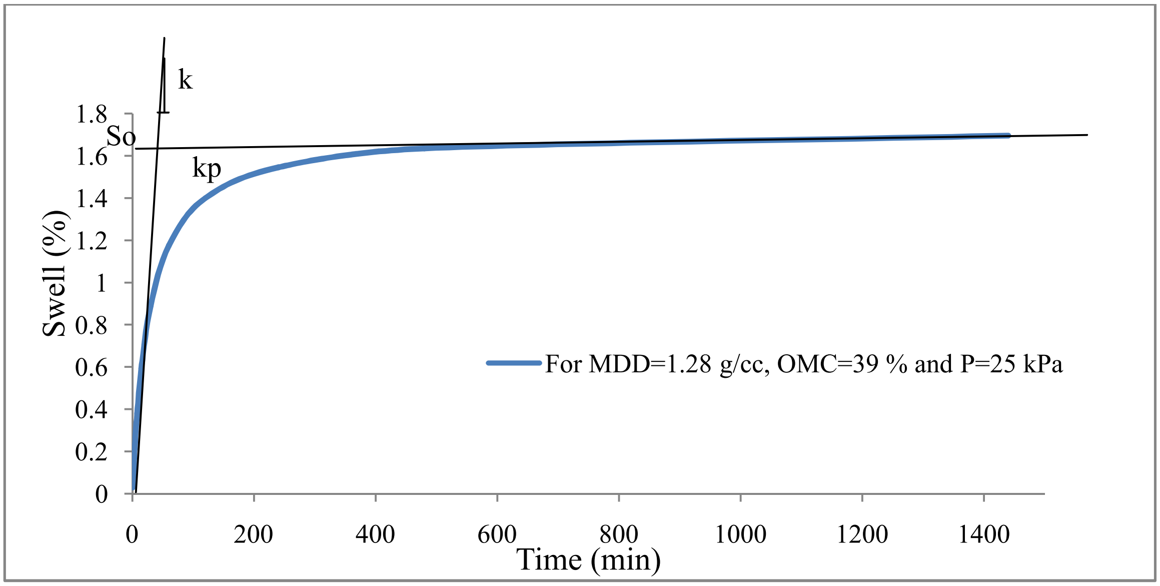

Figure B3 Parameter determination for Bole high school soil

Initial slope of the curve, k = *0.0403*, final slope of the curve, Kp= *6.25E-05*

The reference swell, So=1.62 and the peak swell, Sp= 1.69

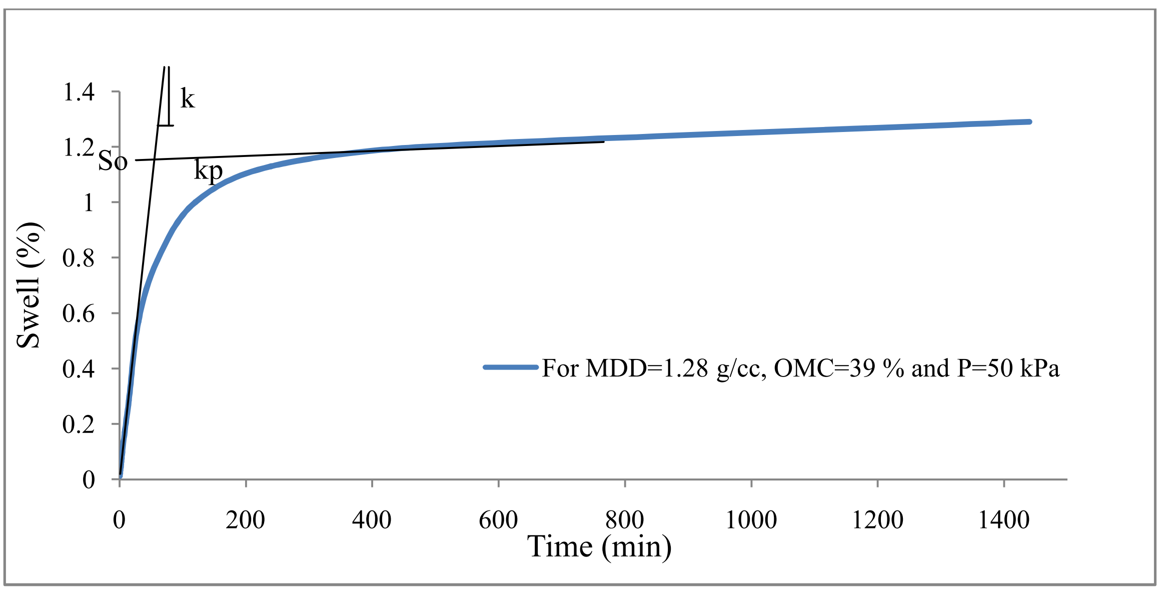

Figure B4 Parameter determination for Bole high school soil

Initial slope of the curve, k = *0.0187*, final slope of the curve, Kp= *5.26E-05*

The reference swell, So=1.18 and the peak swell, Sp= 1.29

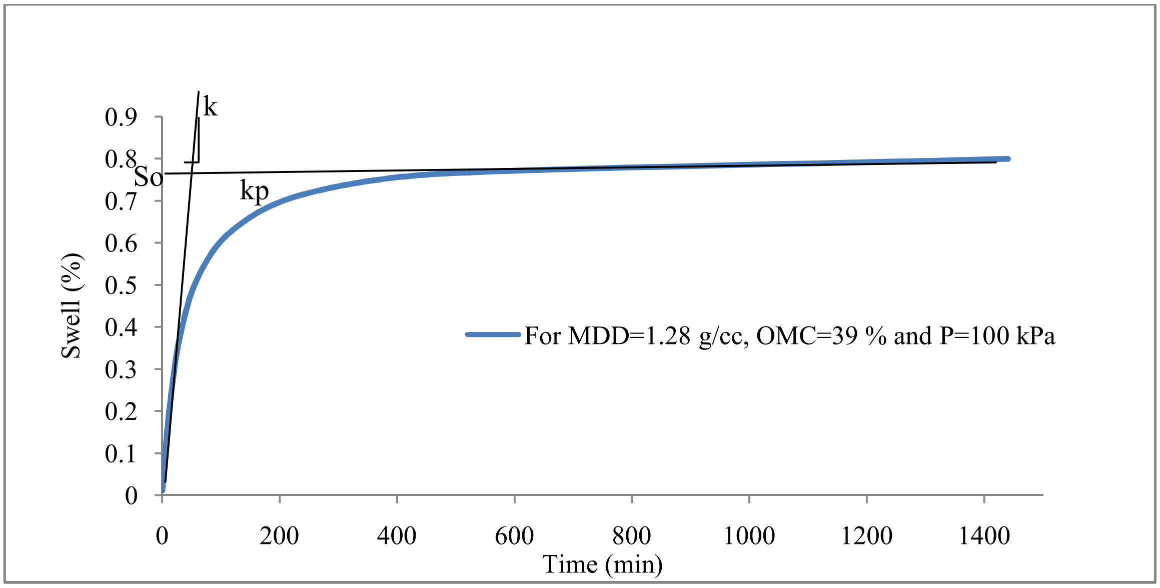

Figure B5 Parameter determination for Bole high school soil

Initial slope of the curve, *k = 0.0107,* final slope of the curve, *Kp= 3.96E-05*

The reference swell, *So*=0.78 and the peak swell, *Sp*= 0.8

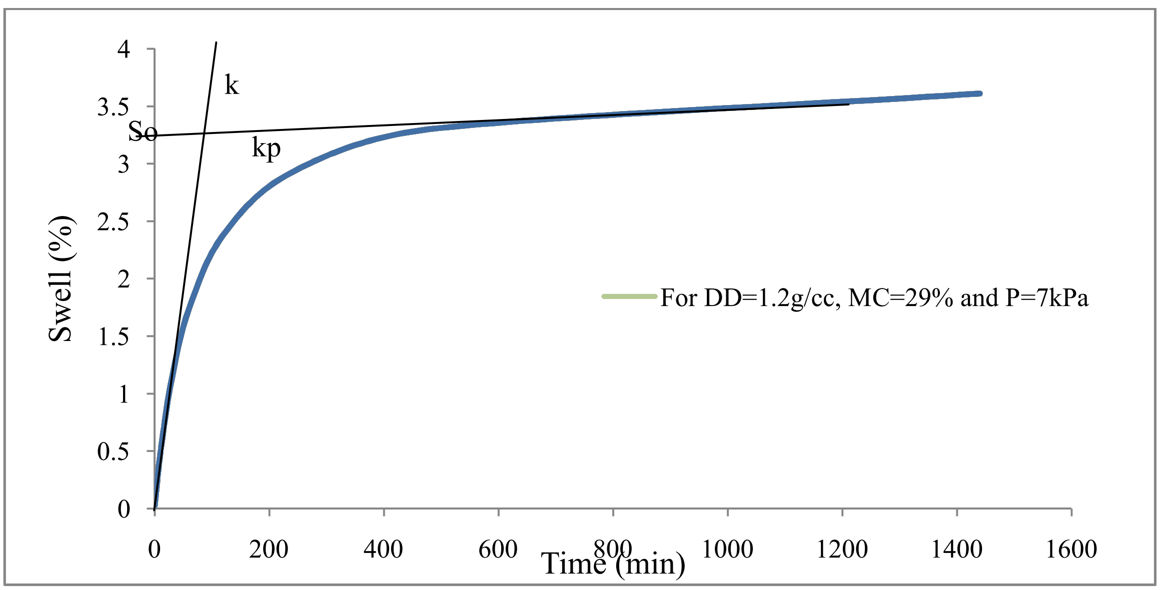

Figure B6 Parameter determination for Kality soil

Initial slope of the curve, *k = 0.037,* final slope of the curve, *Kp= 0.00032*

The reference swell, *So*=3.27 and the peak swell, *Sp*= 3.61

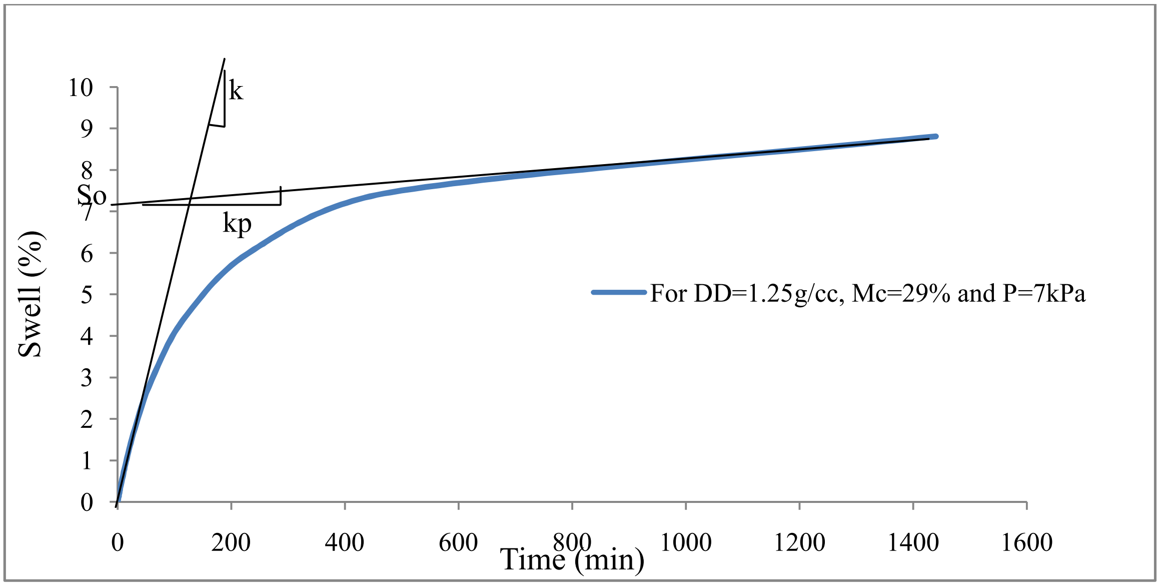

Figure B7 Parameter determination for Kality soil

Initial slope of the curve, k = *0.058,* final slope of the curve, Kp= *0.0014*

The reference swell, So=7.02 and the peak swell, Sp= 8.81

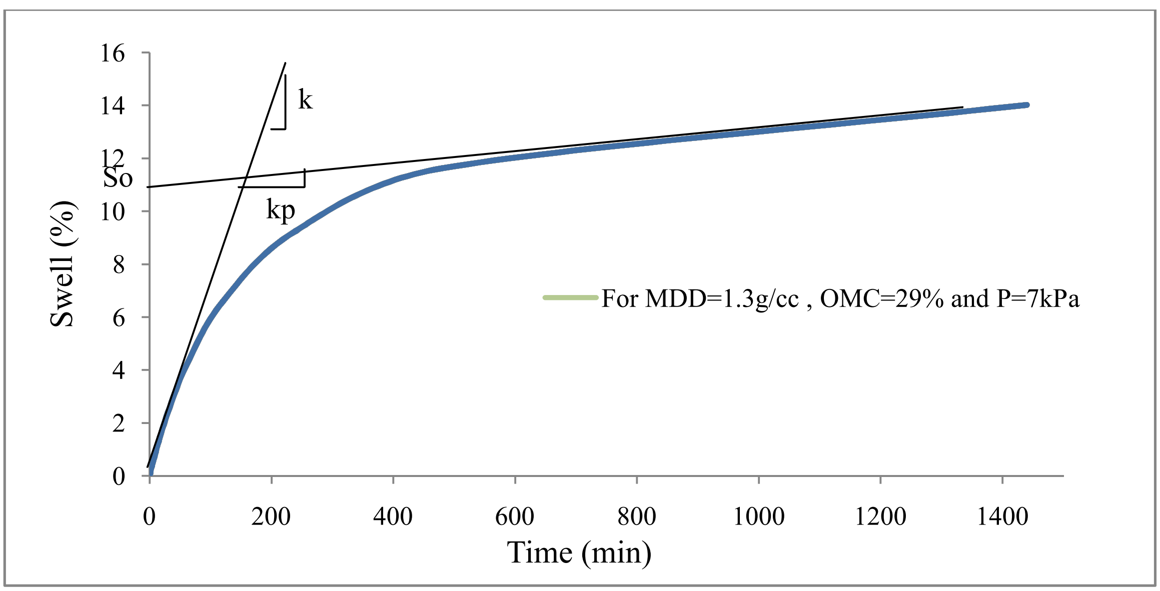

Figure B8 Parameter determination for Kality soil

Initial slope of the curve, k = *0.079,* final slope of the curve, Kp= *0.002468*

The reference swell, So=10.63and the peak swell, Sp= 14.01

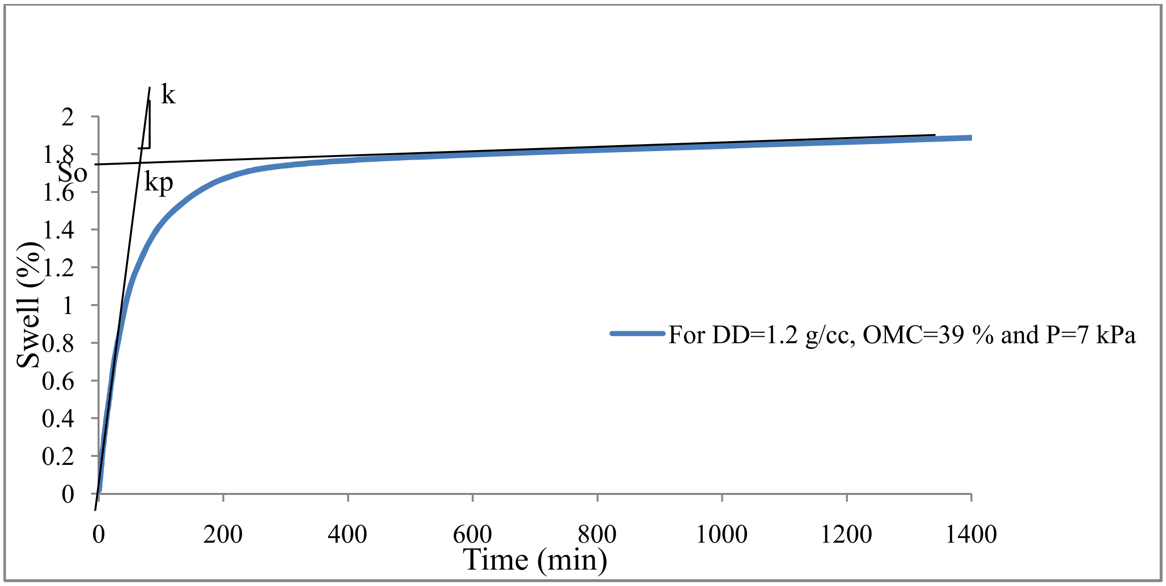

Figure B9 Parameter determination for Bole high school soil

Initial slope of the curve, *k = 0.0265,* final slope of the curve, *Kp= 1.15E-04*

The reference swell, *So*=1.73 and the peak swell, *Sp*= 1.89

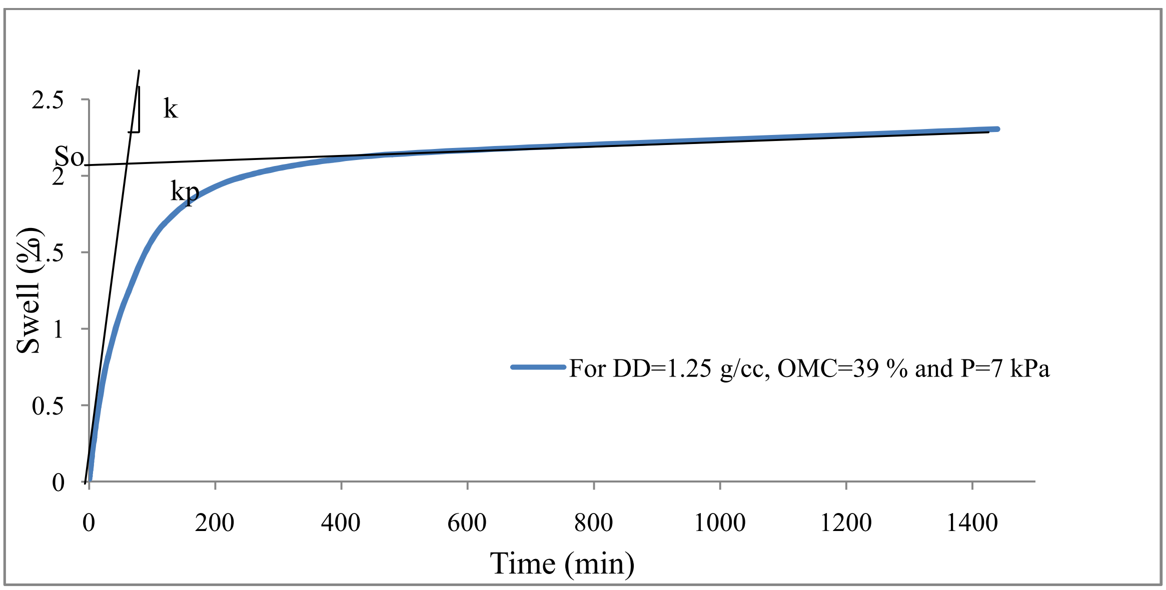

Figure B10 Parameter determination for Bole high school soil

Initial slope of the curve, *k = 0.0268,* final slope of the curve, *Kp= 1.74E-04*

The reference swell, *So*=2.1 and the peak swell, *Sp*= 2.3

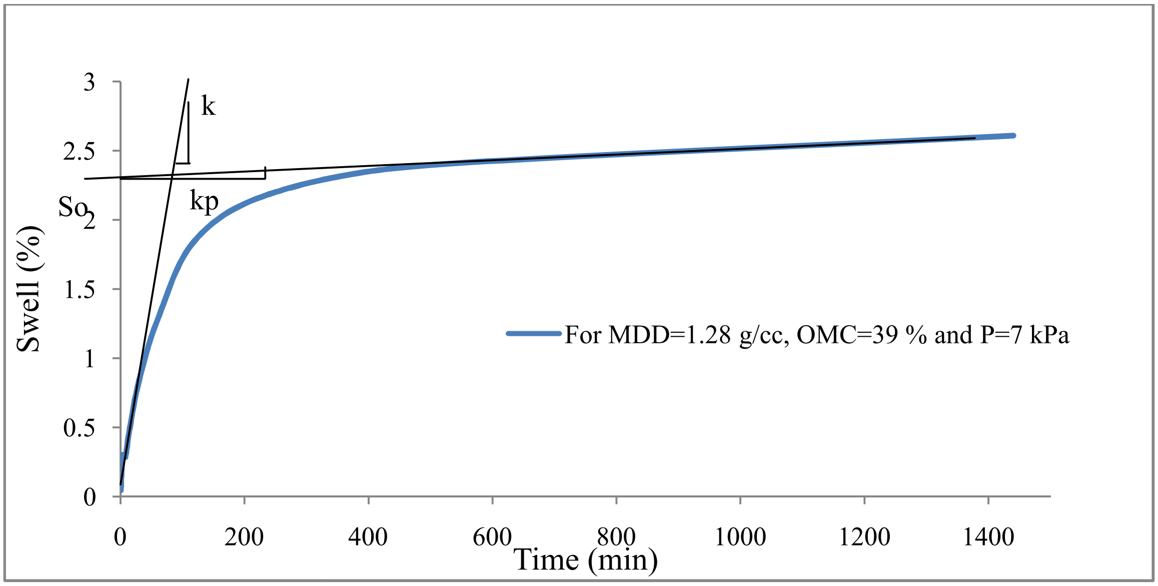

Figure B11 Parameter determination for Bole high school soil

Initial slope of the curve, $k = 0.0269$, final slope of the curve, $Kp = 2.27E\text{-}04$

The reference swell, So=2.27 and the peak swell, Sp= 2.6

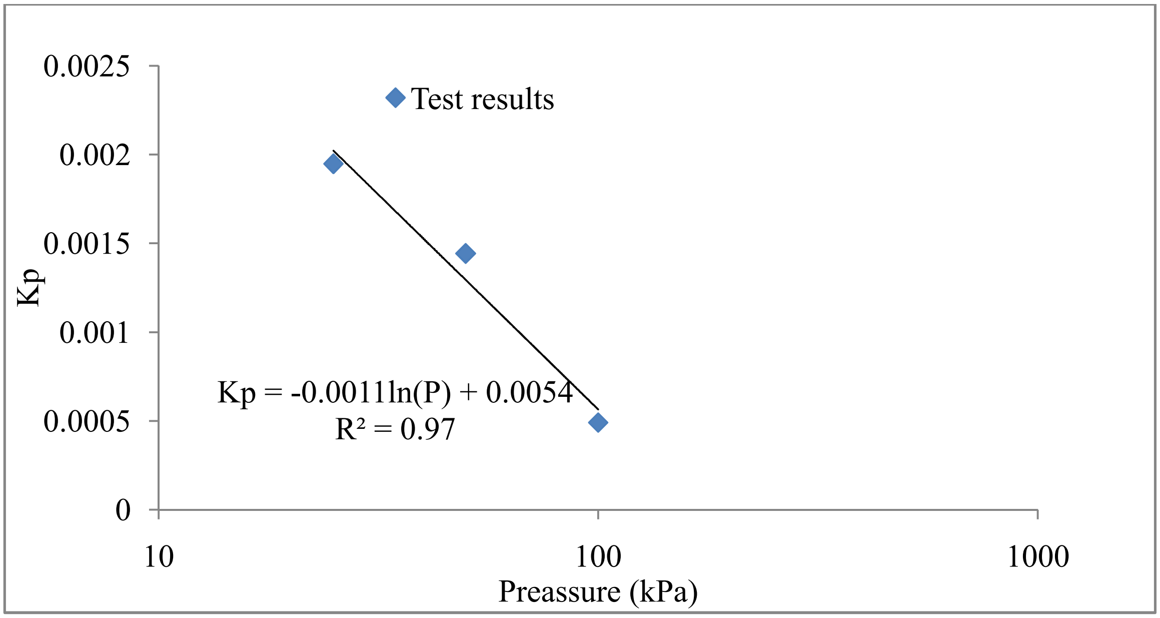

Figure B12 Variation of Kp with applied pressure for test pit No. 1

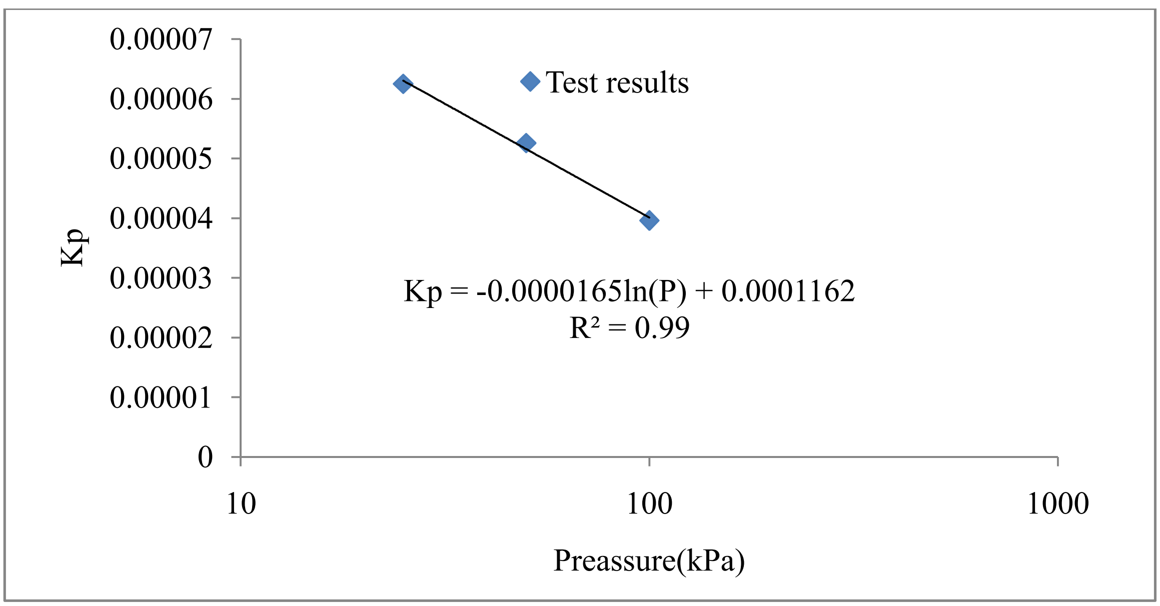

Figure B13 Variation of Kp with applied pressure for test pit No. 2

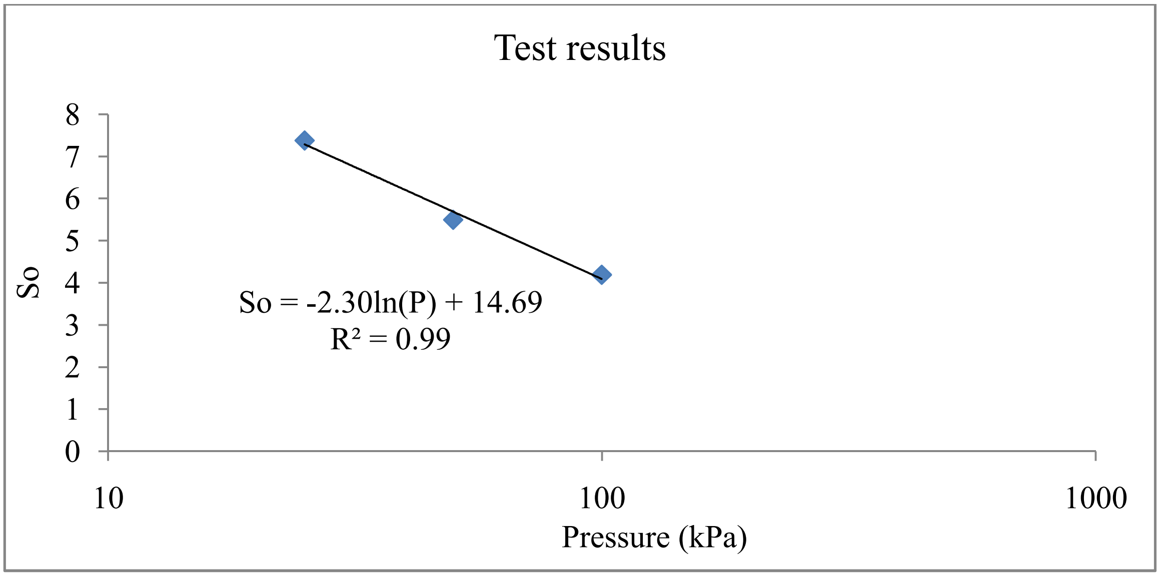

Figure B14 Variation of So with applied pressure for test pit No. 1

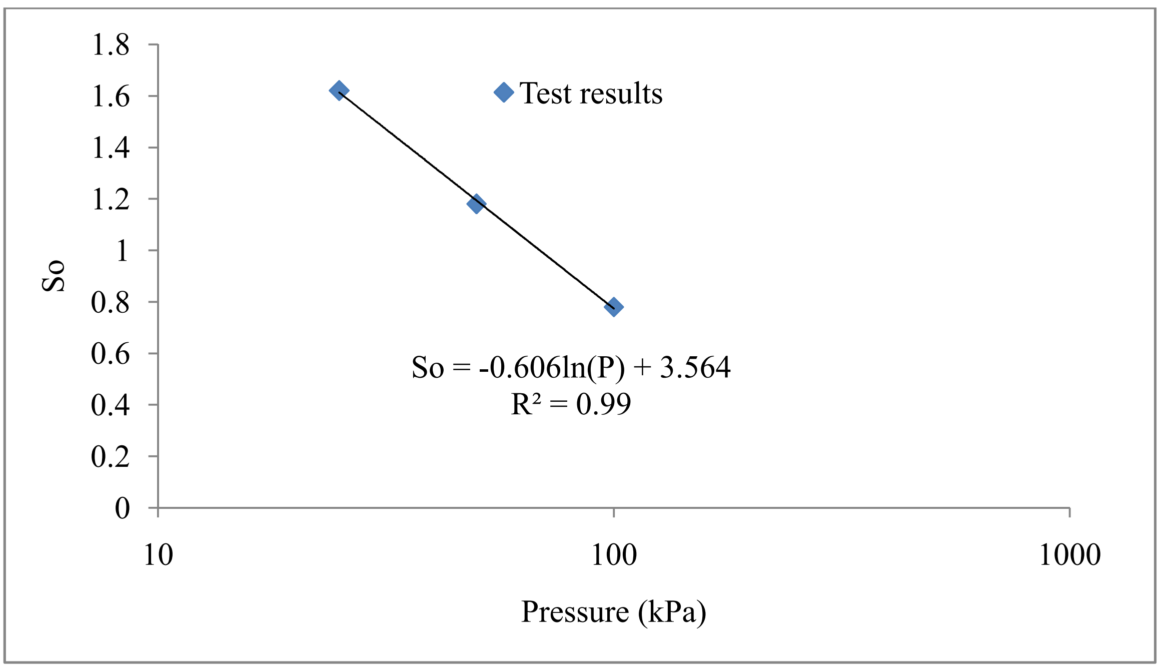

Figure B15 Variation of So with applied pressure for test pit No. 2

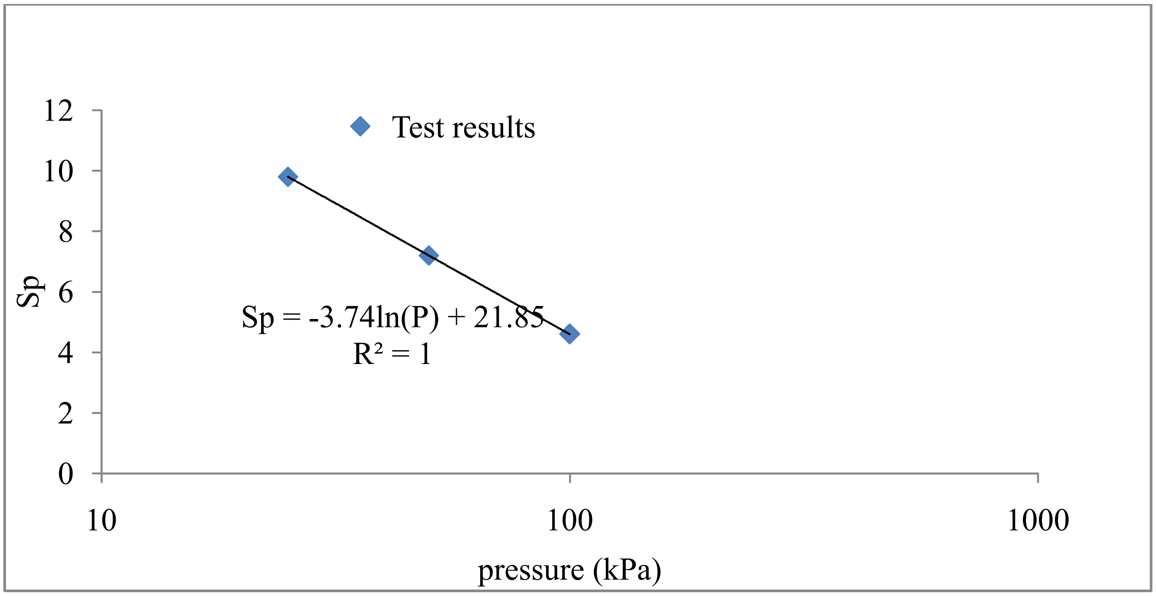

Figure B16 Variation of Sp with applied pressure for test pit No. 1

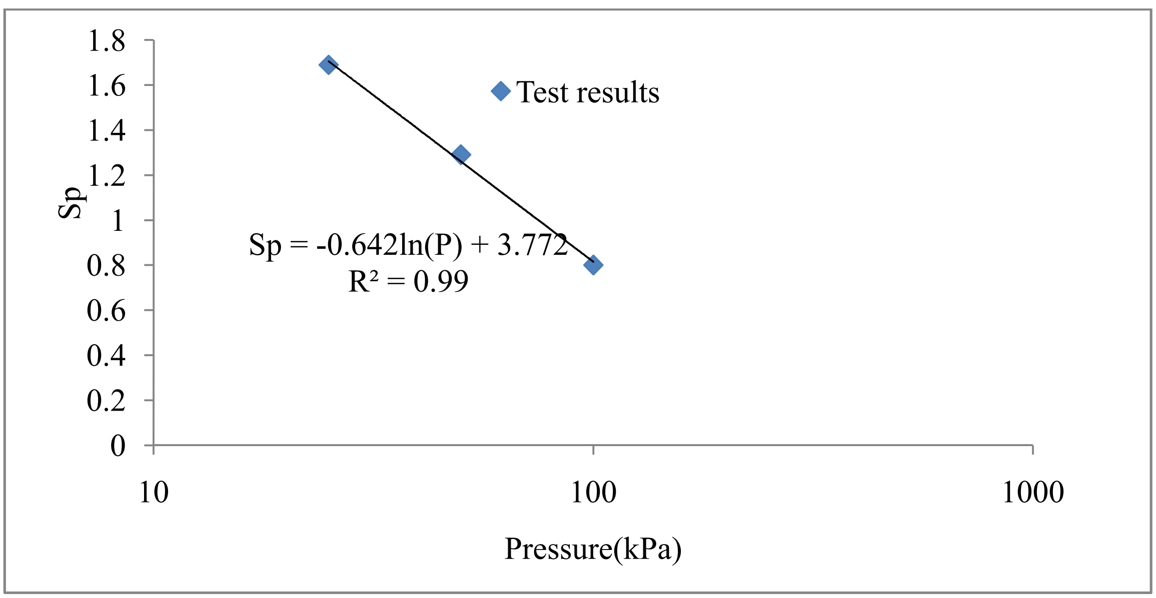

Figure B17 Variation of SP with applied pressure for test pit No. 2

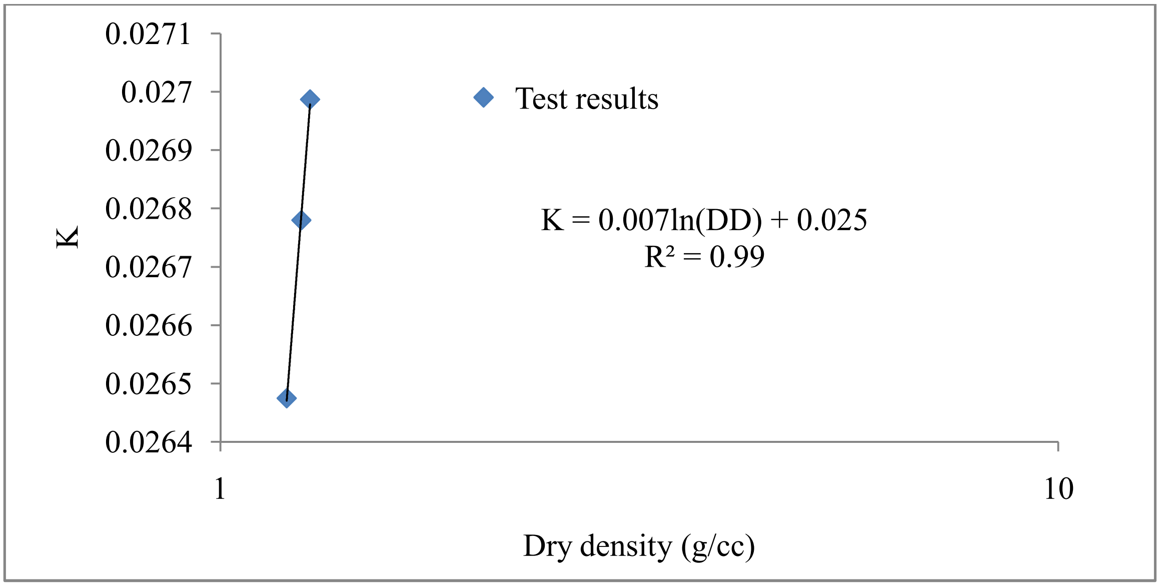

Figure B18 Variation of K with dry density for test pit No. 2

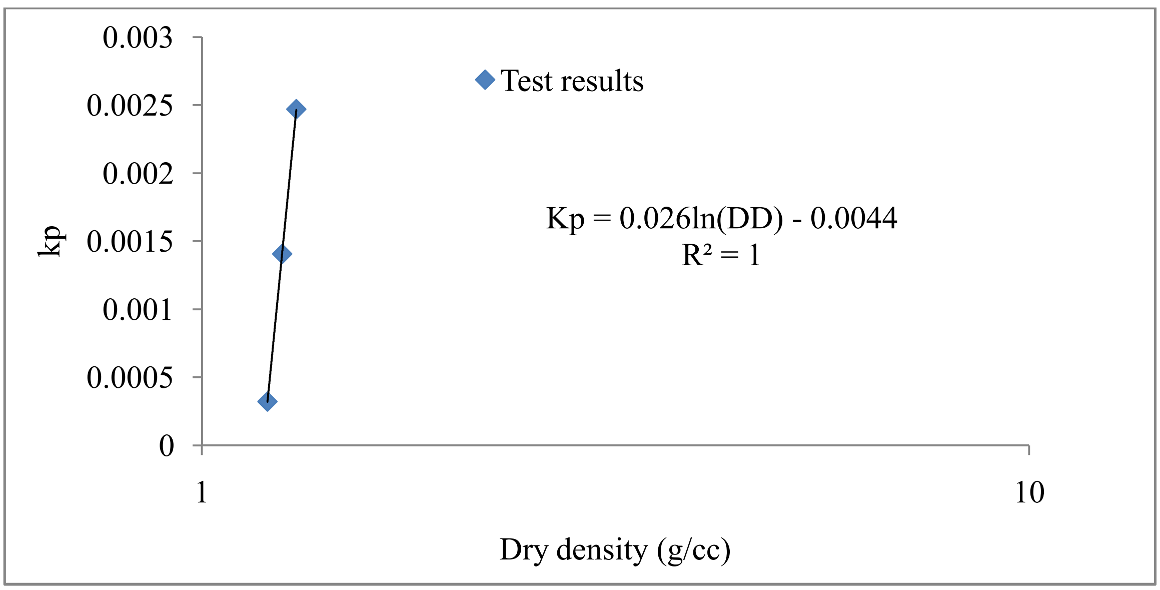

Figure B19 Variation of Kp with dry density for test pit No. 1

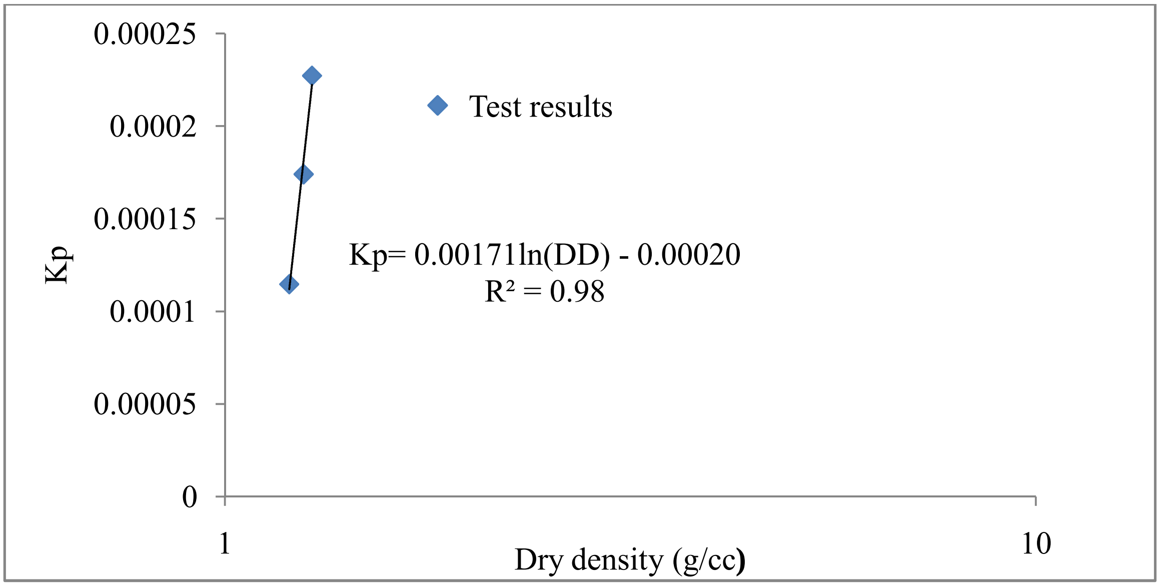

Figure B20 Variation of Kp with dry density for test pit No. 2

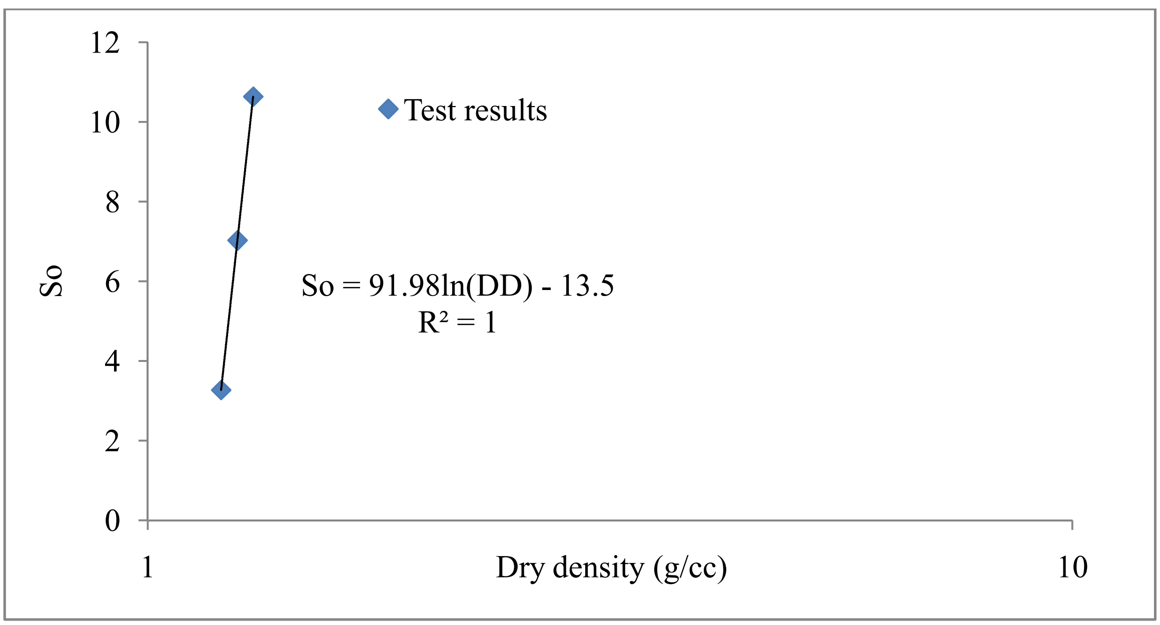

Figure B21 Variation of Kp with dry density for test pit No. 1

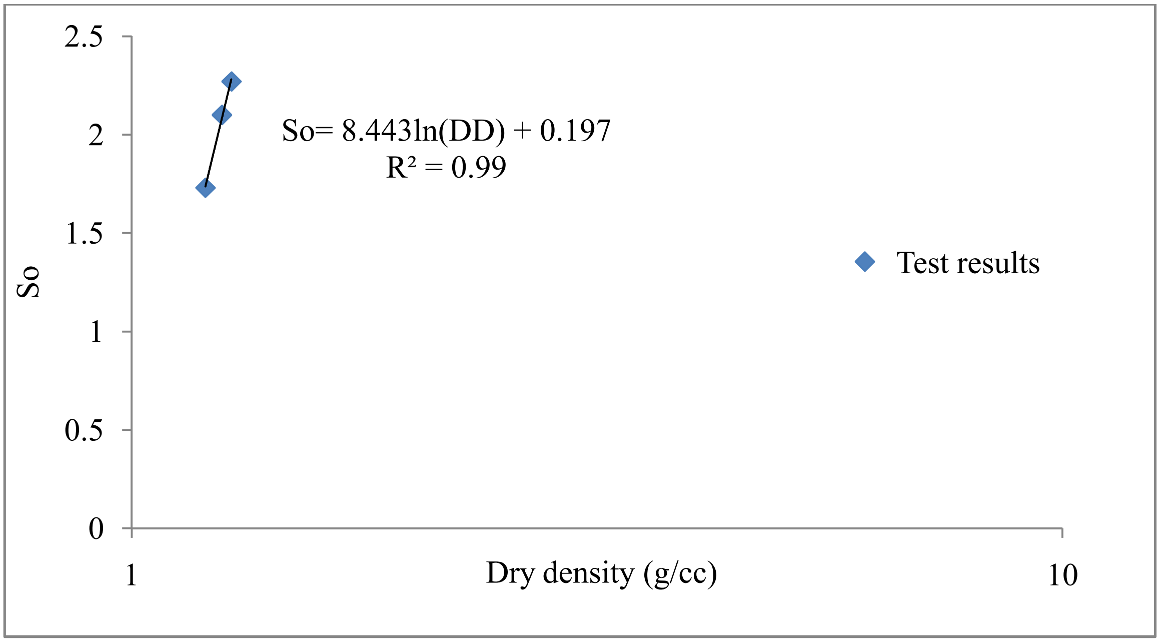

Figure B22 Variation of Kp with dry density for test pit No. 2

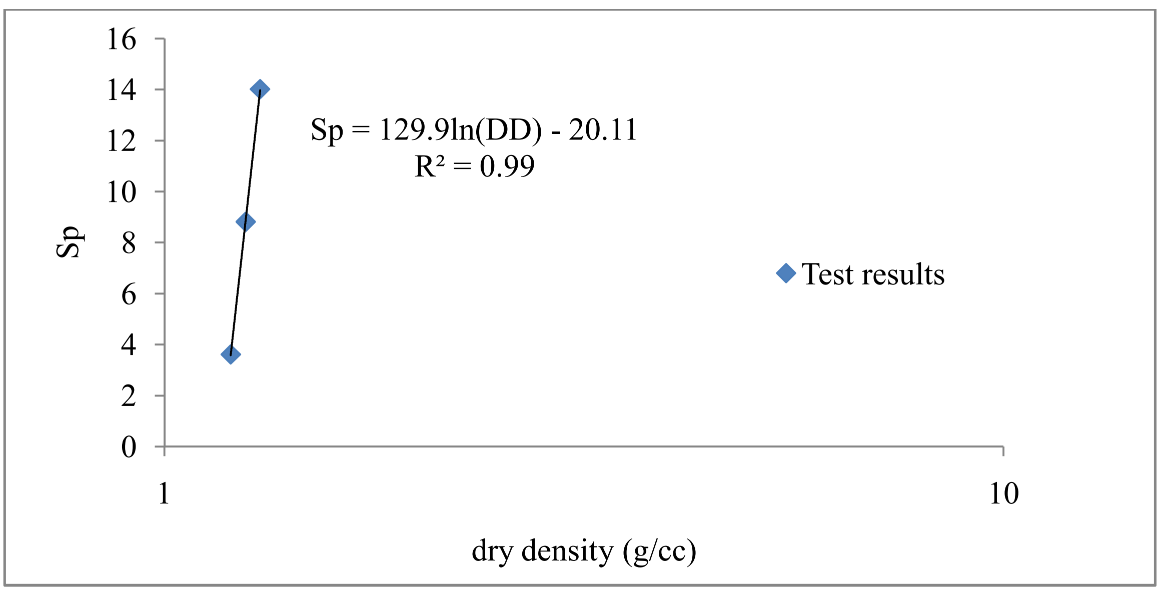

Figure B23 Variation of Sp with dry density for test pit No. 1

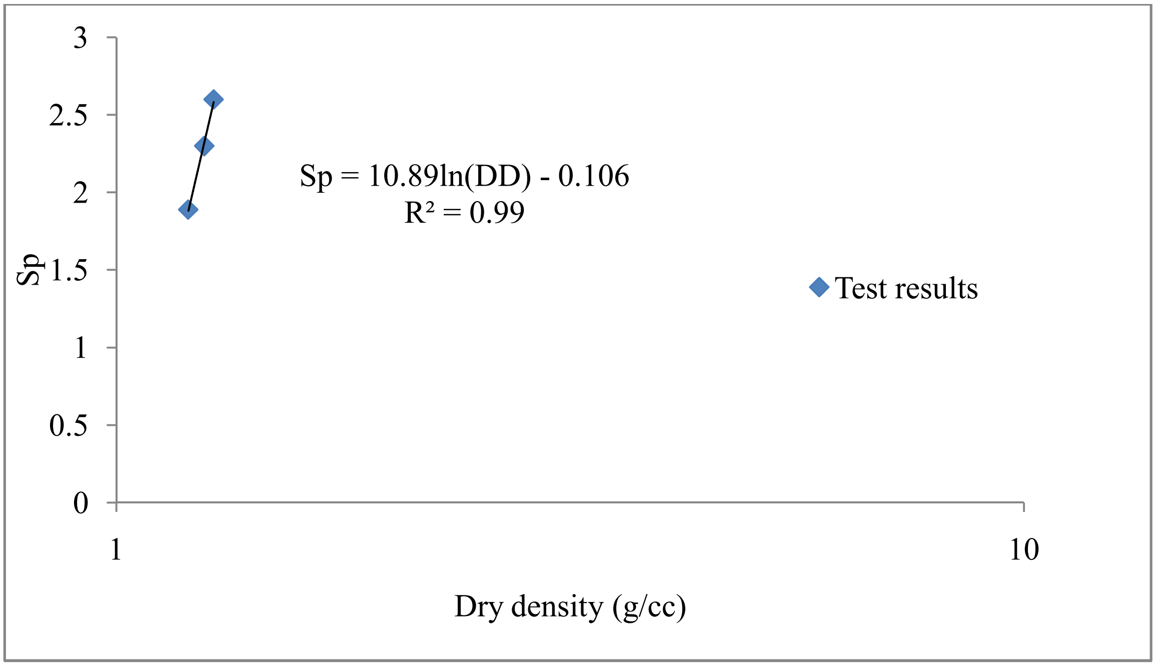

Figure B24 Variation of Sp with dry density for test pit No. 2

Appendix C
Predicted swelling using the proposed model and comparisons between predicted swelling and measured swell

Table C1 Predicted swelling using the proposed model for Kality soil (MDD= 1.3 g/cc, OMC=29 % and P=25 kPa)

m=0.0689 and lnm=-2.67

T(min)	kpT	(k-kp)	(K-Kp)*T	(k-kp)T/so	T1	S1	kp/(k-kp)	ln[(s1/s0-kp/(k-kp)]	n	(k-kp)T/s0^n	[1+((k-kP)*T/So)^n]^1/n	S
0.5	9E-04	0.0604	0.0302	0.0041	120.7	1.58	0.0308	-1.685	1.59	0.00016	1.000103639	0.031
1	0.002	0.0604	0.0604	0.0083	120.7	1.58	0.0308	-1.685	1.59	0.00049	1.000311528	0.062
2	0.004	0.0604	0.1207	0.0165	120.7	1.58	0.0308	-1.685	1.59	0.00149	1.000936309	0.124
4	0.007	0.0604	0.2414	0.0331	120.7	1.58	0.0308	-1.685	1.59	0.00447	1.002813074	0.248
8	0.015	0.0604	0.4829	0.0663	120.7	1.58	0.0308	-1.685	1.59	0.01344	1.008442402	0.494
15	0.028	0.0604	0.9054	0.1242	120.7	1.58	0.0308	-1.685	1.59	0.03646	1.022810918	0.913
30	0.056	0.0604	1.8107	0.2485	120.7	1.58	0.0308	-1.685	1.59	0.10961	1.067695118	1.752
60	0.112	0.0604	3.6215	0.4970	120.7	1.58	0.0308	-1.685	1.59	0.3295	1.196452238	3.138
120	0.223	0.0604	7.2429	0.9940	120.7	1.58	0.0308	-1.685	1.59	0.99051	1.542688828	4.918
240	0.446	0.0604	14.486	1.9880	120.7	1.58	0.0308	-1.685	1.59	2.97756	2.385720156	6.518
480	0.892	0.0604	28.972	3.9760	120.7	1.58	0.0308	-1.685	1.59	8.9508	4.250295567	7.709
1440	2.677	0.0604	86.916	11.9281	120.7	1.58	0.0308	-1.685	1.59	51.2243	12.0742838	9.876

Where: $T1 = \frac{So}{k - kp}$ $\quad S1 = Sp\left[2\frac{T1}{Tp} - \left[\frac{T1}{Tp}\right]^2\right]$ $\quad n = \frac{\ln m}{\ln\left[\frac{S1}{S0} - \frac{kp}{k - kp}\right]}$

Table C2 Predicted swelling using the proposed model for Kality soil (MDD= 1.3 g/cc, OMC=29 % and P=50 kPa)

m=0.0689 and lnm=-2.67

T(min)	kpT	(k-kp)	(K-Kp)*T	(k-kp)T/so	T1	S1	kp/(k-kp)	ln[(s1/s0-kp/(k-kp)]	n	(k-kp)T/s0^n	[1+((k-kP)*T/So)^n]^1/n	S
0.5	5E-04	0.0529	0.0265	0.0046	107.5	1.04	0.0207	-1.823	1.47	0.00038	1.00026	0.027
1	0.001	0.0529	0.0529	0.0093	107.5	1.04	0.0207	-1.823	1.47	0.00104	1.00071	0.054
2	0.002	0.0529	0.1059	0.0186	107.5	1.04	0.0207	-1.823	1.47	0.00289	1.0019	0.108
4	0.004	0.0529	0.2118	0.0372	107.5	1.04	0.0207	-1.823	1.47	0.00798	1.00543	0.215
8	0.009	0.0529	0.4235	0.0744	107.5	1.04	0.0207	-1.823	1.47	0.02207	1.01498	0.426
15	0.016	0.0529	0.7941	0.1395	107.5	1.04	0.0207	-1.823	1.47	0.05553	1.03750	0.782
30	0.033	0.0529	1.5882	0.2790	107.5	1.04	0.0207	-1.823	1.47	0.15358	1.10224	1.474
60	0.066	0.0529	3.1765	0.5580	107.5	1.04	0.0207	-1.823	1.47	0.42478	1.27278	2.561
120	0.132	0.0529	6.3529	1.1160	107.5	1.04	0.0207	-1.823	1.47	1.17486	1.69786	3.873
240	0.263	0.0529	12.7059	2.2321	107.5	1.04	0.0207	-1.823	1.47	3.24948	2.67982	5.004
480	0.526	0.0529	25.4118	4.464	107.5	1.04	0.0207	-1.823	1.47	8.98752	4.79691	5.824
1440	1.579	0.0529	76.2355	13.392	107.5	1.04	0.0207	-1.823	1.47	45.0731	13.5944	7.187

Where: $T1 = \dfrac{So}{k - kp}$ $\quad S1 = Sp\left[2\dfrac{T1}{Tp} - \left[\dfrac{T1}{Tp}\right]^2\right]$ $\quad n = \dfrac{\ln m}{\ln\left[\dfrac{S1}{S0} - \dfrac{kp}{k - kp}\right]}$

Table C3 Predicted swelling using the proposed model for Kality soil (MDD= 1.3 g/cc, OMC=29 % and P=100 kPa)

m=0.0689 and lnm=-2.67

T(min)	kpT	(k-kp)	(K-Kp)*T	(k-kp)T/so	T1	S1	kp/(k-kp)	ln[(s1/s0-kp/(k-kp)]	n	(k-kp)T/s0^n	[1+((k-kP)*T/So)^n]^1/n	S
0.5	2E-04	0.045	0.023	0.0055	90.0	0.56	0.0073	-2.05	1.31	0.0011	1.0008	0.023
1	3E-04	0.045	0.045	0.0111	90.0	0.56	0.0073	-2.05	1.31	0.0028	1.00212	0.046
2	7E-04	0.045	0.091	0.0222	90.0	0.56	0.0073	-2.05	1.31	0.0069	1.00525	0.091
4	0.001	0.045	0.182	0.0444	90.0	0.56	0.0073	-2.05	1.31	0.0170	1.01298	0.181
8	0.003	0.045	0.364	0.0889	90.0	0.56	0.0073	-2.05	1.31	0.0422	1.03206	0.356
15	0.005	0.045	0.683	0.1666	90.0	0.56	0.0073	-2.05	1.31	0.0959	1.07252	0.642
30	0.01	0.045	1.366	0.3333	90.0	0.56	0.0073	-2.05	1.31	0.2375	1.17692	1.170
60	0.02	0.045	2.731	0.6665	90.0	0.56	0.0073	-2.05	1.31	0.5882	1.42419	1.938
120	0.04	0.045	5.463	1.3330	90.0	0.56	0.0073	-2.05	1.31	1.4565	1.98777	2.788
240	0.08	0.045	10.926	2.6661	90.0	0.56	0.0073	-2.05	1.31	3.6069	3.21449	3.479
480	0.16	0.045	21.852	5.3322	90.0	0.56	0.0073	-2.05	1.31	8.9318	5.78276	3.939
1440	0.481	0.045	65.555	15.9965	90.0	0.56	0.0073	-2.05	1.31	37.593	16.3208	4.4981

Where:

$$T1 = \frac{So}{k - kp}$$

$$S1 = Sp\left[2\frac{T1}{Tp} - \left[\frac{T1}{Tp}\right]^2\right]$$

$$n = \frac{\ln m}{\ln\left[\frac{S1}{S0} - \frac{kp}{k - kp}\right]}$$

Table C4 Predicted swelling using the proposed model for Bole H. S. soil (MDD= 1.28 g/cc, OMC=39 % and P=25 kPa)

m=0.01619 and lnm=-4.123

T(min)	kpT	(k-kp)	(K-Kp)*T	(k-kp)T/So	T_1	S_1	kp/(k-kp)	$\ln[(S_1/S_0-kp/(k-kp)]$	n	$[(k-kp)T/S_0]^n$	$[1+((k-kP)*T/S_o)^n]^{1/n}$	S (%)
0.5	3E-05	0.043	0.021	0.0131	37.91	0.09	0.0015	-2.92916	1.41	0.00226	1.00160	0.021
1	6E-05	0.043	0.043	0.0263	37.91	0.09	0.0015	-2.92916	1.41	0.00599	1.004254	0.042
2	1E-04	0.043	0.085	0.0527	37.91	0.09	0.0015	-2.92916	1.41	0.01590	1.011271	0.08
4	3E-04	0.043	0.170	0.1055	37.91	0.09	0.0015	-2.92916	1.41	0.04219	1.029791	0.166
8	5E-04	0.043	0.341	0.2110	37.91	0.09	0.0015	-2.92916	1.41	0.11192	1.078283	0.316
15	9E-04	0.043	0.638	0.3956	37.91	0.09	0.0015	-2.92916	1.41	0.27116	1.185834	0.539
30	0.002	0.043	1.277	0.7913	37.91	0.09	0.0015	-2.92916	1.41	0.71939	1.469642	0.870
60	0.004	0.043	2.554	1.5827	37.91	0.09	0.0015	-2.92916	1.41	1.90855	2.135013	1.199
120	0.008	0.043	5.107	3.1655	37.91	0.09	0.0015	-2.92916	1.41	5.06344	3.597917	1.427
240	0.015	0.043	10.214	6.3310	37.91	0.09	0.0015	-2.92916	1.41	13.43345	6.662350	1.548
480	0.03	0.043	20.429	12.6621	37.91	0.09	0.0015	-2.92916	1.41	35.63930	12.91346	1.612
1440	0.091	0.043	61.286	37.9862	37.91	0.09	0.0015	-2.92916	1.41	167.31840	38.14738	1.697

Where: $T1 = \frac{So}{k - kp}$ $\quad S1 = Sp\left[2\frac{T1}{Tp} - \left[\frac{T1}{Tp}\right]^2\right]$ $\quad n = \frac{\ln m}{\ln\left[\frac{S1}{S0} - \frac{kp}{k-kp}\right]}$

Table C5 Predicted swelling using the proposed model for Bole H. S. soil (MDD= 1.28 g/cc, OMC=39 % and P=50 kPa)

m=0.01619 and lnm=-4.123

T(min)	kpT	(k-kp)	(K-Kp)*T	(k-kp)T/S_o	T_1	S_1	kp/(k-kp)	ln[(S_1/S_0-kp/(k-kp)]	n	$((k\text{-}kp)T/s0)^n$	$[1+((k\text{-}kP)*T/So)^n]^{1/n}$	S (%)
0.5	3E-05	0.029	0.014	0.0120	41.6	0.07	0.0018	-2.84211	1.45	0.00164	1.00113	0.014
1	5E-05	0.029	0.029	0.0240	41.6	0.07	0.00189	-2.84211	1.45	0.00448	1.00309	0.027
2	1E-04	0.029	0.057	0.0481	41.6	0.07	0.0018	-2.84211	1.45	0.01225	1.00843	0.057
4	2E-04	0.029	0.115	0.0962	41.6	0.07	0.0018	-2.84211	1.45	0.03349	1.02297	0.112
8	4E-04	0.029	0.229	0.1924	41.6	0.07	0.0018	-2.84211	1.45	0.09156	1.06225	0.217
15	8E-04	0.029	0.431	0.3608	41.6	0.07	0.0018	-2.84211	1.45	0.22793	1.15204	0.375
30	0.002	0.029	0.861	0.7217	41.6	0.07	0.0018	-2.84211	1.45	0.62305	1.39631	0.618
60	0.003	0.029	1.723	1.4434	41.6	0.07	0.0018	-2.84211	1.45	1.70313	1.98465	0.871
120	0.006	0.029	3.445	2.8868	41.6	0.07	0.0018	-2.84211	1.45	4.65551	3.30123	1.049
240	0.012	0.029	6.889	5.7737	41.6	0.07	0.0018	-2.84211	1.45	12.72587	6.08278	1.145
480	0.025	0.029	13.780	11.547	41.6	0.07	0.0018	-2.84211	1.45	34.78637	11.77529	1.195
1440	0.074	0.029	41.339	34.642	41.6	0.07	0.0018	-2.84211	1.45	171.23604	34.78180	1.263

Where: $T1 = \dfrac{So}{k-kp}$ $\quad S1 = Sp\left[2\dfrac{T1}{Tp} - \left[\dfrac{T1}{Tp}\right]^2\right]$ $\quad n = \dfrac{\ln m}{\ln\left[\dfrac{S1}{S0} - \dfrac{kp}{k-kp}\right]}$

Table C6 Predicted swelling using the proposed model for Bole H. S. soil (MDD= 1.28 g/cc, OMC=39 % and P=100 kPa)

m=0.01619 and lnm=-4.123

T(min)	kpT	(k-kp)	(K-Kp)*T	(k-kp)T/so	T_1	S_1	kp/(k-kp)	ln[(s1/s0-kp/(k-kp)]	n	(k-kp)T/s0^n	[1+((k-kP)*T/So)^n]^1/n	S
0.5	2E-05	0.015	0.007	0.0096	52	0.06	0.0027	-2.62897	1.57	0.00068	1.00043	0.007
1	4E-05	0.015	0.015	0.0192	52	0.06	0.0027	-2.62897	1.57	0.00203	1.00129	0.014
2	8E-05	0.015	0.029	0.038	52	0.06	0.0027	-2.62897	1.57	0.00602	1.00383	0.029
4	2E-04	0.015	0.059	0.077	52	0.06	0.0027	-2.62897	1.57	0.01787	1.01136	0.058
8	3E-04	0.015	0.119	0.153	52	0.06	0.0027	-2.62897	1.57	0.05301	1.03348	0.115
15	6E-04	0.015	0.223	0.288	52	0.06	0.0027	-2.62897	1.57	0.14209	1.08840	0.205
30	0.001	0.015	0.446	0.576	52	0.06	0.0027	-2.62897	1.57	0.42140	1.25133	0.357
60	0.002	0.015	0.891	1.153	52	0.06	0.0027	-2.62897	1.57	1.24975	1.6769	0.533
120	0.005	0.015	1.783	2.305	52	0.06	0.0027	-2.62897	1.57	3.70637	2.68477	0.668
240	0.01	0.015	3.566	4.611	52	0.06	0.0027	-2.62897	1.57	10.99198	4.87422	0.741
480	0.019	0.015	7.131	9.222	52	0.06	0.0027	-2.62897	1.5684	32.59886	9.40138	0.777
1440	0.058	0.015	21.393	27.666	52	0.06	0.0027	-2.62897	1.5684	182.60186	27.7624	0.828

Where: $T1 = \dfrac{So}{k - kp}$ $\quad S1 = Sp\left[2\dfrac{T1}{Tp} - \left[\dfrac{T1}{Tp}\right]^2\right]$ $\quad n = \dfrac{\ln m}{\ln\left[\dfrac{S1}{S0} - \dfrac{kp}{k - kp}\right]}$

Table C7 Predicted swelling using the proposed model for Kality soil (MDD= 1.3 g/cc, OMC=29 % and P=7 kPa)

m=0.0689 and lnm=-2.67

T(min)	kpT	(k-kp)	(K-Kp)*T	(k-kp)T/so	T_1	S_1	kp/(k-kp)	ln(s1/s2-kp/(k-kp)	n	(k-kp)T/s0^n	[1+((k-kP)*T/So)^n]^1/n	S
0.5	0.001	0.078	0.0388	0.004	137	2.53	0.0295	-1.56941	1.70	7.018E-05	1.00004	0.05
1	0.002	0.078	0.0777	0.01	137	2.53	0.0295	-1.56941	1.70	0.000228	1.00013	0.08
2	0.004	0.078	0.1555	0.01	137	2.53	0.0295	-1.56941	1.70	0.000745	1.00043	0.16
4	0.009	0.078	0.3110	0.03	137	2.53	0.0295	-1.56941	1.70	0.002429	1.00140	0.32
8	0.018	0.078	0.6220	0.06	137	2.53	0.0295	-1.56941	1.70	0.007918	1.00463	0.64
15	0.035	0.078	1.1663	0.11	137	2.53	0.0295	-1.56941	1.70	0.023120	1.01350	1.19
30	0.069	0.078	2.3326	0.22	137	2.53	0.0295	-1.56941	1.70	0.075355	1.04354	2.30
60	0.138	0.078	4.6653	0.44	137	2.53	0.0295	-1.56941	1.70	0.245599	1.13751	4.24
120	0.277	0.078	9.3307	0.88	137	2.53	0.0295	-1.56941	1.70	0.800458	1.41197	6.88
240	0.551	0.078	18.661	1.76	137	2.53	0.0295	-1.56941	1.70	2.608857	2.12322	9.34
480	1.102	0.078	37.323	3.51	137	2.53	0.0295	-1.56941	1.70	8.502801	3.74698	11.06
1440	3.307	0.078	111.969	10.5	137	2.53	0.0295	-1.56941	1.70	55.31269	10.6423	13.83

Where: $T1 = \frac{So}{k - kp}$ $\quad S1 = Sp\left[2\frac{T1}{Tp} - \left[\frac{T1}{Tp}\right]^2\right]$ $\quad n = \frac{\ln m}{\ln\left[\frac{S1}{S0} - \frac{kp}{k - kp}\right]}$

Table C8 Predicted swelling using the proposed model for Kality soil (DD= 1.25 g/cc, OMC=29 % and P=7 kPa)

m=0.0689 and lnm=-2.67

T(min)	kpT	(k-kp)	(K-Kp)*T	(k-kp)T/S_o	T_1	S_1	kp/(k-kp)	ln(S_1/S_o-kp/(k-kp)	n	((k-kp)T/S_0)^n	[1+((k-kP)*T/S_o)^n]$^{1/n}$	S
0.5	0.0007	0.058	0.029	0	121	1.43	0.0234	-1.71196	1.56	0.00018	1.00012	0.029
1	0.0014	0.058	0.058	0.01	121	1.43	0.0234	-1.71196	1.56	0.00055	1.00035	0.059
2	0.0027	0.058	0.116	0.02	121	1.43	0.0234	-1.71196	1.56	0.00163	1.00104	0.118
4	0.0054	0.058	0.232	0.03	121	1.43	0.0234	-1.71196	1.56	0.0048	1.00309	0.236
8	0.0108	0.058	0.463	0.07	121	1.43	0.0234	-1.71196	1.56	0.01428	1.00912	0.469
15	0.0203	0.058	0.868	0.12	121	1.43	0.0234	-1.71196	1.56	0.03815	1.02425	0.868
30	0.0407	0.058	1.737	0.25	121	1.43	0.0234	-1.71196	1.56	0.1126	1.07072	1.663
60	0.0813	0.058	3.474	0.49	121	1.43	0.0234	-1.71196	1.56	0.33287	1.20187	2.972
120	0.1627	0.058	6.949	0.99	121	1.43	0.0234	-1.71196	1.56	0.98326	1.54993	4.646
240	0.3253	0.058	13.898	1.98	121	1.43	0.0234	-1.71196	1.56	2.90441	2.39096	6.138
480	0.6506	0.058	27.797	3.96	121	1.43	0.0234	-1.71196	1.56	8.57919	4.24631	7.196
1440	1.9518	0.058	83.391	11.9	121	1.43	0.0234	-1.71196	1.56	47.7522	12.02958	8.884

Where: $T1 = \frac{So}{k - kp}$ $S1 = Sp\left[2\frac{T1}{Tp} - \left[\frac{T1}{Tp}\right]^2\right]$ $n = \frac{\ln m}{\ln\left[\frac{S1}{S0} - \frac{kp}{k - kp}\right]}$

Table C9 Predicted swelling using the proposed model for Kality soil (DD= 1.2 g/cc, OMC=29 % and P=7 kPa)

m=0.0689 and lnm=-2.67

T(min)	kpT	(k-kp)	(K-Kp)*T	(k-kp)T/S_o	T_1	S_1	kp/(k-kp)	ln(s1/s2-kp/(k-kp)	n	((k-kp)T/S_o) ^{n}	[1+((k-kP)*T/S_o)^n]$^{1/n}$	S
0.5	0.0002	0.037	0.0186	0.01	87.8	0.42	0.0101	-2.12795	1.26	0.00150	1.00119	0.019
1	0.0004	0.037	0.0372	0.01	87.8	0.42	0.0101	-2.12795	1.26	0.00360	1.00286	0.038
2	0.0008	0.037	0.0745	0.02	87.8	0.42	0.0101	-2.12795	1.26	0.00861	1.00684	0.075
4	0.0015	0.037	0.1490	0.05	87.8	0.42	0.0101	-2.12795	1.26	0.02059	1.01635	0.148
8	0.003	0.037	0.2980	0.09	87.8	0.42	0.0101	-2.12795	1.26	0.04923	1.03896	0.2896
15	0.0056	0.037	0.5588	0.17	87.8	0.42	0.0101	-2.12795	1.26	0.10850	1.08539	0.520
30	0.0113	0.037	1.1176	0.34	87.8	0.42	0.0101	-2.12795	1.26	0.25935	1.20133	0.941
60	0.0225	0.037	2.2352	0.68	87.8	0.42	0.0101	-2.12795	1.26	0.61989	1.46770	1.545
120	0.0451	0.037	4.4705	1.37	87.8	0.42	0.0101	-2.12795	1.26	1.48165	2.06064	2.215
240	0.0902	0.037	8.9411	2.73	87.8	0.42	0.0101	-2.12795	1.26	3.54142	3.33253	2.773
480	0.1803	0.037	17.88	5.47	87.8	0.42	0.0101	-2.12795	1.26	8.46465	5.97667	3.172
1440	0.541	0.037	53.646	16.4	87.8	0.42	0.0101	-2.12795	1.26	33.68282	16.79234	3.736

Where: $T1 = \dfrac{So}{k - kp}$ $\quad S1 = Sp\left[2\dfrac{T1}{Tp} - \left[\dfrac{T1}{Tp}\right]^2\right]$ $\quad n = \dfrac{\ln m}{\ln\left[\dfrac{S1}{S0} - \dfrac{kp}{k-kp}\right]}$

Table C10 Predicted swelling using the proposed model for Bole H. S. soil (MDD= 1.28 g/cc, OMC=39 % and P=7 kPa)

m=0.01619 and lnm=-4.123

T(min)	kpT	(k-kp)	(K-Kp)*T	(k-kp)T/S_o	T_1	S_1	kp/(k-kp)	ln(S_1/S_2-kp/(k-kp)	n	((k-kp)T/S_0)^n	[1+((k-kP)*T/So)^n]$^{1/n}$	S
0.5	0.0001	0.03	0.014	0.01	83.9	0.29	0.008	-2.12171	1.94	4.75E-05	1.00002	0.014
1	0.0002	0.03	0.027	0.01	83.9	0.29	0.008	-2.12171	1.94	0.00018	1.00009	0.027
2	0.0004	0.03	0.054	0.02	83.9	0.29	0.008	-2.12171	1.94	0.00070	1.00036	0.055
4	0.0009	0.03	0.109	0.05	83.9	0.29	0.008	-2.12171	1.94	0.00270	1.00139	0.109
8	0.0018	0.03	0.217	0.09	83.9	0.29	0.008	-2.12171	1.94	0.0104	1.00533	0.218
15	0.0033	0.03	0.408	0.18	83.9	0.29	0.008	-2.12171	1.94	0.03527	1.01799	0.404
30	0.0067	0.03	0.816	0.36	83.9	0.29	0.008	-2.12171	1.94	0.13567	1.06765	0.771
60	0.0133	0.03	1.632	0.71	83.9	0.29	0.008	-2.12171	1.94	0.52181	1.24118	1.329
120	0.02666	0.03	3.265	1.43	83.9	0.29	0.008	-2.12171	1.94	2.00695	1.76207	1.879
240	0.05331	0.03	6.529	2.86	83.9	0.29	0.008	-2.12171	1.94	7.71904	3.04738	2.196
480	0.10662	0.03	13.059	5.72	83.9	0.29	0.008	-2.12171	1.94	29.68854	5.82286	2.349
1440	0.31987	0.03	39.177	17.17	83.9	0.29	0.008	-2.12171	1.9434	251.09182	17.20849	2.596

Where: $T1 = \frac{So}{k - kp}$ $S1 = Sp\left[2\frac{T1}{Tp} - \left[\frac{T1}{Tp}\right]^2\right]$ $n = \frac{\ln m}{\ln\left[\frac{S1}{S0} - \frac{kp}{k - kp}\right]}$

Table C11 Predicted swelling using the proposed model for Bole H. S. soil (DD= 1.25g/cc, OMC=39 % and P=7 kPa)

m=0.01619 and lnm=-4.123

T(min)	kpT	(k-kp)	(K-Kp)*T	(k-kp)T/so	T_1	S_1	kp/(k-kp)	$\ln(S_1/S_o$-kp/(k-kp))	n	$((k-kp)T/S_o)^n$	$[1+((k-kP)*T/S_o)^n]^{1/n}$	S (%)
0.5	9.08E-05	0.027	0.014	0.0065	76.9	0.24	0.007	-2.21358	1.86	8.44909E-05	1.00005	0.014
1	0.00018	0.027	0.027	0.0130	76.9	0.24	0.007	-2.21358	1.86	0.00031	1.00016	0.027
2	0.00036	0.027	0.054	0.0260	76.9	0.24	0.007	-2.21358	1.86	0.00112	1.00059	0.05
4	0.00073	0.027	0.108	0.0520	76.9	0.24	0.007	-2.21358	1.86	0.00406	1.00218	0.109
8	0.00145	0.027	0.217	0.1041	76.9	0.24	0.007	-2.21358	1.86	0.01478	1.00791	0.216
15	0.00272	0.027	0.406	0.1952	76.9	0.24	0.0071	-2.21358	1.86	0.04768	1.02532	0.399
30	0.00545	0.027	0.812	0.3904	76.9	0.24	0.007	-2.21358	1.86	0.17341	1.08964	0.751
60	0.01089	0.027	1.625	0.7808	76.9	0.24	0.007	-2.21358	1.86	0.63069	1.30019	1.261
120	0.02179	0.027	3.249	1.5616	76.9	0.24	0.007	-2.21358	1.86	2.29384	1.89637	1.735
240	0.04358	0.027	6.499	3.1232	76.9	0.24	0.007	-2.21358	1.86	8.34274	3.31886	2.002
480	0.08716	0.027	12.999	6.2463	76.9	0.24	0.007	-2.21358	1.86	30.34272	6.35601	2.132
1440	0.26147	0.027	38.996	18.7389	76.9	0.244	0.007	-2.213583	1.86	234.863	18.78176	2.338

Where: $T1 = \frac{So}{k - kp}$ $\quad S1 = Sp\left[2\frac{T1}{Tp} - \left[\frac{T1}{Tp}\right]^2\right]$ $\quad n = \frac{\ln m}{\ln\left[\frac{S1}{S0} - \frac{kp}{k - kp}\right]}$

Table C12 Predicted swelling using the proposed model for Bole H. S. Soil (DD= 1.2g/cc, OMC=39 % and P=7 kPa)

m=0.01619 and lnm=-4.123

T(min)	kpT	(k-kp)	(K-Kp)*T	(k-kp)T/S_o	T_1	S_1	kp/(k-kp)	ln(s1/s2-kp/(k-kp)	n	$((k-kp)T/s0)^n$	$[1+((k-kP)*T/S_o)^n]^{1/n}$	S
0.5	5.8E-05	0.027	0.013	0.00773	64.6	0.165	0.004	-2.39879	1.72	0.00023	1.00014	0.014
1	0.0001	0.027	0.027	0.01547	64.6	0.165	0.004	-2.39879	1.72	0.00077	1.00045	0.027
2	0.0002	0.027	0.054	0.03094	64.6	0.165	0.004	-2.39879	1.72	0.00254	1.00148	0.054
4	0.0004	0.027	0.107	0.06188	64.6	0.165	0.004	-2.39879	1.72	0.00837	1.00486	0.107
8	0.0008	0.027	0.215	0.12377	64.6	0.165	0.004	-2.39879	1.72	0.02756	1.01594	0.212
15	0.0016	0.027	0.403	0.23207	64.6	0.165	0.004	-2.39879	1.72	0.08120	1.04647	0.387
30	0.0033	0.027	0.806	0.46415	64.6	0.165	0.004	-2.39879	1.72	0.26731	1.14777	0.706
60	0.0067	0.027	1.612	0.92831	64.6	0.165	0.004	-2.39879	1.72	0.87997	1.44374	1.123
120	0.0134	0.027	3.224	1.85662	64.6	0.165	0.004	-2.39879	1.72	2.89680	2.20622	1.47
240	0.0269	0.027	6.447	3.71325	64.6	0.165	0.004	-2.39879	1.72	9.536	3.93505	1.66
480	0.0536	0.027	12.895	7.42650	64.6	0.165	0.004	-2.39879	1.72	31.3921	7.56323	1.76
1440	0.1609	0.027	38.685	22.2795	64.6	0.165	0.004	-2.39879	1.72	207.472	22.34194	1.89

Where: $T1 = \frac{So}{k - kp}$ $S1 = Sp\left[2\frac{T1}{Tp} - \left[\frac{T1}{Tp}\right]^2\right]$ $n = \frac{\ln m}{\ln\left[\frac{S1}{S0} - \frac{kp}{k - kp}\right]}$

Table C13 Comparisons of Eqn. 2.3 and Eqn. 2.6 (OMC=29 % and MDD=1.3 g/cc)

time (min)	P=100kPa			P=50 kPa			P=25 kPa		
	eqn 2.3	eqn 2.6	meaured	eqn 2.3	eqn 2.6	meaured	eqn 2.3	eqn 2.6	meaured
0.5	0.023841	0.023	0.03	0.02927	0.027	0.035	0.0379	0.031	0.04
1	0.047451	0.046	0.059	0.058294	0.054	0.06	0.075559	0.062	0.078
2	0.09399	0.091	0.115	0.115615	0.108	0.115	0.150164	0.124	0.155
4	0.184432	0.181	0.225	0.227434	0.215	0.225	0.296585	0.248	0.3
8	0.355448	0.356	0.44	0.44041	0.426	0.44	0.578744	0.494	0.58
15	0.626584	0.642	0.775	0.782255	0.782	0.81	1.040847	0.913	1.035
30	1.110738	1.17	1.39	1.405776	1.474	1.61	1.914246	1.752	1.88
60	1.810033	1.938	2.29	2.337276	2.561	2.5	3.29793	3.138	3.17
120	2.641568	2.788	3.075	3.495316	3.873	3.85	5.164452	4.918	4.825
240	3.42928	3.479	3.71	4.646374	5.004	4.975	7.202702	6.518	6.53
480	4.030176	3.939	4.135	5.562236	5.824	5.815	8.97348	7.709	7.932
1440	4.563239	4.498	4.605	6.403746	7.187	7.2	10.73254	9.876	9.8

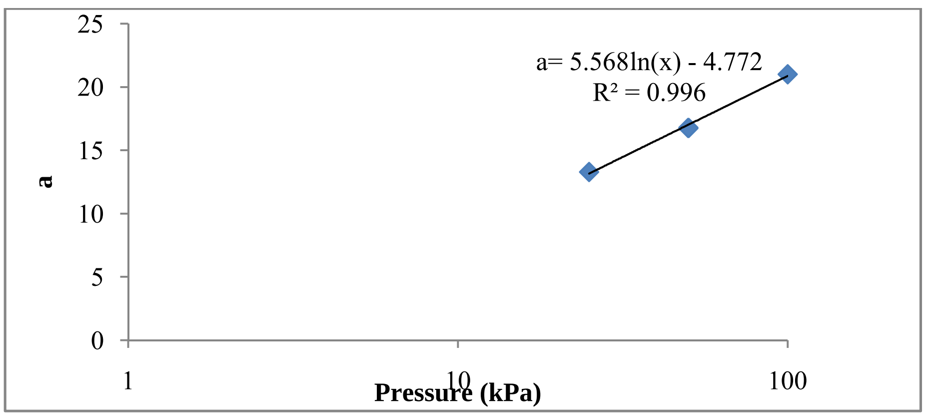

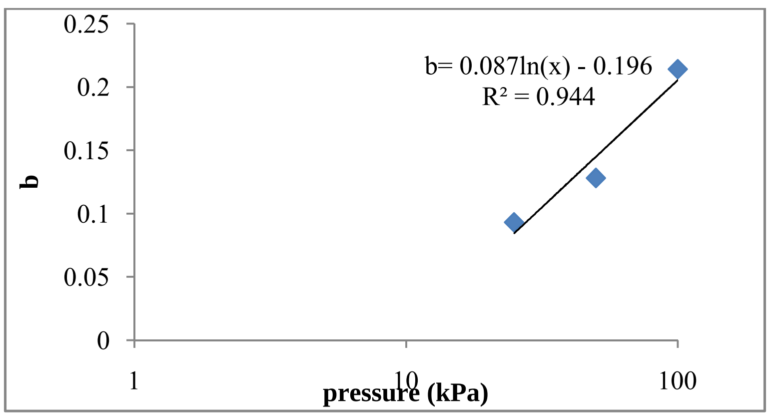

Table C14 Comparisons of Eqn. 2.3 and Eqn. 2.6 (OMC=39 % and MDD=1.28g/cc) for Bole high school soil

time (min)	P=100kPa			P=50 kPa			P=25 kPa		
	eqn 2.3	eqn 2.6	meaured	eqn 2.3	eqn 2.6	meaured	eqn 2.3	eqn 2.6	meaured
0.5	0.010706	0.007	0.0115	0.01518	0.014	0.012	0.026078	0.021	0.03
1	0.021149	0.014	0.0225	0.029974	0.027	0.023	0.05144	0.042	0.059
2	0.041281	0.029	0.0435	0.058461	0.057	0.045	0.100132	0.08	0.115
4	0.078776	0.058	0.08	0.111393	0.112	0.089	0.190106	0.166	0.215
8	0.144315	0.115	0.15	0.203538	0.217	0.17	0.345196	0.316	0.38
15	0.235906	0.205	0.24	0.33151	0.375	0.285	0.557406	0.539	0.595
30	0.370142	0.357	0.375	0.517401	0.618	0.569	0.85925	0.87	0.89
60	0.517328	0.533	0.515	0.718983	0.871	0.79	1.178276	1.199	1.175
120	0.645711	0.668	0.63	0.892927	1.049	1	1.446879	1.427	1.4
240	0.737182	0.741	0.715	1.015805	1.145	1.13	1.633011	1.548	1.545
480	0.793377	0.777	0.765	1.090862	1.195	1.2	1.74527	1.612	1.635
1440	0.835855	0.828	0.8	1.147382	1.263	1.29	1.829096	1.697	1.695

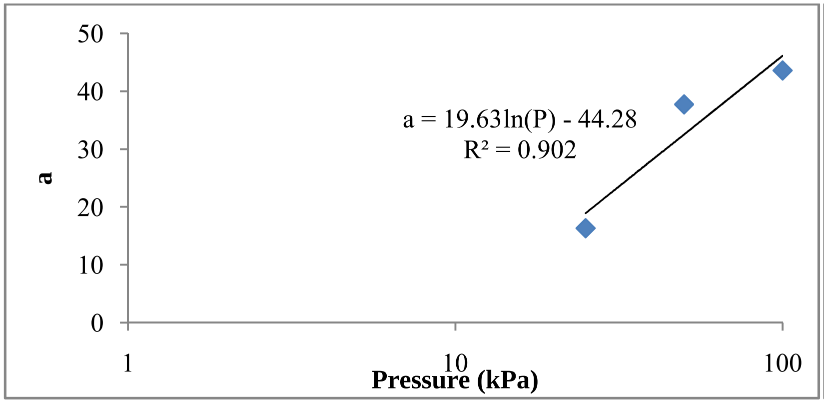

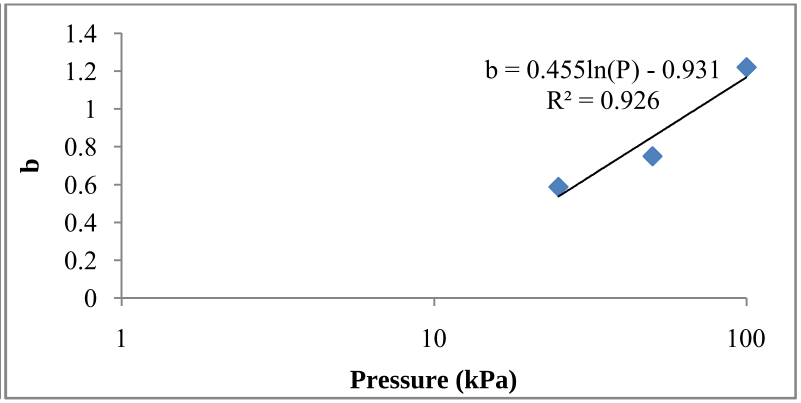

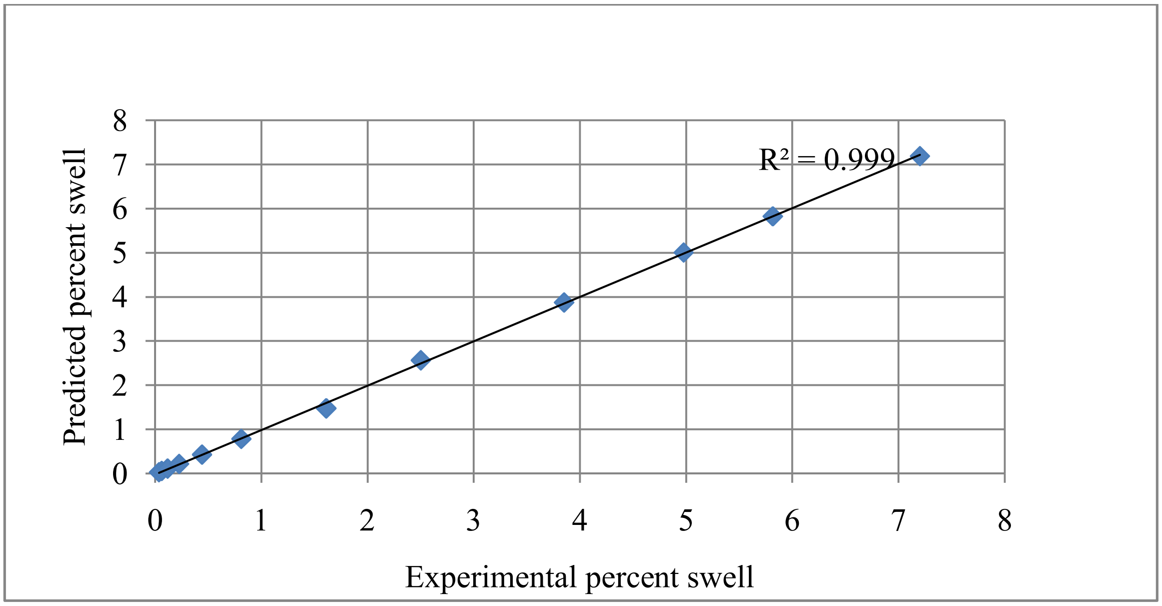

Figure C1 Relationships between experimental swell and predicted swell for Kality soil (OMC=29 %, MDD=1.3 g/cc and P=50 kPa)

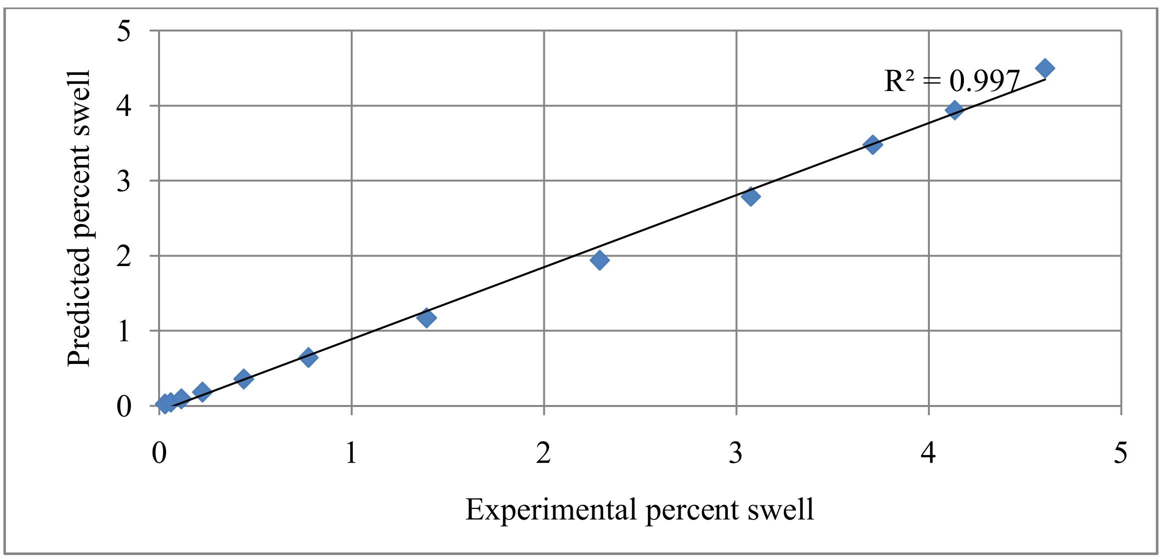

Figure C2 Relationships between experimental swell and predicted swell for Kality soil (OMC=29 %, MDD=1.3 g/cc and P=100 kPa)

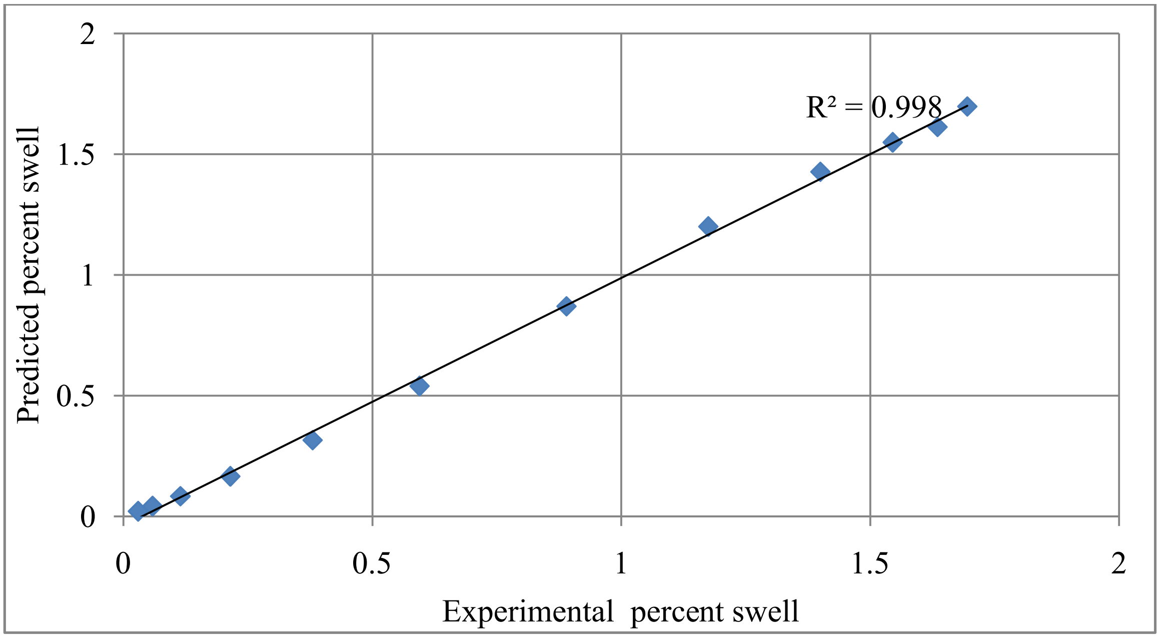

Figure C3 Relationships between experimental swell and predicted swell for Bole high school soil (OMC=39 %, MDD=1.28 g/cc and P=25 kPa)

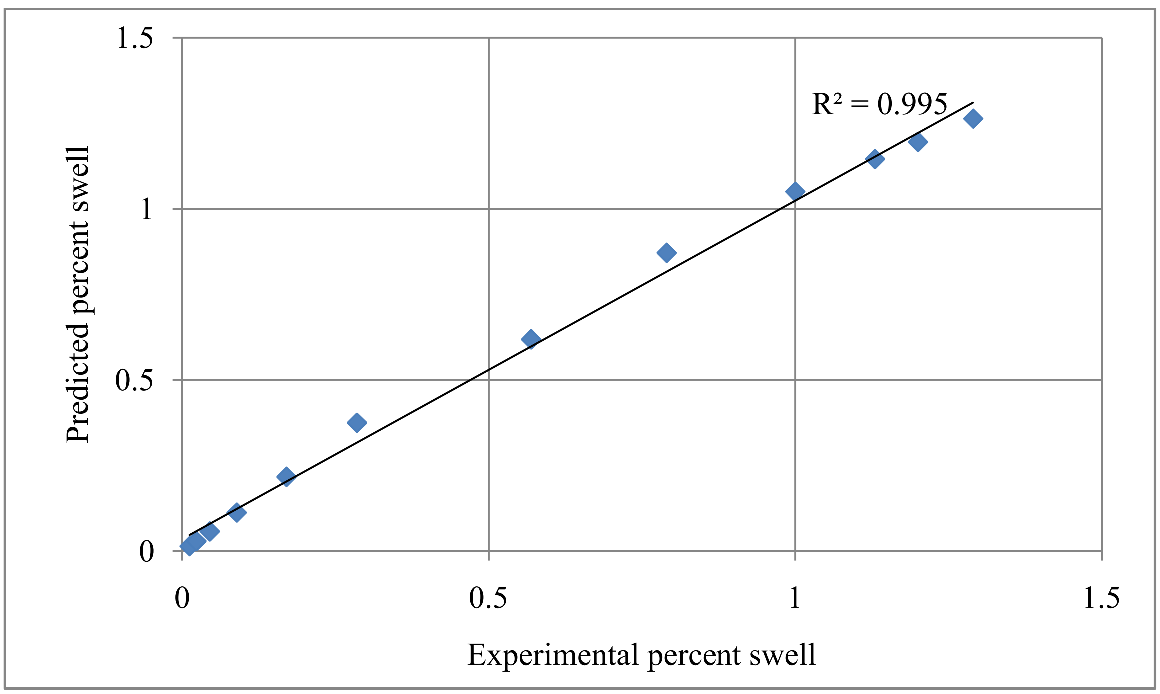

Figure C4 Relationships between experimental swell and predicted swell for Bole high school soil (OMC=39 %, MDD=1.28 g/cc and P=50 kPa)

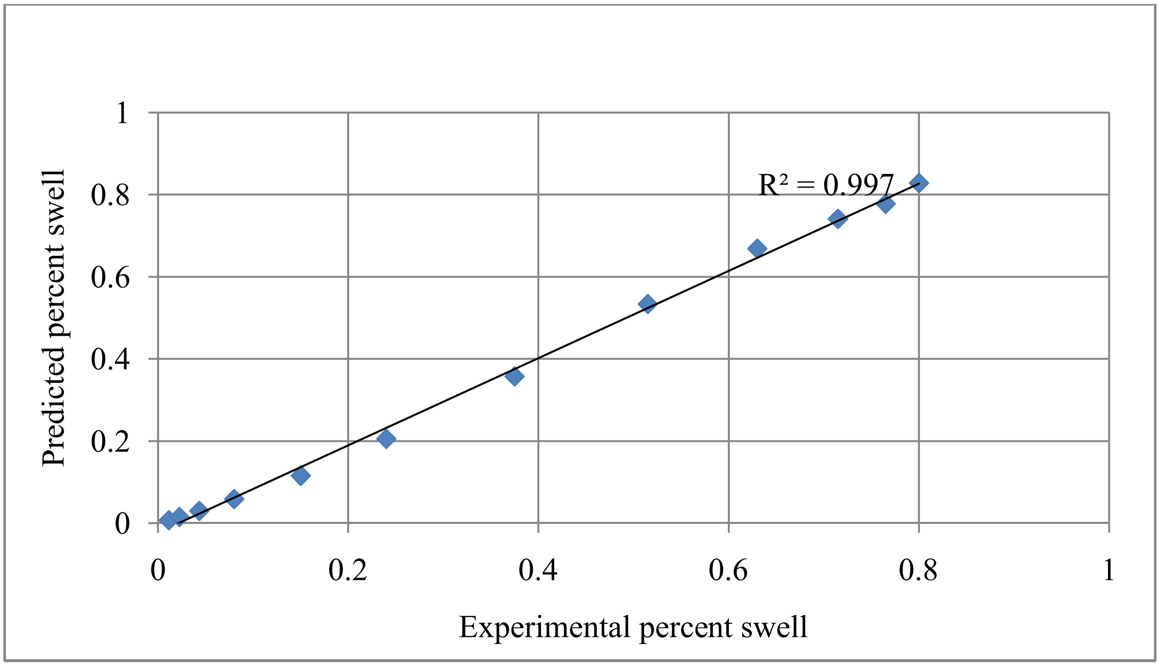

Figure C5 Relationships between experimental swell and predicted swell for Bole high school soil (OMC=39 %, MDD=1.28 g/cc and P=100 kPa)

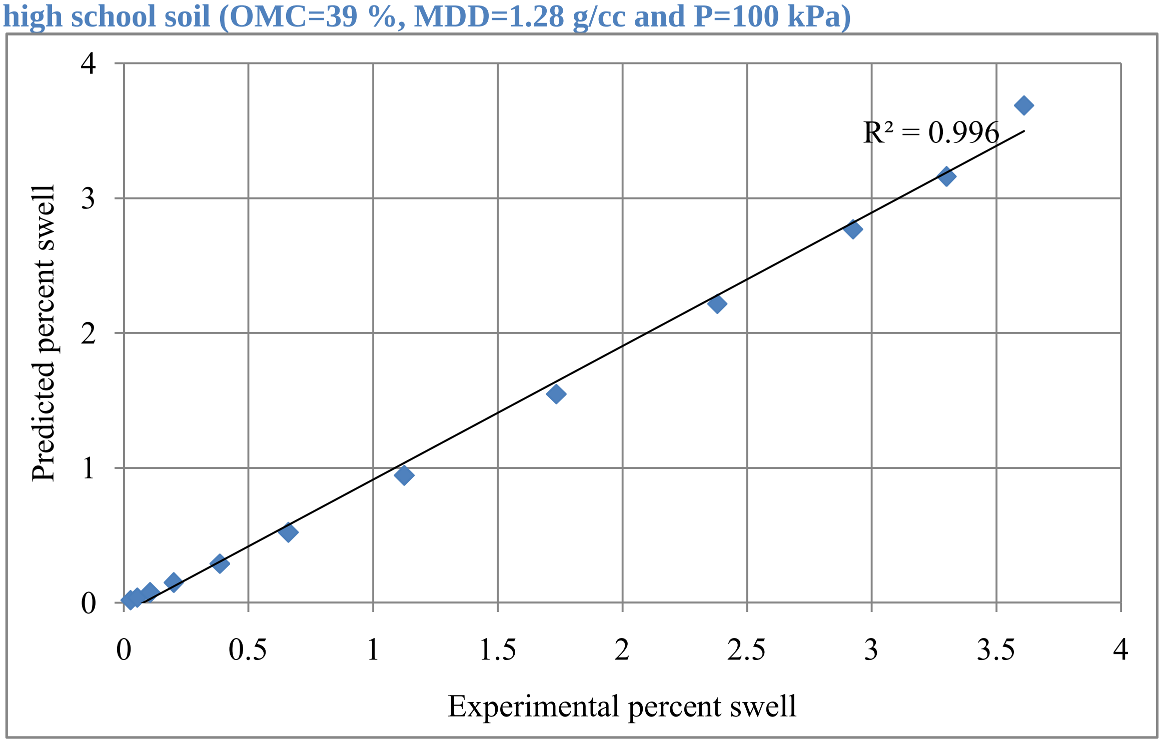

Figure C6 Relationships between experimental swell and predicted swell for Kality soil (OMC=29 %, MDD=1.2 g/cc and P=7 kPa)

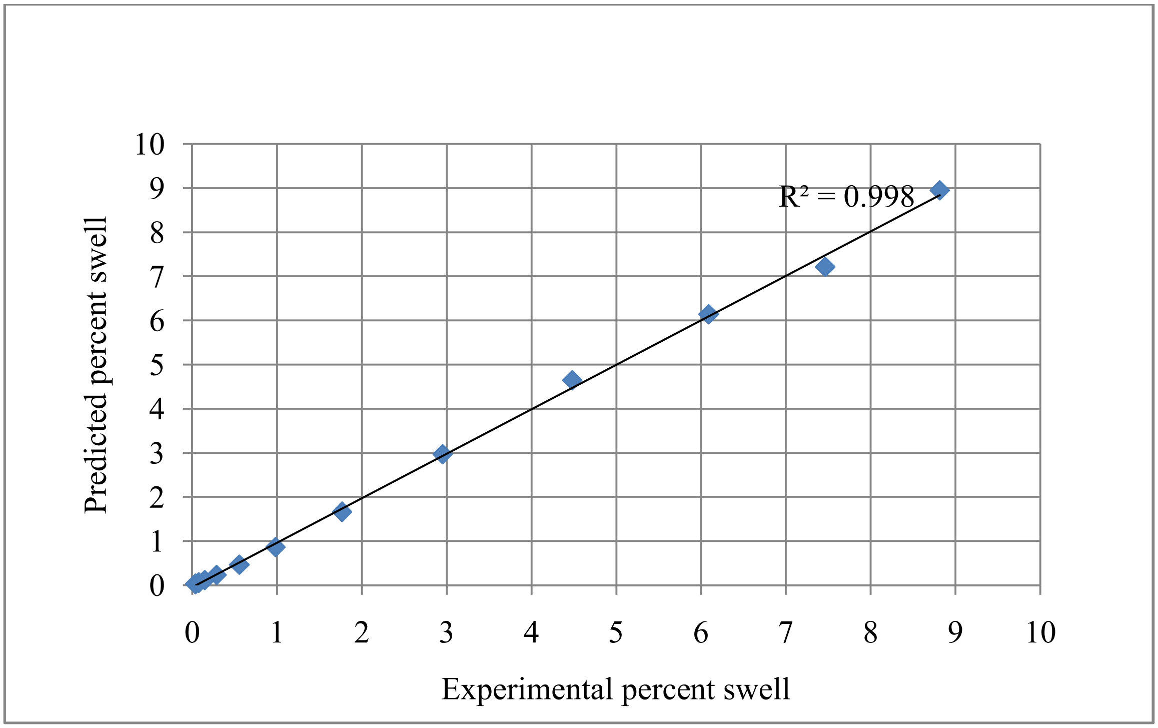

Figure C7 Relationships between experimental swell and predicted swell for Kality soil (OMC=29 %, MDD=1.25 g/cc and P=7 kPa)

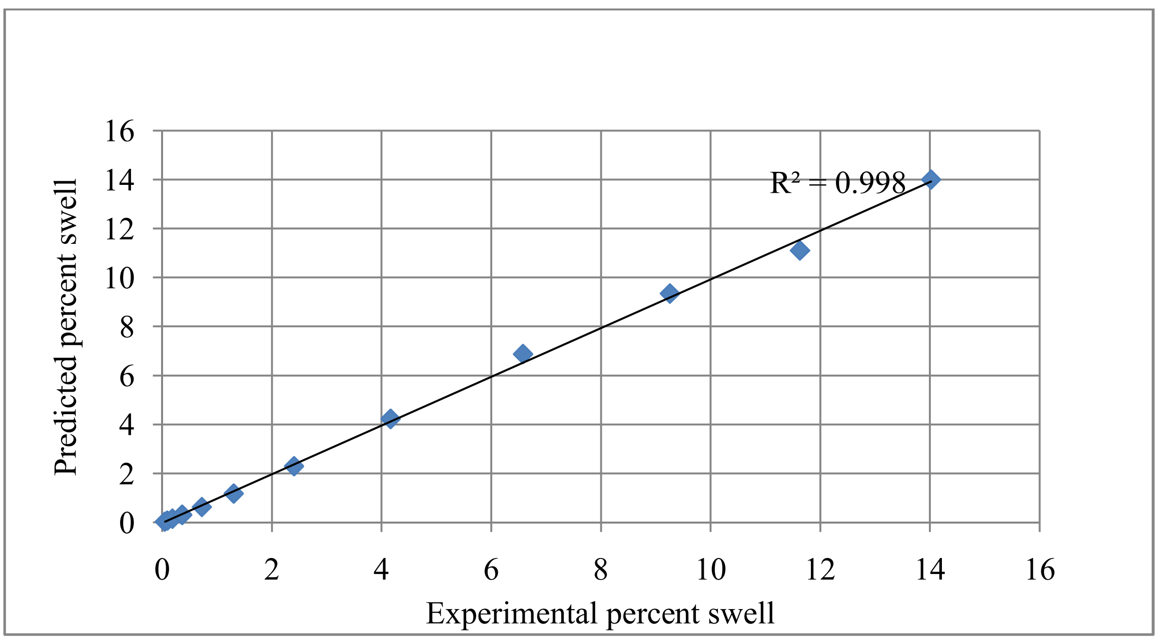

Figure C8 Relationships between experimental swell and predicted swell for Kality soil (OMC=29 %, MDD=1.3 g/cc and P=7 kPa)

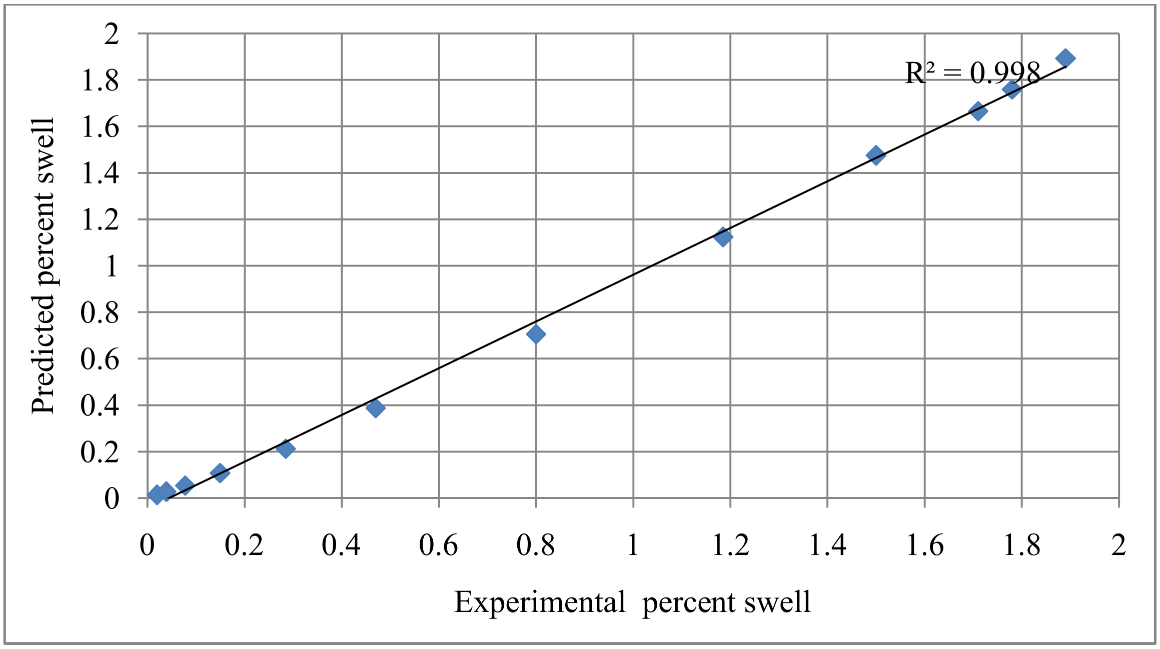

Figure Relationships between experimental swell and predicted swell for Bole high school soil (OMC=39 %, MDD=1.2 g/cc and P=7 kPa)

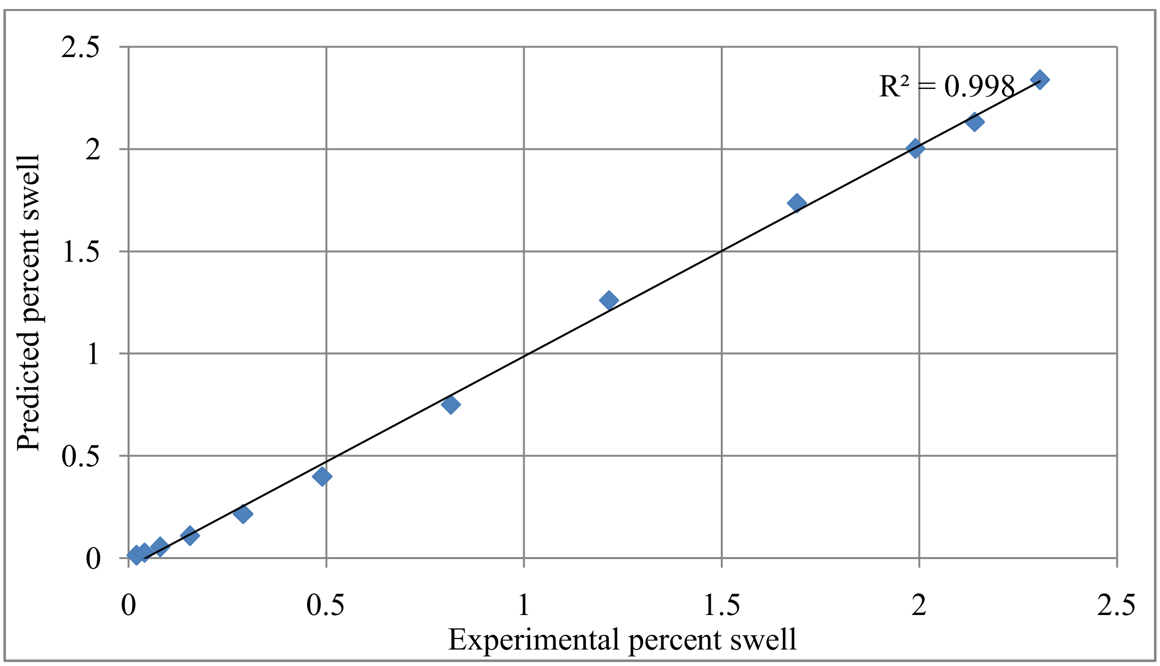

Figure C10 Relationships between experimental swell and predicted swell for Bole high school soil (OMC=39 %, MDD=1.25 g/cc and P=7 kPa)

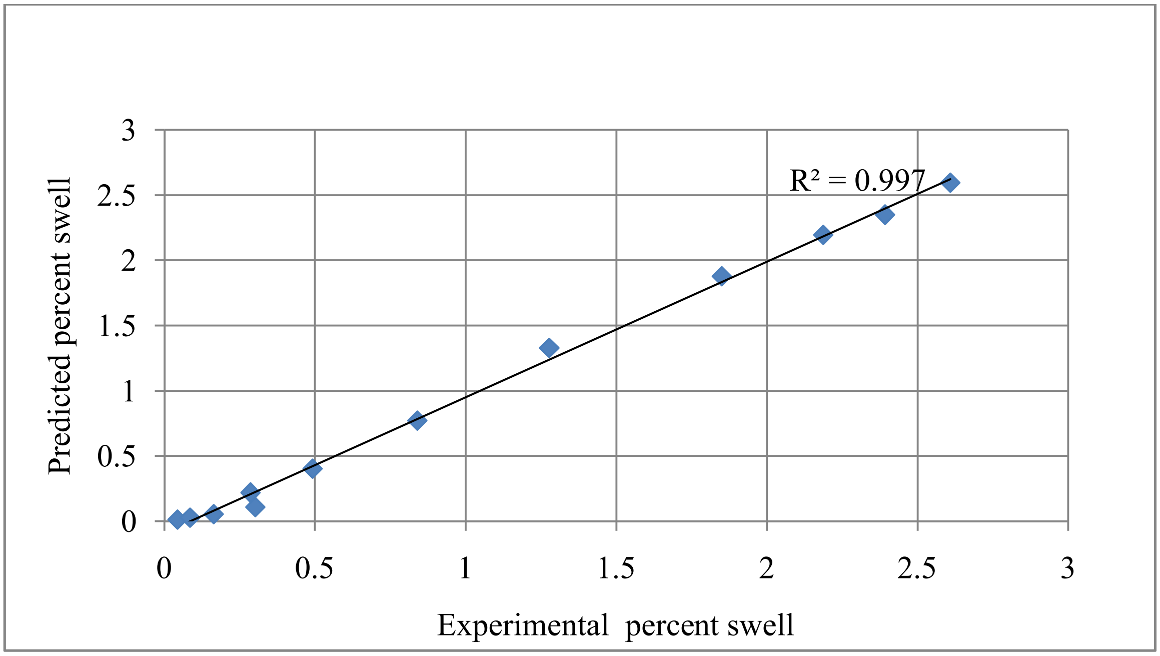

Figure C11 Relationships between experimental swell and predicted swell for Bole high school soil (OMC=39 %, MDD=1.28 g/cc and P=7 kPa)

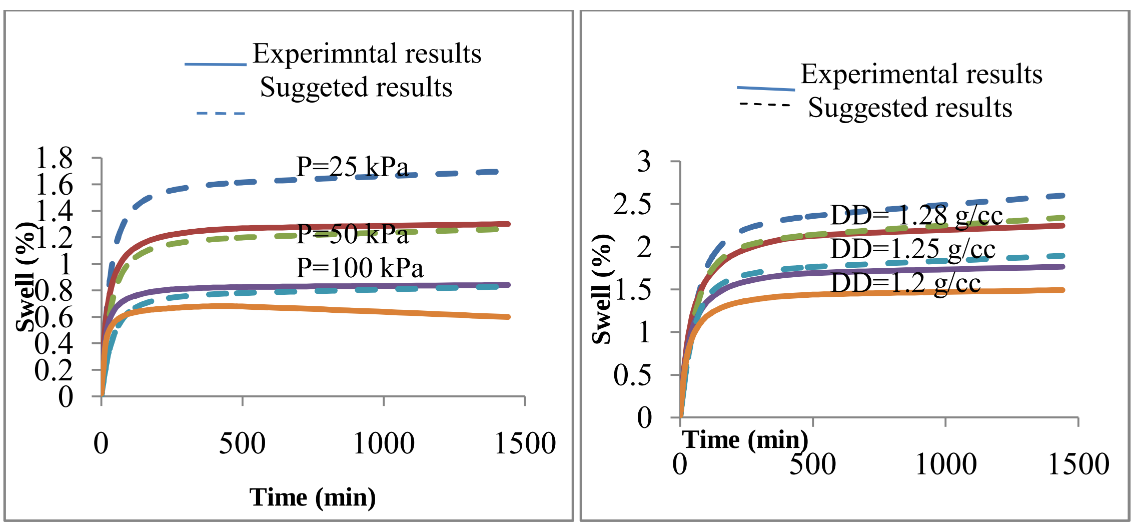

Figure C12 Swell time relationship for soil close to Bole Airport using the model developed for Bole High school soil

.